Synthesis of Group (IV) Transition Metal Complexes and their Applications as Catalysts for Ethylene Polymerization

Dissertation

zur Erlangung des akademischen Grades eines
Doktors der Naturwissenschaften (Dr. rer. nat.)
der Fakultät für Biologie, Chemie und Geowissenschaften
der
Universität Bayreuth

Vorgelegt von
Khalil Ahmad
aus Jhang, Pakistan

Bayreuth 2010

This thesis fulfils the requirements of the doctoral degree of the Faculty of Biology, Chemistry and Geological Sciences at the Universität Bayreuth.

Thesis submitted: 10.02.2010

Date of Scientific Colloquium: 19.03.2010

Examination Committee:

Prof. Dr. Helmut G. Alt	1. Referee
Prof. Dr. Jürgen Senker	2. Referee
Prof. Dr. Rainer Schobert	
Prof. Dr. Peter Strohriegl	Chairman

The following work was performed during the period April 2006 to October 2009 under the supervision of Prof. Dr. Helmut G. Alt at the Lehrstuhl für Anorganische Chemie II der Universität Bayreuth.

My sincere acknowledgement to my supervisor

Herrn Professor Dr. Helmut G. Alt

for his guidance, encouragement and enthusiastic support which enabled me to complete this research work.

I am grateful to HEC Pakistan and DAAD for the financial support.

Acknowledgement

I am thankful to Dr. Christian Görl for his guidance in research work and thesis writing and to Julian Lang for his help.

I am very grateful to Andrea Rimkus, Dr. Ezzat Khan and Dr. Awal Noor for their help in GC/MS and NMR measurements.

I would like to express my gratitude to my labmates: Dr. Christine Denner, Dr. Haif Alshammari, Dr. Silke Taubmann, Dr. Sandra Taubmann, Dr. Hamdi Elagab, Mohamed Abdelbagi, Frank Lüdel, Tanja Englmann and Matthias Dötterl for their help, support and valuable suggestions.

I am thankful to Fakhera Heinrich, Dr. Saddaf Qayyum and Muhammad Hafeez for their moral support during the course of my stay here in Bayreuth.

I would like to express my gratitude to all members in AC II for providing a friendly and cooperative atmosphere.

Finally I would like to extend my thanks to my family members in Pakistan for their constant encouragement and moral support throughout the period of my studies.

To

My Father

&

The Soul of my Mother

Abbreviations

α-	alpha-
Å	Angström
β-	beta-
n-Bu	n-butyl
℃	Degree Celsius
cat.	catalyst
$CDCl_3$	deuterated chloroform
CD_2Cl_2	deuterated methylene chloride
δ	chemical shift in ppm
d	doublet in NMR spectroscopy
dd	doublet of doublet in NMR spectroscopy
DMF	dimethylformamide
DMSO	dimethylsulphoxide
Et	ethyl
g	gram
GC	gas chromatography
h	hour
Hz	hertz
i-Pr	iso-propyl
kg	kilogram
M	metal
MAO	methylaluminoxane
Me	methyl
mg	milligram
min	minute
mL	milliliter
mol	mole
mmol	millimole
m/e	mass/elemental electric charge
M_n	number average molar mass
M_w	weight average molar mass

MS	mass spectrometry
NMR	Nuclear Magnetic Resonance
n.a.	not assigned
n.d.	not determined
PE	polyethylene
Ph	phenyl
PP	polypropylene
ppm	parts per million
r.t.	room temperature
s	second
THF	tetrahydrofuran
TMA	trimethylaluminum
t	triplet in NMR spectroscopy
X	halide

Contents

1. Introduction

1.1 General

Polyolefin industry is one of the fastest growing industries. Polyolefin materials include polyethylenes (PEs), polypropylenes (PPs), ethylene/α-olefin copolymers, and ethylene/propylene/diene elastomers (EPDMs) etc. Their total annual production is over 100 million tons which is still increasing. Polyolefins are replacing other polymers which is evident from the fact that their share of total polymer production increased from 30 percent in 1970 to 60 percent in 2002[1]. This is due to the combination of their cost efficiency with exceptional properties like chemical inertness, high mechanical strength, low density, flexibility, processibility and recyclability. The common applications of polyolefins are their use in food packages, plastic bags, squeeze bottles, containers, storage boxes, toys, disposable diapers, bullet-proof vests, gasoline tanks and components of automotive and engineering industry.

Polyethylene is the most common polyolefin. It was accidentally synthesized by the German chemist Pechmann in 1898 and characterised by his colleagues Bamberger and Tschirner[2]. Its industrial scale production started at the British company Imperial Chemical Industrial (ICl) in 1939 using a radical polymerization process under high pressure[3].

The first catalytic synthesis of polyethylene was discovered by Banks and Hogan at Phillips Petroleum in 1951. They used chromium trioxide supported on silica gel (Phillips catalyst) to polymerize ethylene at milder conditions[4]. In 1953 the German chemist Ziegler used titanium halides along with organoaluminum compounds (e.g. trimethylaluminum, diethylaluminum chloride) to polymerize ethylene even at milder conditions compared with the Phillips catalyst[5, 6]. Still the major amount of the polyethylene is produced with the Phillips and Ziegler catalyst systems as they are cheap. Later on, Natta used the Ziegler catalyst system to polymerize propylene[7]. For their achievements[8, 9], Ziegler and Natta were awarded the Nobel Prize in chemistry in 1963. The advantage of both the Phillips and the Ziegler catalyst is that they can be heterogenized on an inorganic support like aluminum oxide or silica gel thus avoiding the fouling (the produced polymer accumulates on the reactor walls and disturbs the reaction control) of the reactor walls. The disadvantage of these catalyst systems is that they are multi-site catalysts, and each site produces a polymer of different molecular weight resulting in complex polymer mixtures with varying molecular weights and microstructures. Due to their heterogeneous nature it is hard to predict structure-property relationships of these catalyst systems.

The next evolution step in the field of catalytic olefin polymerization has been the metallocene catalysts. Soon after Ziegler's discovery, the first catalytically active metallocene system Cp_2TiCl_2-$AlEt_2Cl$ (Cp = η^5-C_5H_5) for olefin polymerization was reported by Breslow and Natta[10, 11]. Due to their homogeneous nature, these metallocene systems were useful as model compounds for kinetic studies but they were not attractive for commercial use because of their low activities.

In 1980, the discovery of Sinn and Kaminsky[12, 13] that the use of methylaluminoxane (MAO) as a cocatalyst results in a tremendous increase of the activity of metallocene complexes lead to the revival of interest in this field. MAO is obtained by the partial hydrolysis of trimethylaluminum (TMA).

Activation of metallocene complexes with MAO can be explained by the Cossee-Arlman[14-16] mechanism (Scheme 1). According to this mechanism, MAO is added to the metallocene complexes and replaces one or both chloride ligands with methyl groups from trimethylaluminum (TMA). In the next step the remaining chloride ligand or one methyl group is abstracted by the strongly Lewis acidic aluminum centers to form a metallocene cation which has a vacant site at the metal center. An olefin molecule can now coordinate to the vacant site. In the next step, the methyl ligand migrates to the olefin ligand ("olefin insertion") and generates a vacant site on the backside of the catalyst molecule. Now the same procedure can start again (catalytic cycles).

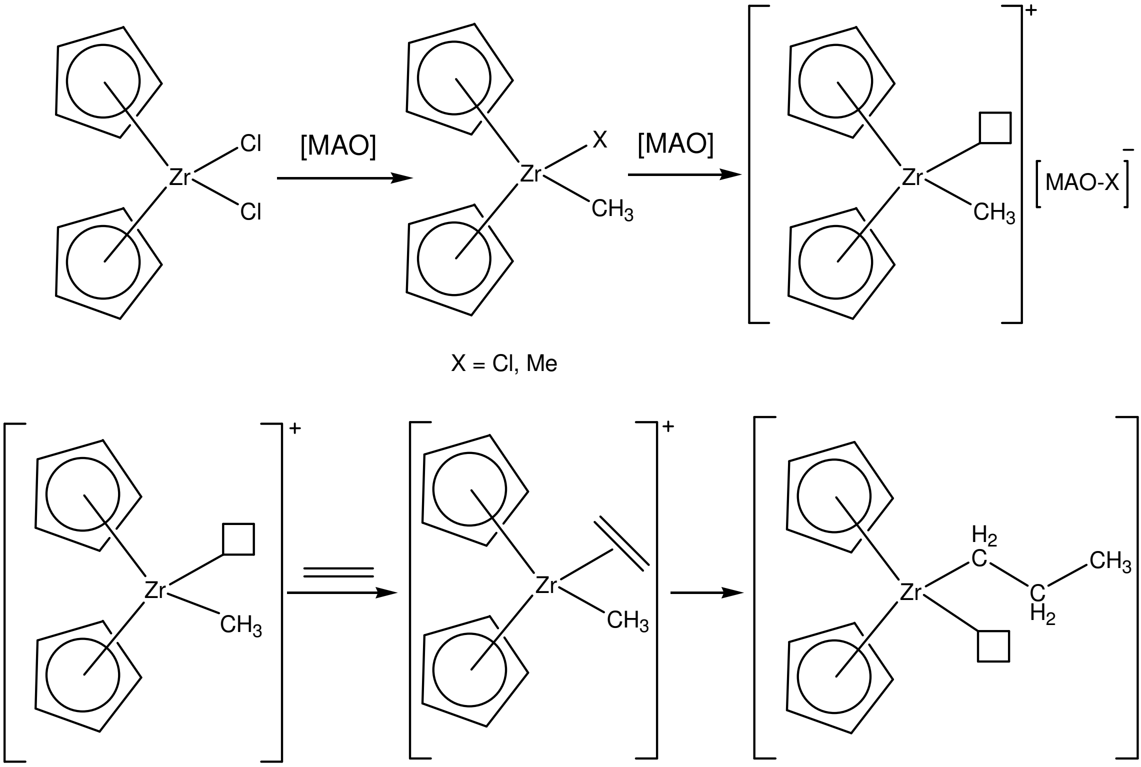

Scheme 1: Cossee-Arlman mechanism for the activation of a metallocene complex with MAO and ethylene insertion.

Metallocene complexes are usually single site catalysts which produce polymers with controlled molecular weights, specific tacticities, improved molecular weight distributions and better comonomer distributions as well as new olefinic materials like high performance linear low density polyethylene and cyclic olefin copolymers.

Although metallocene complexes are very efficient catalysts for olefin polymerization, they cannot incorporate polar olefins such as acrylates, vinyl acetate, vinyl halides and acrylonitriles because early transition metals have a strong tendency to coordinate to the electronegative atoms of the monomers instead of the olefin.

Keim's discovery[17-21] that nickel (II) complexes bearing P-O chelating ligands can oligomerize ethylene to give higher olefins lead to the Shell higher olefin process (SHOP). In 1995 Brookhart discovered that activated nickel (II) and palladium (II) diimine complexes can polymerize ethylene[22-24] which triggered the increased interest in late transition metal catalysts. These late transition metal complexes produce branched polymers. Another advantage is the low oxophilicity of late transition metals which provides the opportunity to copolymerize ethylene and other α-olefins with polar comonomers like acrylates.

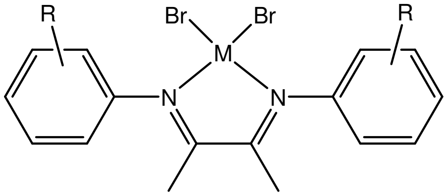

R = Alkyl, Halogen

M = Ni, Pd

Scheme 2: General structure of α-diimine complexes.

In 1996, McConville[25, 26] reported chelating diamide complexes of titanium as catalyst precursors for the polymerization of higher olefins. These catalysts induce living polymerization of 1-hexene with very high activities.

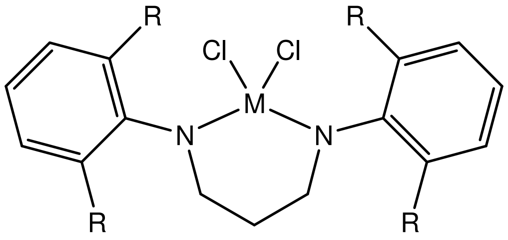

M = Ti, Zr
R = Alkyl

Scheme 3: General structure of chelating diamide complexes.

In 1998 Brookhart[27, 28] and Gibson[29, 30] independently discovered a new class of catalysts based on iron and cobalt complexes with 2,6-bis(imino)pyridine ligands for oligomerization and polymerization of olefins. These complexes can be easily tuned to produce oligomers[31-33] or polymers[34-36] by changing the substituents on the iminoaryl groups. Due to their good compatibility with other early and late transition metal copolymerization catalysts, they can be used as oligomerization catalysts in tandem catalytic processes to produce branched polyethylene[37, 38].

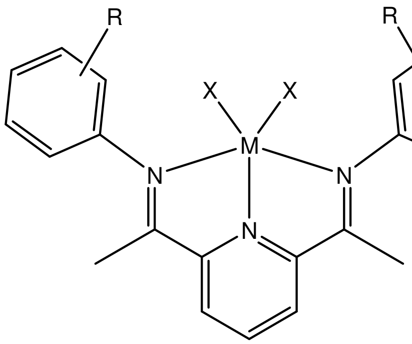

R = Alkyl, Halogen

M = Fe, Co

X = Cl, Br

Scheme 4: General structure of 2,6-bis(imino)pyridine transition metal complexes.

In 1998, Fujita reported bis (phenoxyimine) zirconium dichloride complexes[39-43] as a new class of catalysts for olefin polymerization. These catalysts show very high activities for ethylene polymerization[44-46] and are named FI catalysts (the term FI catalysts originates from the Japanese pronunciation of the ligand, Fenokishi-Imin Haiishi (Haiishi means ligand), FI also stands for “Fujita group invented” catalysts).

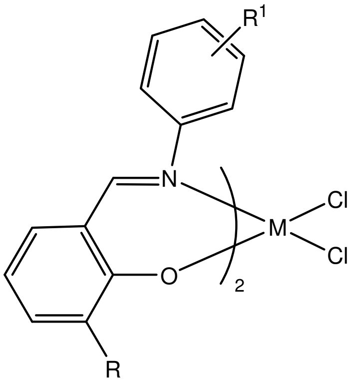

R = Alkyl
R^1 = Alkyl, Halogen
M = Ti, Zr, Hf

Scheme 5: General structure of FI complexes.

1.2 Aim of the work

The ligand structure plays the key role in terms of the activity and selectivity of a catalyst. Minor changes in the ligand structure can lead to dramatic effects on the activity and selectivity of a catalyst. Keeping this in focus, the aim of the work was to synthesize new potential ligands and their transition metal complexes. The proposed potential ligands include

-alkoxy substituted indenyl compounds.
-9-methylfluorenyl substituted indenyl compounds.
-asymmetric diamine compounds.
-Schiff base compounds of 2-(2-aminophenyl)benzothiazole
-indene-phenoxyimine and indene/fluorene-amidine bridged compounds.

Titanium, zirconium and hafnium complexes of the above ligands should be synthesized as catalyst precursors, tested for ethylene polymerization after activation with methylaluminoxane (MAO) and tailored in accordance with the “structure-property relation” for optimum results.

2. General Part

2.1 Alkoxy substituted zirconocene and hafnocene dichloride complexes

2.1.1 General

Metallocene dichloride complexes are precursors of highly active catalysts for α-olefin polymerization. In contrast to traditional Ziegler-Natta catalysts, metallocene complexes are single site catalysts which produce polyolefins with well defined microstructures. Due to facile ligand modification, a very large number of metallocene complexes has been synthesized to improve both the activities of the catalysts and the properties of the produced polyolefins. The size and nature of substituents linked to cyclopentadienyl or indenyl moieties play an important role on the catalytic activity as well as on the molecular weight and molecular weight distribution of the produced polyolefin. Several metallocene complexes containing functional groups linked to cyclopentadienyl or indenyl moieties have been reported[47-70]. Donor atoms can alter the activity of a catalyst by coordinating reversibly or irreversibly to the metal center and block the vacant coordination site. Piccolrovazzi et. al. have found that electron donating alkyl groups on bis (indenyl) zirconium dichloride have a favourable effect on the ethylene polymerization activity of the catalyst while electron withdrawing groups decrease the catalyst activity and the molecular weight of the polyethylene produced[51]. Jutzi et. al. have reported the ethylene polymerization properties of titanium and zirconium complexes containing dimethylamino substituted cyclopentadienyl ligands[63]. Alonso-Moreno et. al. immobilized alkoxy- and siloxy-substituted metallocene catalysts on dehydroxylated silica[70], while Sun et. al. used oxygen bearing bridges for the synthesis of symmetric and asymmetric dinuclear metallocene complexes[71-74]. Here symmetric and asymmetric complexes of zirconium and hafnium with phenoxy and naphthoxy substituted indenyl ligands and their behaviour towards ethylene polymerization after activation with MAO are reported.

2.1.2 Synthesis and characterization of indenyl compounds with phenoxy and naphthoxy substituents

Phenoxy and naphthoxy substituted indenes were synthesized by two methods. In the first method, phenols or naphthols were refluxed with equivalent amounts of ω-bromo-1-

indenylalkanes and potassium carbonate in the presence of catalytic amounts of 18-crown-6 in acetone (Scheme 6, method 1).

In the second method, ω-bromo-1-phenoxyalkanes were first synthesized by refluxing an excess of dibromoalkanes with phenols and potassium carbonate in the presence of catalytic amounts of 18-crown-6 in acetone and then reacting them with equivalent amounts of indenyl lithium (Scheme 6, method 2).

The second method gives quantitative yields for all phenols and naphthols while the first method does not work well for phenols bearing electron donating groups at the ortho position.

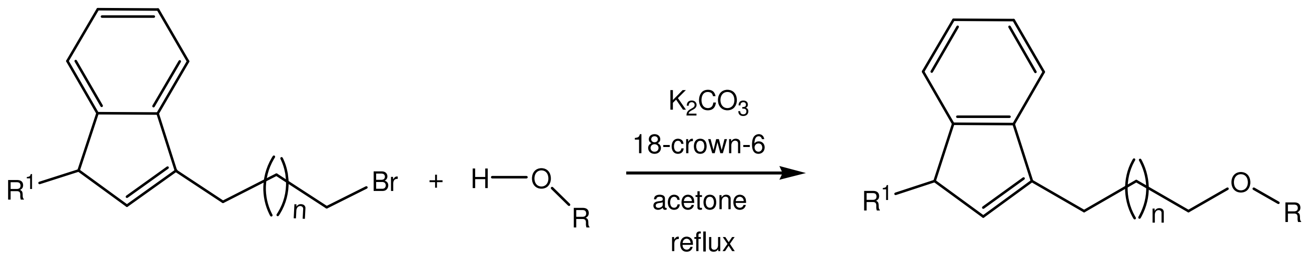

Method 1

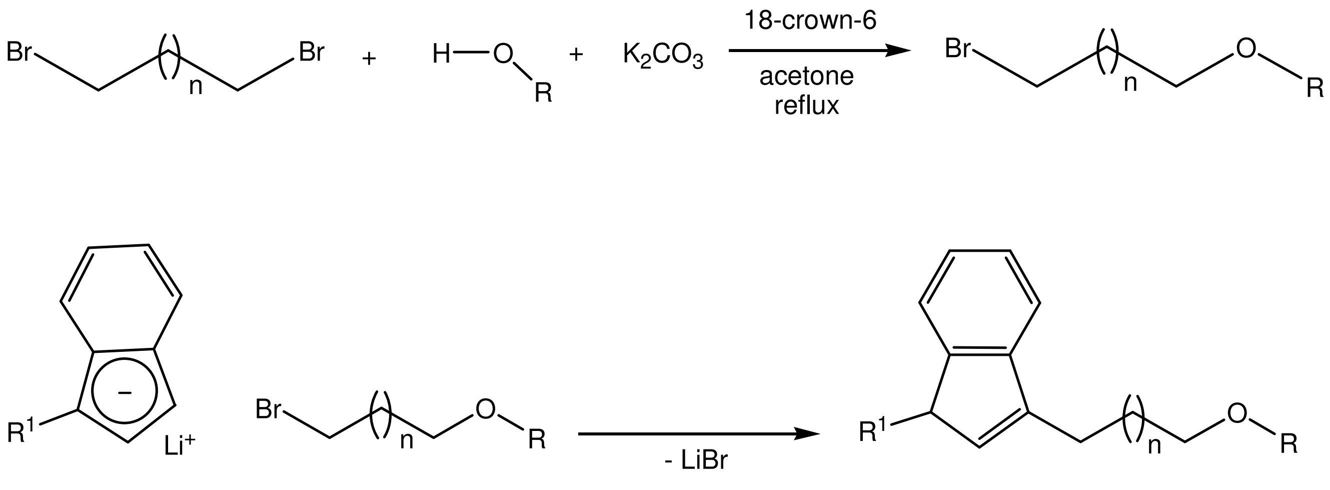

Method 2

Scheme 6: Synthesis of compounds **1**-**14**.

Table 1: Compounds 1-14

No.	n	R^1	R	structure
1	1	H	phenyl	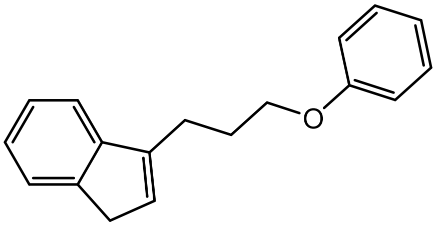
2	2	H	phenyl	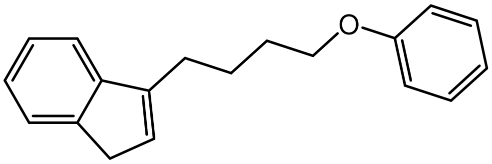
3	3	H	phenyl	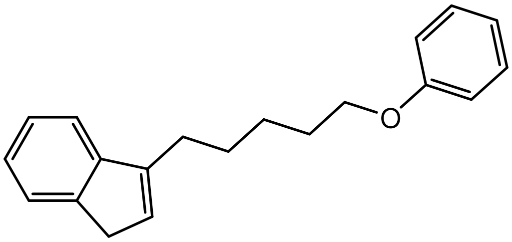
4	1	H	2-t-butyl phenyl	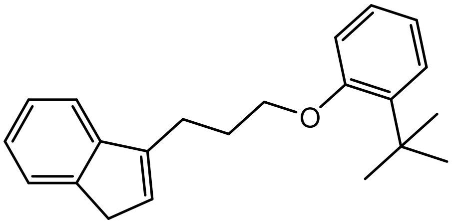
5	2	H	2-t-butyl phenyl	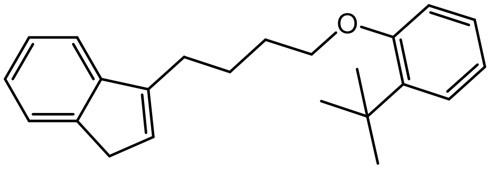
6	3	H	2-t-butyl phenyl	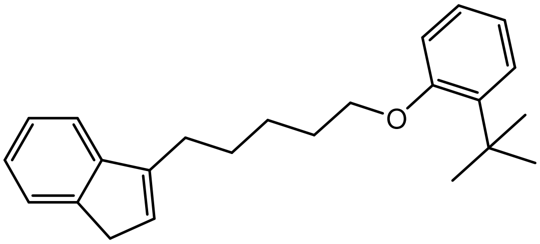
7	1	H	4-t-butyl phenyl	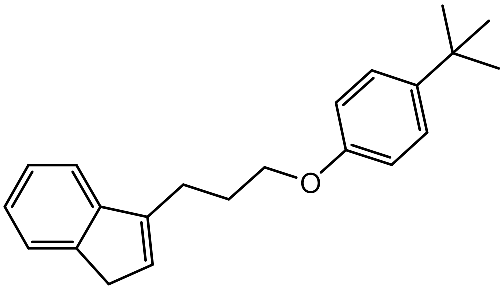

No.	n	R^1	R	structure
8	2	H	4-t-butyl phenyl	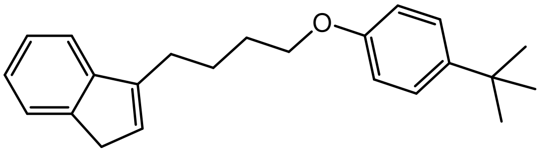
9	3	H	4-t-butyl phenyl	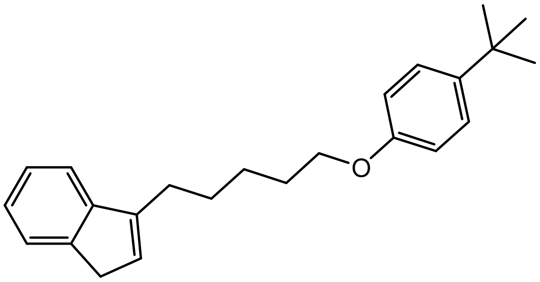
10	1	H	2-phenyl phenyl	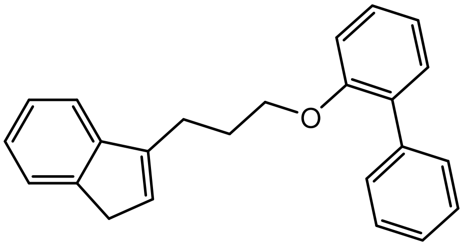
11	1	CH_3	2-phenyl phenyl	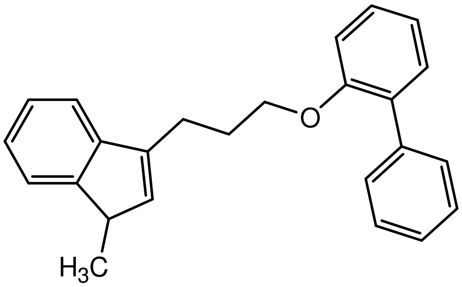
12	2	H	2-phenyl phenyl	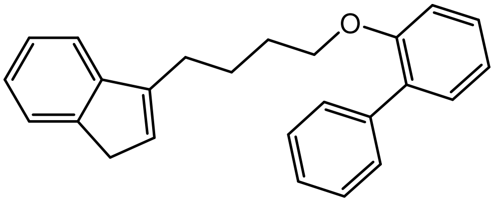
13	3	H	2-phenyl phenyl	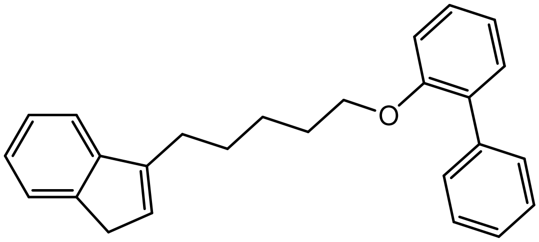
14	1	H	1-naphthyl	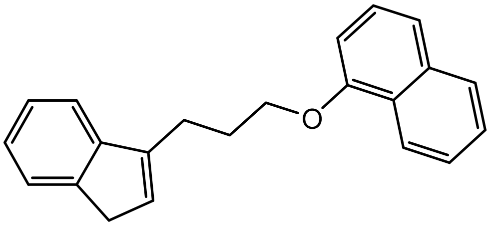

Compounds **1**-**14** were characterized by GC/MS and ^{1}H- and ^{13}C-NMR spectroscopy (Table 2). The MS and NMR spectra of compounds **2**, **4** and **8** are discussed as examples.

The ^{1}H-NMR spectrum of compound **2** (Scheme 7) shows signals at δ = 7.47-7.44 (m, 1H), 7.38-7.35 (m, 1H), 7.32-7.25 (m, 3H), 7.22-7.17 (m, 1H), and 6.95-6.88 (m, 3H) ppm for the nine protons of the two six membered rings. The signal at δ = 6.23 (br, 1H) ppm is due to the indenyl proton H2 while the signal at δ = 4.00 (t, J = 5.8 Hz, 2H) ppm is assigned to the CH_2 protons in neighborhood to the oxygen substituent H11. The indenyl CH_2 protons H1 appear at δ = 3.32 (br, 2H) ppm. The signal at δ = 2.65-2.60 (m, 2H) ppm is assigned to the CH_2 protons H8, while the signal at δ = 1.91-1.87 (m, 4H) ppm can be assigned to H9 and H10.

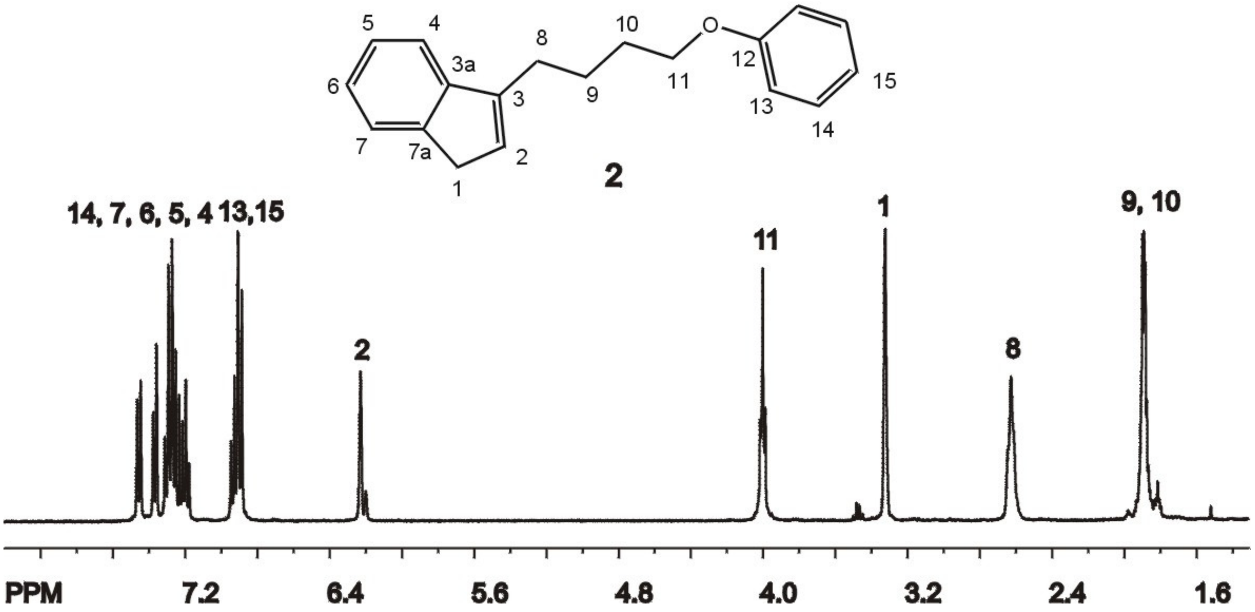

Scheme 7: ^{1}H-NMR spectrum of compound **2**.

The ^{13}C-NMR spectrum of compound **2** (Scheme 8) shows the signal for the quaternary carbon atom C12 at δ = 159.0 ppm. The signals at δ = 145.4, 144.5 and 144.1 ppm are assigned to the indenyl quaternary carbon atoms C7a, C3a and C3. The signal at δ = 129.4 ppm is assigned to C14, while the signals at δ = 128.0, 126.0, 124.5, 123.7, 120.5 and 118.9 ppm derive from C7, C6, C5, C4, C2 and C15. At δ = 114.5 ppm the signal for the CH carbon atom C13 appears. The signal at δ = 67.6 ppm arises from C11, the signal at δ = 37.7 ppm from C1. The signals at δ = 29.2, 27.4 and 24.5 ppm can be assigned to the CH_2 groups of the alkyl chain (C8, C9 and C10).

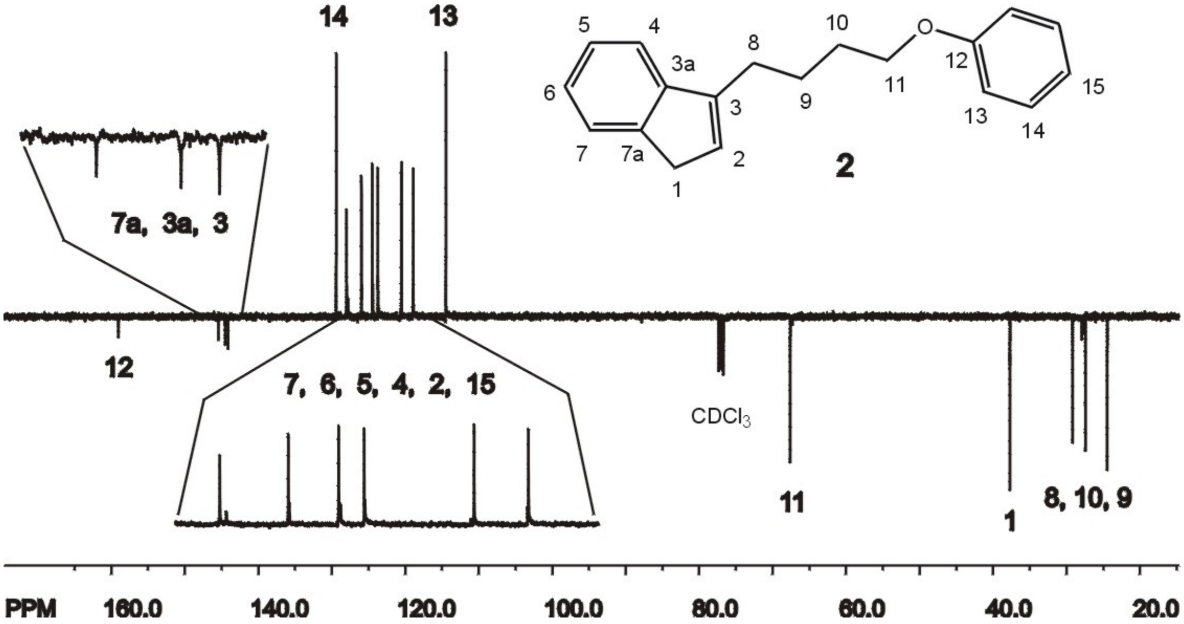

Scheme 8: ^{13}C-NMR spectrum of compound **2**.

The mass spectrum of compound **2** (Scheme 9) shows the molecular ion peak at m/z = 264 with 3% intensity relative to the base peak. The fragmentation at the C11-O bond results into a fragment at m/z = 171 with 90% intensity relative to the base peak, while the fragmentation at the C8-C9 bond results into the base peak at m/z = 129.

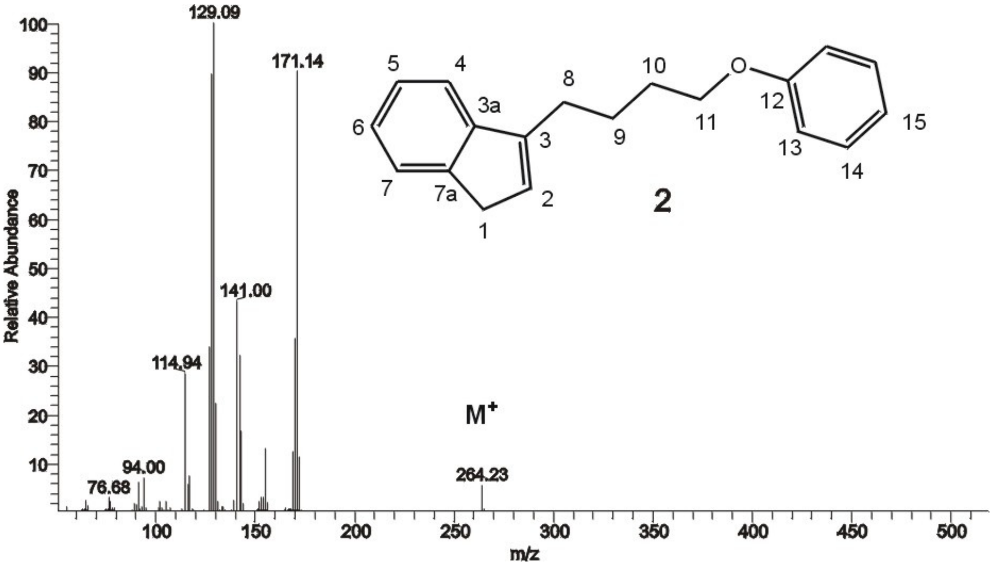

Scheme 9: Mass spectrum of compound **2**.

In the ^{1}H-NMR spectrum of compound **4** (Scheme 10), the signals at δ = 7.56-7.53 (m, 1H), 7.50-7.47 (m, 1H), 7.41-7.37 (m, 2H), 7.32-7.22 (m, 2H) and 7.00-6.92 (m, 2H) ppm derive from the aryl protons H7, H6, H5, H4, H16, H15, H14 and H13. The signal at δ = 6.34 (br, 1H) ppm is assigned to H2, while the signal at δ = 4.14 (t, J = 6.2 Hz, 2H) ppm is due to the H10 protons. The protons of the indenyl CH_2 group appear at δ = 3.42 (br, 2H) ppm. The signals at δ = 2.93-2.87 (m, 2H) and 2.36-2.28 (m, 2H) ppm can be assigned to the H8 and H9 protons. The methyl protons of the tertiary butyl group appear at δ = 1.57 (s, 9H) ppm.

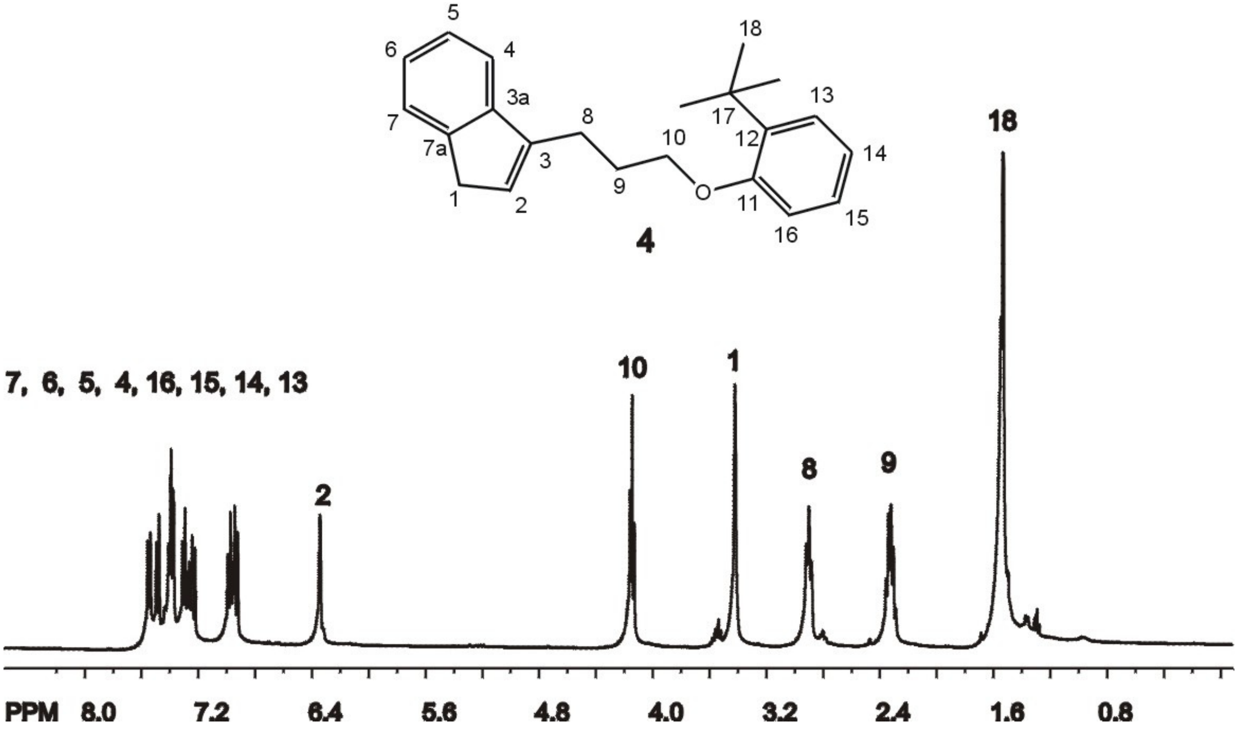

Scheme 10: ^{1}H-NMR spectrum of compound **4**.

In the ^{13}C-NMR spectrum of compound **4** (Scheme 11), the signal for the quaternary carbon atom C11 arises at δ = 157.8 ppm, while the signals at δ = 145.2, 144.5 and 143.6 ppm can be assigned to the indenyl quaternary carbon atoms C7a, C3a and C3. The signal at δ = 137.9 ppm arises from the quaternary carbon atom C12. The signals at δ = 128.2, 127.0, 126.6, 126.0, 124.6, 123.8, 120.1 and 118.9 ppm can be assigned to the CH groups C15, C14, C13, C7, C6, C5, C4 and C2. At δ = 111.7 ppm, the signal for the aryl CH carbon atom C16 can be observed. The signal for CH_2 carbon C10 arises at δ = 67.1 ppm, while the signals at δ = 37.7, 34.8 and 29.9 ppm derive from C1, C17 and C18. The signals at δ = 28.0 and 24.8 ppm can be assigned to the alkyl chain carbon atoms C8 and C9.

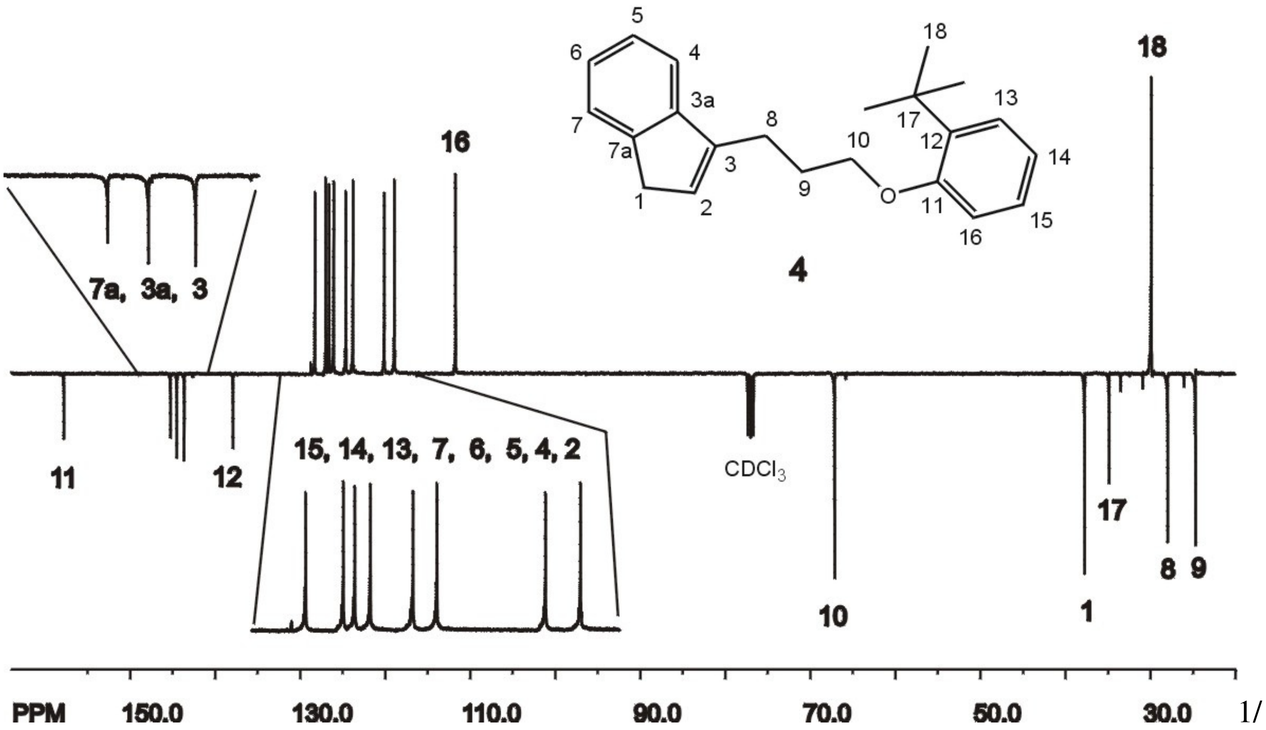

Scheme 11: ^{13}C-NMR spectrum of compound **4**.

The mass spectrum of compound **4** (Scheme 12) shows the molecular ion peak at m/z = 306 with 3% intensity relative to the base peak. Fragmentation of the C10-O bond results into the fragment at m/z = 157 with 44% intensity relative to the base peak, while the fragmentation at the C8-C9 bond results into the base peak at m/z = 129. The indenyl fragment appears at m/z = 115 with 64% intensity relative to the base peak.

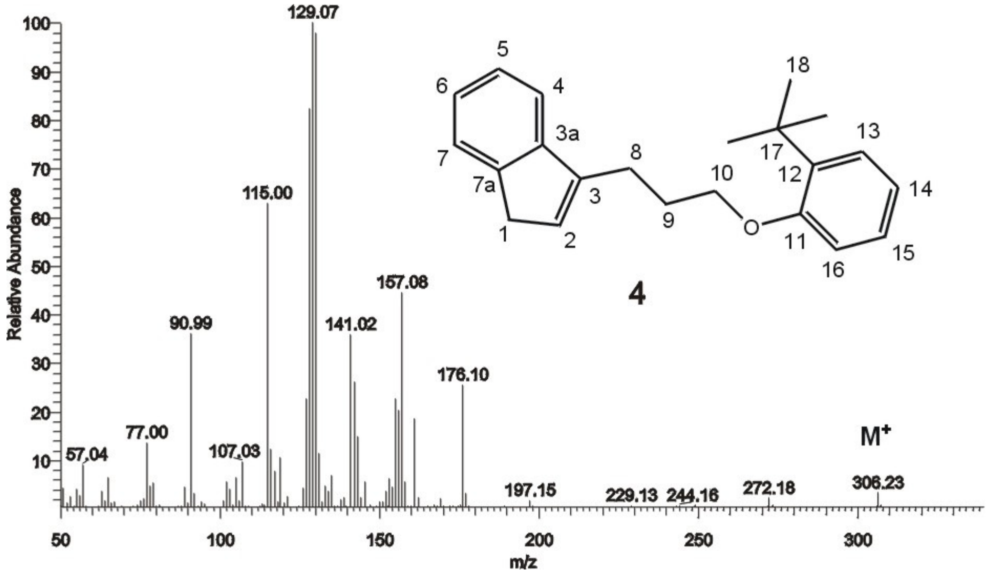

Scheme 12: Mass spectrum of compound **4**.

The ^{1}H-NMR spectrum of compound **8** (Scheme 13) shows signals at δ = 7.45-7.42 (m, 1H), 7.36-7.33 (m, 1H), 7.29-7.24 (m, 3H), 7.20-7.15 (m, 1H) and 6.83-6.79 (m, 2H) ppm for the eight protons H7, H6, H5, H4, H14 and H13. The signal for the indenyl proton H2 arises at δ = 6.20 (br, 1H) ppm. At δ = 3.96 (t, J = 6.0 Hz, 2H) ppm the signal for CH_2 protons H11 appears, while the indenyl CH_2 protons H1 give the signal at δ = 3.30 (br, 2H) ppm. The signal for the methylene protons H8 can be found at δ = 2.63-2.57 (m, 2H) ppm, while the signal at δ = 1.88-1.83 (m, 4H) ppm can be assigned to the residual CH_2 groups H9 and H10. The signal for the tertiary butyl group arises at δ = 1.27 (s, 9H) ppm.

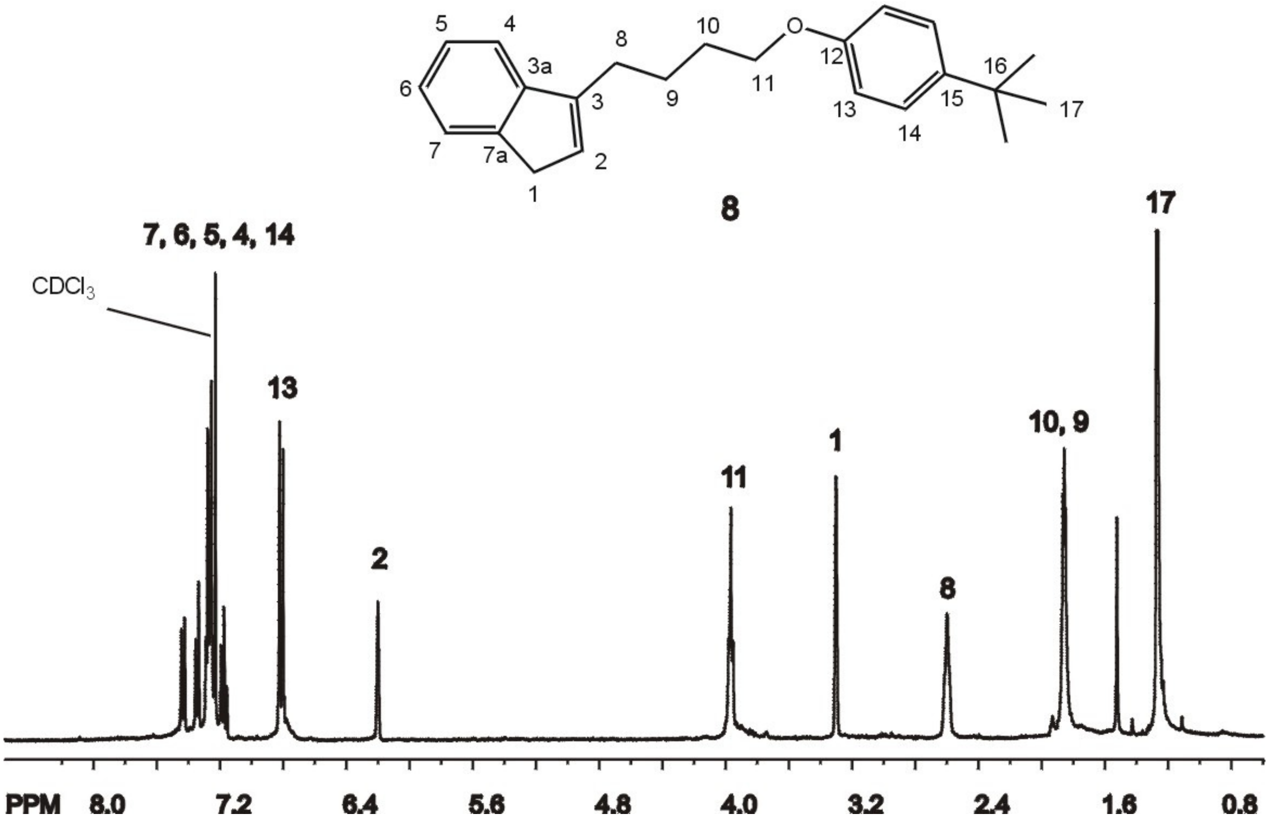

Scheme 13: ^{1}H-NMR spectrum of compound **8**.

The ^{13}C-NMR spectrum of compound **8** (Scheme 14) shows the signal for the quaternary carbon atom C12 at δ = 156.8 ppm, while the signals at δ = 145.5, 144.6, 144.2 and 143.1 ppm can be assigned to the quaternary carbon atoms C15, C7a, C3a and C3. The signals at δ = 128.0, 126.0, 124.5, 123.8 and 119.0 ppm can be assigned to the CH groups C7, C6, C5, C4 and C2 of the indenyl moiety, while the signals at δ = 126.2 and 114.0 ppm derive from the CH carbon atoms C14 and C13 of the phenoxy group. The signal at δ = 67.7 ppm is assigned to the CH_2 group attached to the oxygen atom (C11), while the signal at δ = 37.7 ppm results from the methylene group C1 of the indenyl ring. At δ = 34.0 and 31.5 ppm, the quaternary carbon atom C16 and the methyl carbon C17 can be found, while the signals at δ = 29.2, 27.4 and 24.5 ppm can be assigned to the methylene groups of the alkyl chain.

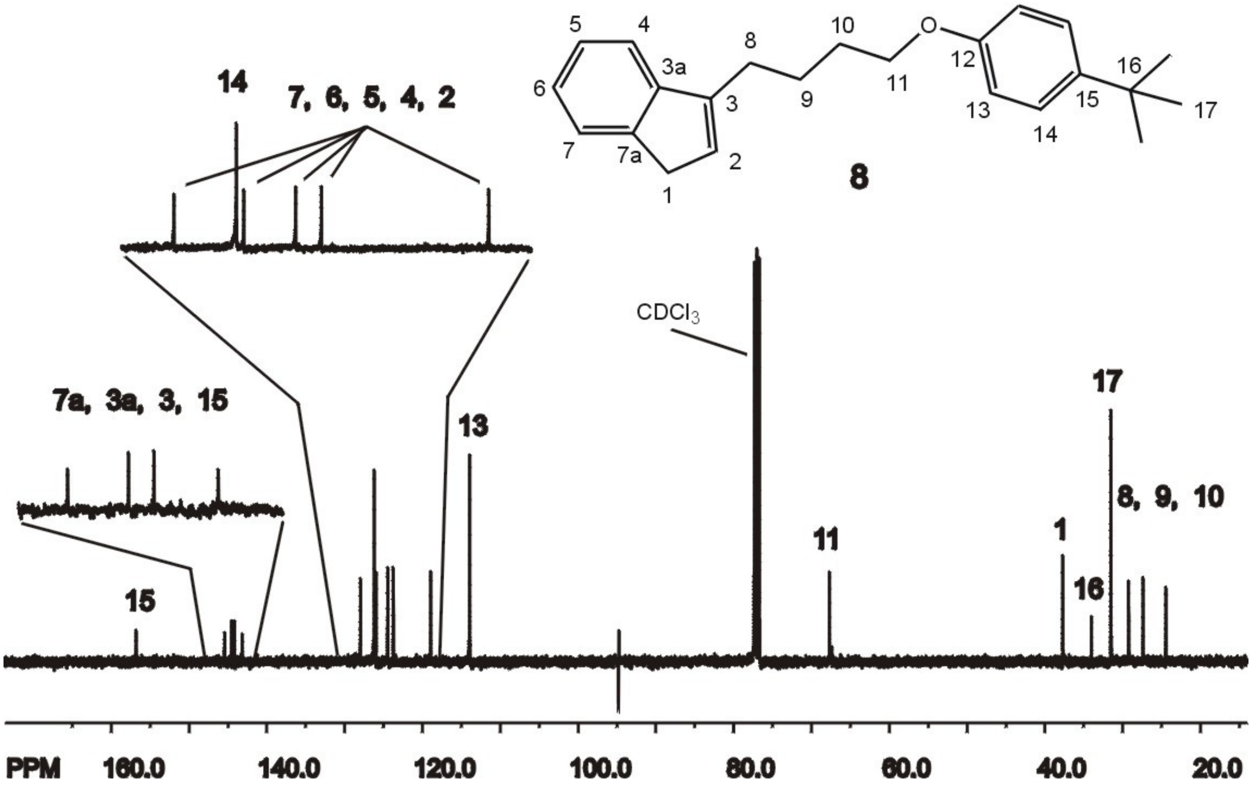

Scheme 14: ^{13}C-NMR spectrum of compound **8**.

The mass spectrum of compound **8** (Scheme 15) shows the molecular ion peak at m/z = 320 with 6% intensity as compared to the base peak. Fragmentation of the C11-O bond results in the base peak at m/z = 171. Fragmentation at the C8-C9 bond results in a fragment with m/z = 129 with 78% intensity relative to the base peak, the indenyl fragment appears at m/z = 115 with 22% intensity relative to the base peak.

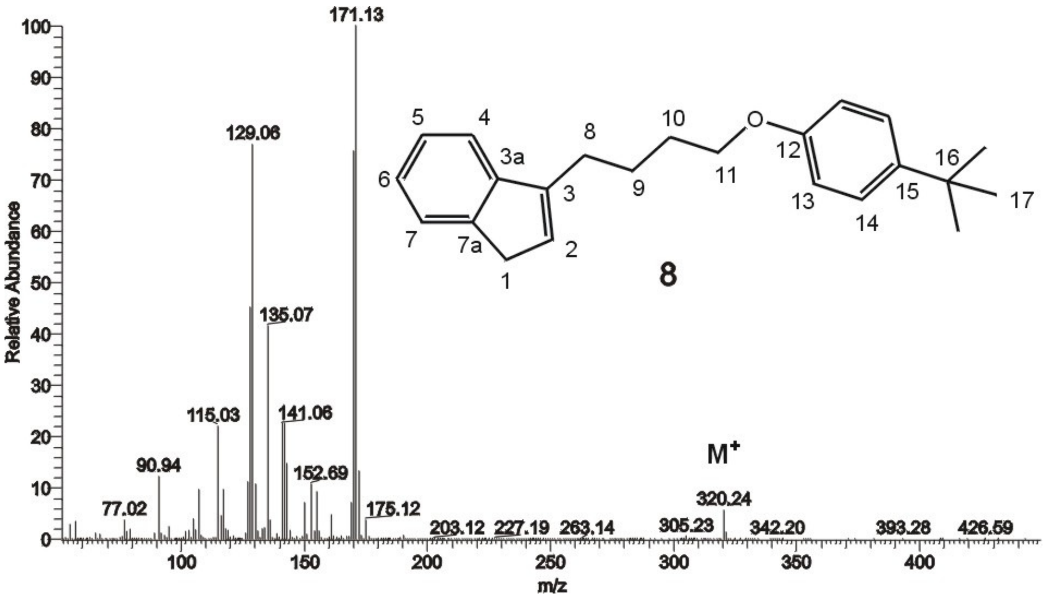

Scheme 15: Mass spectrum of compound **8**.

Table 2: NMR$^{a)}$ and MS data of compounds 1-14.

No.	^{1}H-NMR	^{13}C-NMR	MS [m/z (%)]
1	7.53-7.50 m (1H) 7.46-7.43 m (1H) 7.38-7.31 m (3H) 7.29-7.24 m (1H) 7.01-6.95 m (3H) 6.29 m (br, 1H, Ind-H2) 4.09 t (2H, OCH_2) 3.87 br (2H, Ind-H1) 2.84-2.78 m (2H, CH_2) 2.27-2.20 m (2H, CH_2)	159.0, 145.2, 144.4, 143.6 (C_q) 29.4, 128.2, 126.0, 124.6, 123.7, 120.5, 118.9, 114.5 (CH) 67.2 (OCH_2) 37.7 (CH_2-Ind) 27.6, 24.1 (each CH_2)	250 [M^+] (4) 155 (12) 141 (22) 130 (100) 115 (49)
2	7.47-7.43 m (1H) 7.38-7.35 m (1H) 7.32-7.25 m (3H) 7.22-7.17 m (1H) 6.95-6.88 m (3H) 6.23 m (br, 1H, Ind-H2) 4.00 t (2H, OCH_2) 3.32 br (2H, Ind-H1)	159.0, 145.4, 144.5, 144.1 (C_q) 29.4, 128.0, 126.0, 124.5, 123.7, 120.5, 118.9, 114.5 (CH) 67.6 (OCH_2) 37.7 (CH_2-Ind) 29.2, 27.4, 24.5 (each CH_2)	264 [M^+] (3) 171 (90) 129 (100)

No.	^{1}H-NMR	^{13}C-NMR	MS [m/z (%)]
	2.66-2.59 m (2H, CH$_2$) 1.93-1.85 m (4H, CH$_2$)		
3	7.48-7.44 m (1H) 7.39-7.35 m (1H) 7.32-7.25 m (3H) 7.23-7.17 m (1H) 6.96-6.88 m (3H) 6.20 m (br, 1H, Ind-H2) 3.96 t (2H, OCH$_2$) 3.32 br (2H, Ind-H1) 2.63-2.55 m (2H, CH$_2$) 1.88-1.72 m (4H, CH$_2$) 1.63-1.54 m (2H, CH$_2$)	159.0, 145.4, 144.5, 144.3 (C$_q$) 129.4, 127.8, 126.0, 124.4, 123.7, 120.5, 118.9, 114.5 (CH) 67.7 (OCH$_2$) 37.7 (CH$_2$-Ind) 29.2, 27.8, 27.6, 26.1 (each CH$_2$)	278 [M$^+$] (1) 185 (49) 129 (100) 115 (27)
4	7.56-7.53 m (1H) 7.50-7.47 m (1H) 7.41-7.37 m (2H) 7.32-7.22 m (2H) 7.00-6.92 m (2H) 6.34 m (br, 1H, Ind-H2) 4.14 t (2H, OCH$_2$) 3.42 br (2H, Ind-H1) 2.93-2.87 m (2H, CH$_2$) 2.36-2.28 m (2H, CH$_2$) 1.57 s (9H, CH$_3$)	157.8, 145.2, 144.5, 143.6, 137.9 (C$_q$) 128.2, 127.0, 126.6, 126.0, 124.6, 123.8, 120.0, 118.9, 111.7 (CH) 67.1 (OCH$_2$) 37.7 (CH$_2$-Ind) 34.8 (Cq) 29.9 (CH$_3$) 28.0, 24.8 (each CH$_2$)	306 [M$^+$] (3) 157(44) 129 (100) 115 (64)
5	7.46-7.43 m (1H) 7.38-7.35 m (1H) 7.30-7.25 m (2H) 7.21-7.12 m (2H) 6.88-6.83 m (2H) 6.22 m (br, 1H, Ind-H2) 4.01 t (2H-OCH$_2$) 3.32 br (2H, Ind-H1) 2.66-2.61 m (2H, CH$_2$)	157.8, 145.4, 144.6, 144.1, 138.0 (C$_q$) 127.9, 127.0, 126.6, 126.0, 124.5, 124.8, 120.0, 119.0, 111.7 (CH) 67.5 (OCH$_2$) 37.7 (CH$_2$-Ind) 34.9 (C$_q$) 29.8 (CH$_3$)	320 [M$^+$] (2) 171 (100) 129 (68) 115 (18)

No.	^{1}H-NMR	^{13}C-NMR	MS [m/z (%)]
	1.97-1.91 m (4H, CH_2) 1.38 s (9H, CH_3)	29.5, 27.5, 24.9 (each CH_2)	
6	7.46-7.43 m (1H) 7.39-7.35 m (1H) 7.31-7.26 m (2H) 7.21-7.12 m (2H) 6.90-6.82 m (2H) 6.20 m (br, 1H, Ind-H2) 3.97 t (2H, OCH_2) 3.31 br (2H, Ind-H1) 2.63-2.57 m (2H, CH_2) 1.94-1.86 m (2H, CH_2) 1.83-1.75 m (2H, CH_2) 1.68-1.61 m (2H, CH_2) 1.41 s (9H, CH_3)	157.7, 145.2, 144.4, 144.2, 137.8 (C_q) 127.6, 126.8, 126.4, 125.8, 124.4, 123.6, 119.9, 118.8, 111.6 (CH) 67.4 (OCH_2) 37.6 (CH_2-Ind) 34.7 (C_q) 29.7 (CH_3) 29.4, 27.6, 27.5, 26.3 (each CH_2)	334 [M^+] (1) 185 (100) 129 (60) 115 (22)
7	7.47-7.43 m (1H) 7.39-7.35 m (1H) 7.32-7.25 m (3H) 7.22-7.16 m (1H) 6.87-6.82 m (2H) 6.23 m (br, 1H, Ind-H2) 4.02 t (2H, OCH_2) 3.31 br (2H, Ind-H1) 2.77-2.69 m (2H, CH_2) 2.21-2.11 m (2H, CH_2) 1.29 s (9H, CH_3)	156.8, 145.3, 144.5, 143.7, 143.2 (C_q) 128.2, 128.1, 126.2, 126.0, 124.6, 123.8, 119.0, 114.0 (CH) 67.3 (OCH_2) 37.8 (CH_2-Ind) 34.0 (C_q) 31.5 (CH_3) 27.7, 24.2 (each CH_2)	306 [M^+] (8) 176(78) 161 (81) 129 (100) 115 (56)
8	7.45-7.42 m (1H) 7.36-7.33 m (1H) 7.29-7.24 m (3H) 7.20-7.15 m (1H) 6.83-6.79 m (2H) 6.20 m (br, 1H, Ind-H2) 3.96 t (2H, OCH_2)	156.8, 145.5, 144.6, 144.2, 143.1 (C_q) 128.0, 126.2, 126.0, 124.5, 123.8, 119.0, 114.0 (CH) 67.7 (OCH_2) 37.7 (CH_2-Ind) 34.0 (C_q)	320 [M^+] (6) 171 (100) 129 (78) 115 (22)

No.	^{1}H-NMR	^{13}C-NMR	MS [m/z (%)]
	3.30 br (2H, Ind-H1) 2.63-2.57 m (2H, CH_2) 1.88-1.83 m (4H, CH_2) 1.27 s (9H, CH_3)	31.5 (CH_3) 29.2, 27.4, 24.5 (each CH_2)	
9	7.46-7.43 m (1H) 7.37-7.34 m (1H) 7.30-7.26 m (3H) 7.21-7.16 m (1H) 6.84-6.81 m (2H) 6.19 m (br, 1H, Ind-H2) 3.94 t (2H, OCH_2) 3.31 br (2H, Ind-H1) 2.60-2.54 m (2H, CH_2) 1.86-1.71 m (4H, CH_2) 1.61-1.52 m (2H, CH_2) 1.29 s (9H, CH_3)	156.8, 145.5, 144.5, 144.4, 143.1 (C_q) 127.8, 126.1, 125.9, 124.4, 123.7, 118.9, 113.9 (CH) 67.8 (OCH_2) 37.7 (CH_2-Ind) 34.0 (C_q) 31.5 (CH_3) 29.2, 27.8, 27.7, 26.1 (each CH_2)	334 [M^+] (3) 204 (6) 185 (100) 135 (74) 117 (65) 115 (23)
10	7.65-7.62 m (2H) 7.50-7.43 m (3H) 7.41-7.30 m (5H) 7.26-7.22 m (1H) 7.09-7.05 m (1H) 7.02-6.99 m (1H) 6.20 m (br, 1H, Ind-H2) 4.08 t (2H, OCH_2) 3.34 br (2H, Ind-H1) 2.72-2.66 m (2H, CH_2) 2.16-2.08 m (2H, CH_2)	155.9, 145.2, 144.4, 143.6, 138.6, 131.0 (C_q) 129.9, 129.6, 128.5, 128.2, 127.8, 126.7, 126.0, 124.5, 123.7, 120.8, 118.9, 112.4 (CH) 67.7 (OCH_2) 37.7 (CH_2-Ind) 27.8, 24.2 (each CH_2)	326 [M^+] (6) 196 (100) 141 (53) 128 (96) 115 (76)
11	7.52-7.48 m (2H) 7.35-7.10 m (9H) 6.97-6-92 m (1H) 6.90-6.87 m (1H) 6.00 m (br, 1H, Ind-H2) 3.95 t (2H,OCH_2)	155.9, 149.9, 144.2, 141.8, 138.7, 131.0 (C_q) 135.5, 130.9, 129.6, 128.6, 127.9, 126.8, 126.2, 124.8, 122.6, 120.8, 119.0, 112.5 (CH) 67.7 (OCH_2)	340 [M^+] (6) 196 (35) 171 (100) 129 (95) 115 (32

No.	^{1}H-NMR	^{13}C-NMR	MS [m/z (%)]
	3.35-3.28 m (1H, Ind-H1) 2.56-2.49 m (2H, CH_2) 2.03-1.94 m (2H, CH_2) 1.18 d (3H, CH_3)	43.6 (CH-Ind) 27.8, 24.1 (CH_2) 16.3 (CH_3)	
12	7.57-7.54 m (2H) 7.46-7.43 m (1H) 7.39-7.26 m (7H) 7.21-7.17 m (1H) 7.03-6.99 m (1H) 6.97-6.94 m (1H) 6.14 m (br, 1H, Ind-H2) 3.99 t (2H, CH_2) 3.30 br (2H,Ind-CH_2) 2.57-2.51 m (2H, CH_2) 1.84-1.78 m (4H, CH_2)	155.9, 145.4, 144.4, 144.1, 138.6, 130.9 (C_q) 130.8, 129.5, 128.5, 127.8, 126.7, 125.9, 124.4, 123.6, 120.8, 118.9, 112.4 (CH) 68.1 (OCH_2) 37.6 (CH_2-Ind) 29.1, 27.3, 24.5 (each CH_2)	340 [M^+] (3) 171 (100) 129 (84) 115 (44)
13	7.60-7.49 m (2H) 7.47-7.14 m (9H) 7.05-6.88 m (2H) 6.14 m (br, 1H, Ind-H2) 3.93 t (2H, OCH_2) 3.29 br (2H,Ind-CH_2) 2.57-2.45 m (2H, CH_2) 1.80-1.61 m (4H, CH_2) 1.56-1.42 m (2H, CH_2)	155.9, 145.4, 144.4, 144.3, 138.6, 130.9 (C_q) 130.8, 129.5, 128.4, 127.7, 127.6, 126.6, 125.9, 124.4, 123.6, 120.7, 118.8, 112.4 (CH) 68.2 (OCH_2) 37.6 (CH_2-Ind) 29.0, 27.6, 27.5, 26.0 (each CH_2)	354 [M^+] (1) 224 (8) 185 (100) 128 (76) 117 (54) 115 (42)
14	8.46-8.40 m (1H) 7.92-7.84 m (1H) 7.60-7.54 m (3H) 7.52-7.49 m (2H) 7.46-7.37 m (2H) 7.34-7.28 m (1H) 6.88-6.83 m (1H) 6.34 m (br, 1H, Ind-H2) 4.26 t (2H, OCH_2)	154.7, 145.3, 144.5, 143.6, 134.5, 125.7 (C_q) 128.3, 127.4, 126.3, 126.0, 125.9, 125.1, 124.6, 123.8, 122.0, 120.0, 118.9, 104.5 (CH) 67.4 (OCH_2) 37.7 (CH_2-Ind) 27.7, 24,4 (each CH_2)	300 [M^+] (88) 170 (100) 129 (88) 115 (78)

No.	^{1}H-NMR	^{13}C-NMR	MS [m/z (%)]
	3.41 br (2H,Ind-CH$_2$) 2.98-2.90 m (2H, CH$_2$) 2.43-2.35 m (2H, CH$_2$)		

[a] δ (ppm) rel. CHCl$_3$ (7.24 ppm, ^{1}H-NMR) and rel. CDCl$_3$ (77.0 ppm, ^{13}C-NMR) at 298 K

2.1.3 Synthesis and characterization of the transition metal complexes

2.1.3.1 Synthesis of symmetric complexes

Two equivalents of substituted indenes were deprotonated by the addition of two equivalents of n-butyllithium (n-BuLi) followed by the addition of one equivalent of zirconium tetrachloride or hafnium tetrachloride to yield the desired symmetric zirconocene and hafnocene dichloride complexes. The general synthesis of the symmetric zirconocene and hafnocene dichloride complexes is given in Scheme 16.

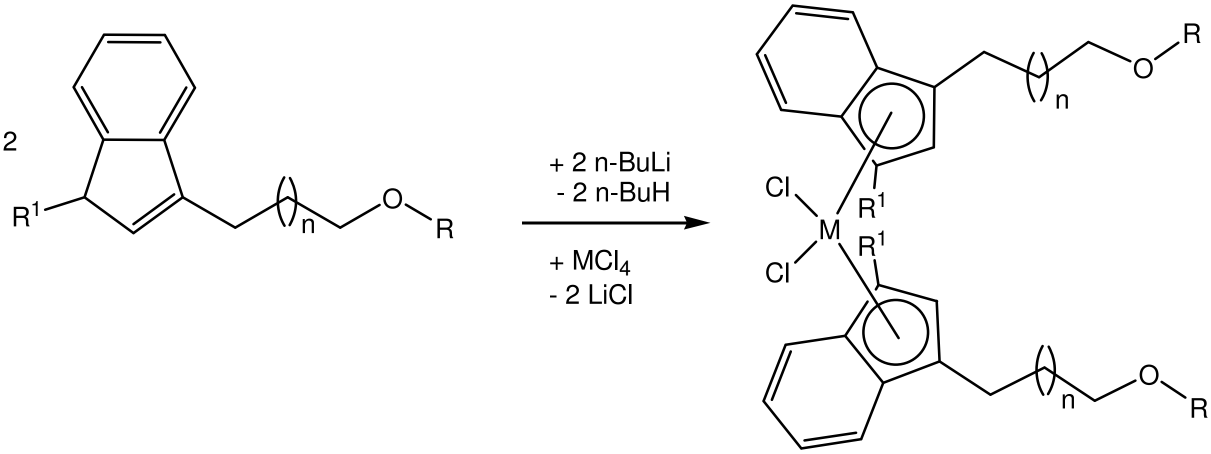

Complex No.	M	n	R^1	R
15	Zr	1	H	phenyl
16	Zr	2	H	phenyl
17	Zr	3	H	phenyl
18	Zr	1	H	2-t-butyl phenyl

Complex No.	M	n	R^1	R
19	Zr	2	H	2-t-butyl phenyl
20	Zr	3	H	2-t-butyl phenyl
21	Zr	1	H	4-t-butyl phenyl
22	Zr	2	H	4-t-butyl phenyl
23	Zr	3	H	4-t-butyl phenyl
24	Zr	1	H	2-phenyl phenyl
25	Hf	1	H	2-phenyl phenyl
26	Zr	1	CH_3	2-phenyl phenyl
27	Zr	2	H	2-phenyl phenyl
28	Zr	3	H	2-phenyl phenyl
29	Zr	1	H	1-naphthyl
30	Hf	1	H	1-naphthyl

Scheme 16: General synthesis equation of the prepared symmetric zirconocene and hafnocene dichloride complexes.

2.1.3.2 Synthesis of asymmetric complexes

For the synthesis of asymmetric complexes, one equivalent of a substituted indene was deprotonated with one equivalent of n-butyllithium followed by the addition of one equivalent of indenyl zirconium trichloride. The general synthesis equation for the asymmetric zirconocene dichloride complexes is given in Scheme 17.

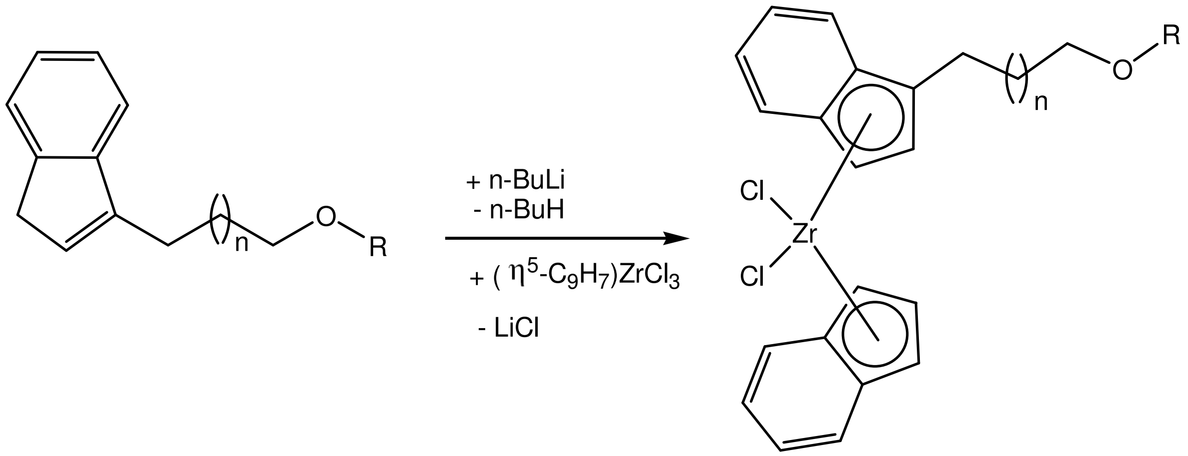

Complex No.	N	R
31	1	4-t-butyl phenyl
32	2	4-t-butyl phenyl
33	3	4-t-butyl phenyl
34	1	2-phenyl phenyl
35	3	2-phenyl phenyl
36	1	1-naphthyl

Scheme 17: General synthesis equation of the prepared asymmetric zirconocene dichloride complexes.

2.1.3.3 Characterization of complexes

Complexes **15**-**36** were characterized by ^{1}H- and ^{13}C-NMR spectroscopy (Table 3) and elemental analysis (see experimental part). As the complexes of the prochiral substituted indenyl ligands can yield a mixture of rac and meso diastereomers[70], the ^{1}H- and ^{13}C-NMR spectra of these complexes show a mixture of rac and meso isomers. The ^{1}H- and ^{13}C-NMR spectra of some selected complexes are discussed as examples.

The ^{1}H-NMR spectrum of complex **16** (Scheme 18) shows signals for both rac and meso isomers. At δ = 7.57-7.54 (m, 2H), 7.52-7.47 (m, 4H), 7.38-7.35 (m, 2H), 7.30-7.04 (m,16H) and 6.86-6.75 (m, 12H) ppm arise the signals for the aromatic CH groups (H7, H6, H5, H4, H15, H14 and H13). At δ = 6.25 (d, J = 3.2 Hz, 2H), 5.97 (d, J = 3.2 Hz, 2H), 5.77 (d, J = 3.2 Hz, 2H) and 5.57 (d, J = 3.2 Hz, 2H) ppm, the signals for the rac and meso indenyl protons H2 and H3 can be found. The multiplet at δ = 3.90-3.80 (m, 8H) ppm can be assigned to the methylene protons H11, while the signal for the H8 protons arises at δ = 3.00-2.60 (2m, 8H) ppm. The signals for the methylene groups (H9 and H10) appear at δ = 1.82-1.56 (m, 16H) ppm.

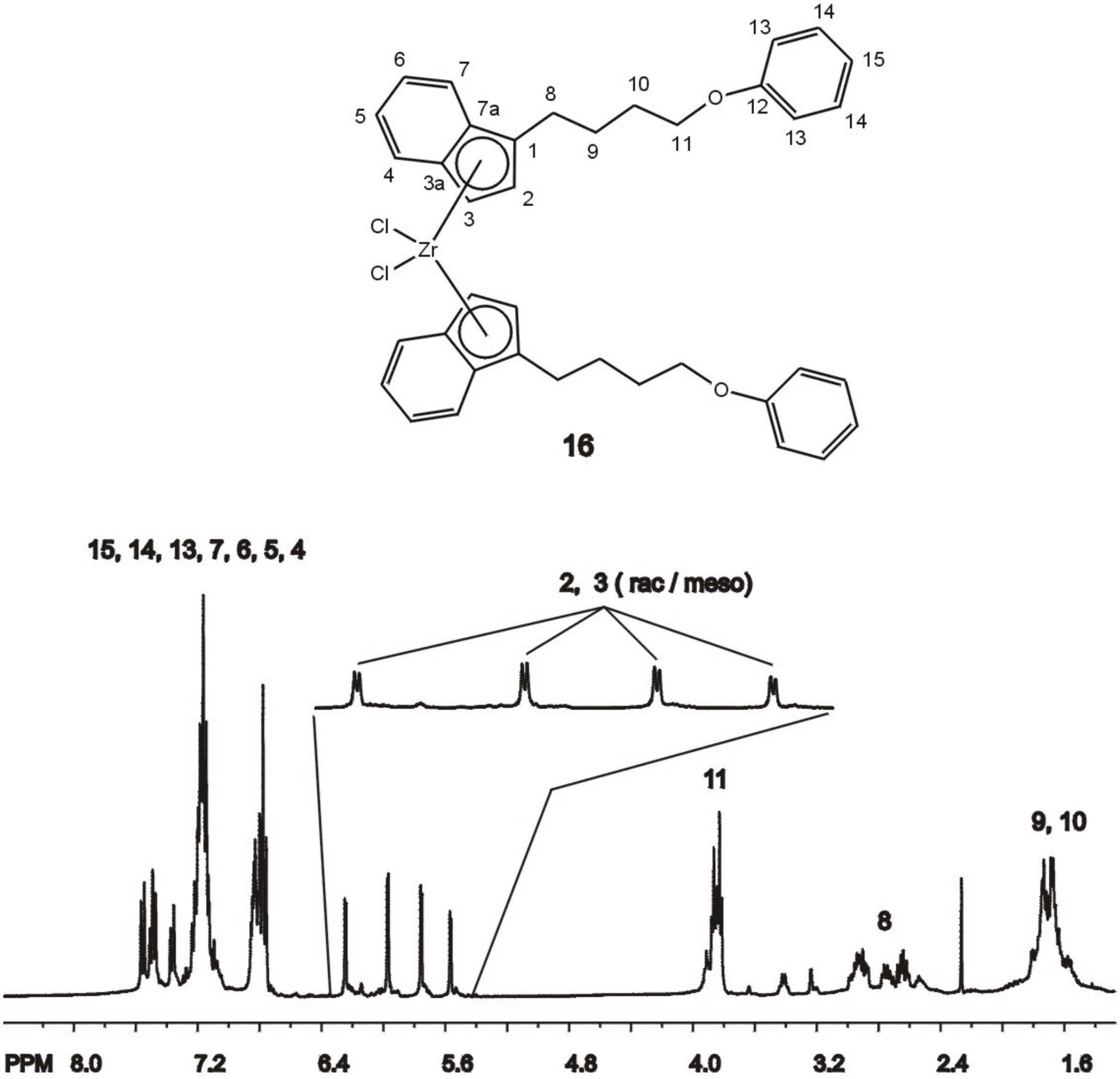

Scheme 18: ^{1}H-NMR spectrum of complex **16**.

In the ^{13}C-NMR spectrum of compound **16** (Scheme 19), two sets of signals appear due to rac and meso isomers. Only one set of signals is discussed here. The signal for the quaternary carbon atom C12 arises at δ = 158.9 ppm, while the signals at δ = 127.3, 125.9 and 123.0 ppm are assigned to the quaternary carbon atoms C7a, C3a and C1. The signals for the CH groups of the phenoxy ring (C15, C14, and C13) can be found at δ = 129.4, 120.5 and 114.4 ppm respectively. The signals for the indenyl CH carbon atoms C7, C6, C5, C4 and C3 arise at δ = 126.3, 125.6, 125.5, 123.8 and 122.0 ppm. The signal for the CH carbon atom C2 appears at δ = 99.1 ppm. The methylene group attached to the oxygen atom (C11) gives the signal at δ = 67.4 ppm. The signals at δ = 29.1, 27.9 and 26.6 ppm are assigned to the alkyl chain methylene groups C8, C9 and C10.

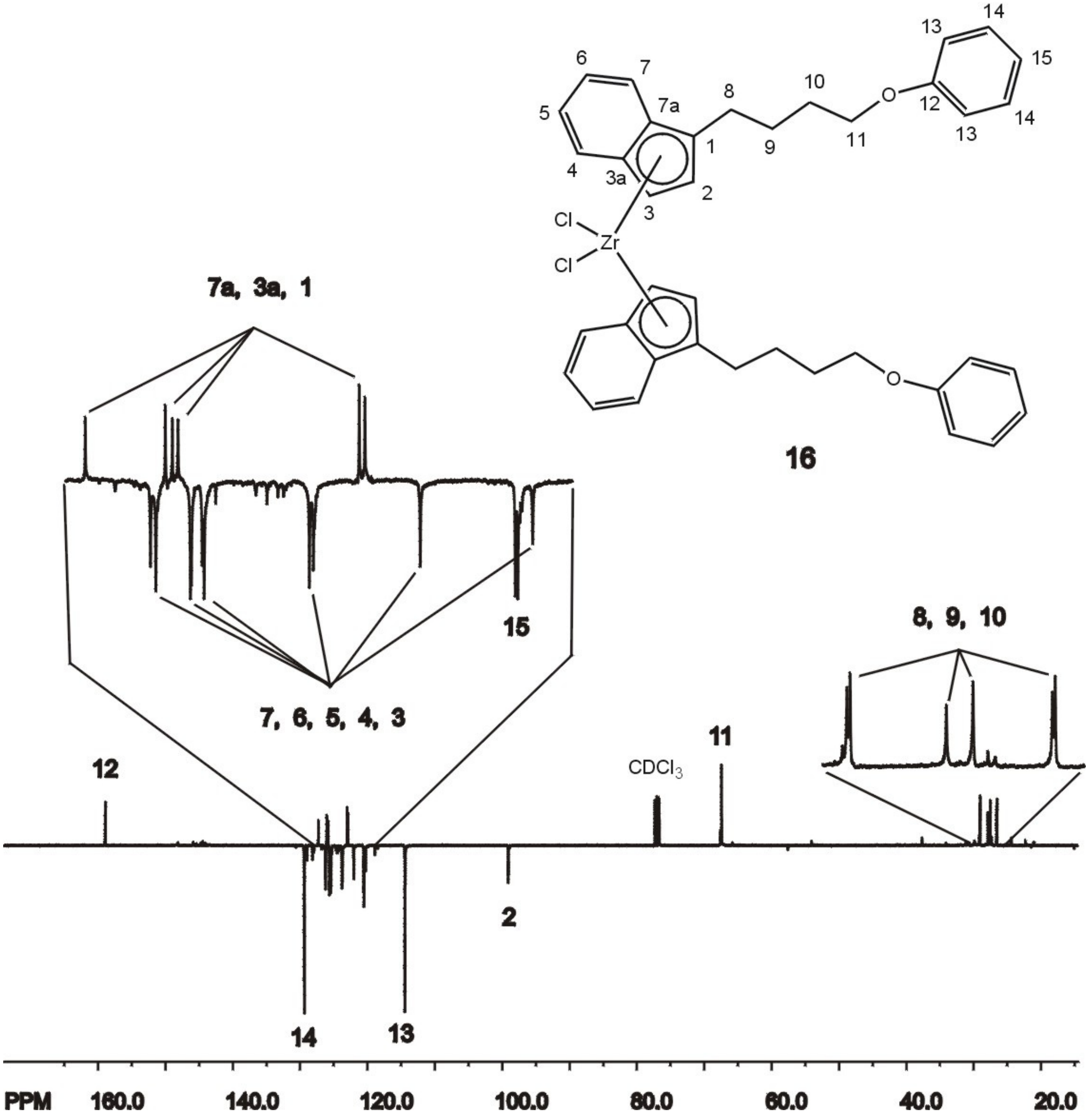

Scheme 19: ^{13}C-NMR spectrum of complex **16**.

The ^{1}H-NMR spectrum of complex **18** (Scheme 20) shows signals at δ = 7.55-7.51 (m, 4H), 7.35-7.30 (m, 6H), 7.20-7.07 (m, 6H), 7.02-6.88 (m, 12H) and 6.62-6.55 (m, 4H) ppm for 32 protons (rac and meso H7, H6, H5, H4, H16, H15, H14 and H13). Four signals appear at δ = 6.14 (d, J = 3.2 Hz, 2H), 5.92 (d, J = 3.2 Hz), 5.50 (d, J = 3.2 Hz) and 5.47 (d, J = 3.2 Hz) ppm for the indenyl protons H2 and H3 (rac and meso). Rac and meso protons of the alkyl chain (H10) appear at δ = 3.60-3.50 (m, 8H) ppm. Two signals at δ = 3.25-3.13 (m, 4H) and 3.05-2.93 (m, 4H) ppm can be assigned to rac and meso H8. The signal at δ = 2.00-1.76 (m, 8H) ppm can be assigned to rac and meso H9. The signals for the tertiary butyl groups (H18) appear at δ = 1.56 (s, 18H) and 1.52 (s, 18H) ppm.

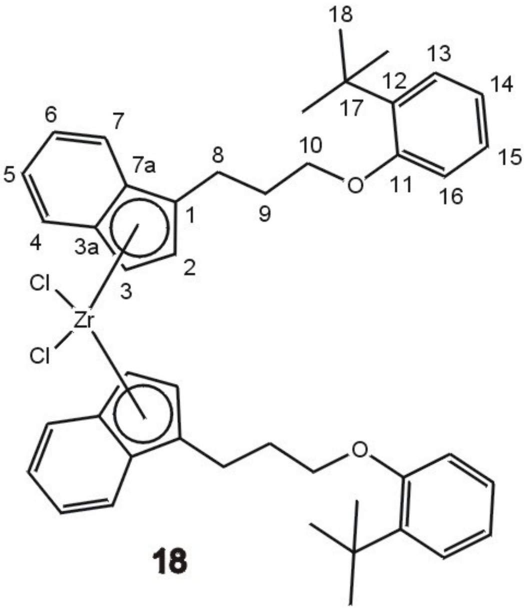

18

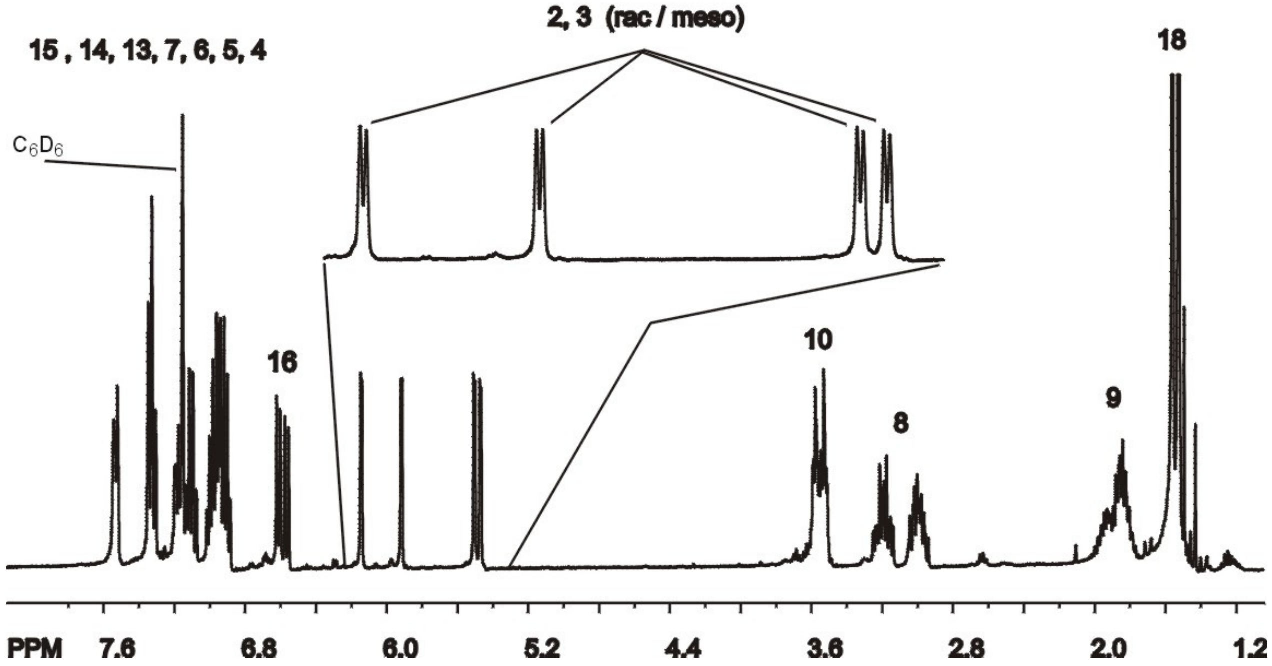

Scheme 20: ^{1}H-NMR spectrum of complex **18**.

The ^{13}C-NMR spectrum of complex **18** (Scheme 21) shows two sets of signals for both rac and meso isomers. Only one set of signals will be described here. The signal for the quaternary carbon atom C11 appears at δ = 158.0 ppm. At δ = 138.0 ppm the signal for the quaternary carbon atom C12 shows up. The signals for the indenyl quaternary carbon atoms C7a, C3a and C1 appear at δ = 127.4, 126.4 and 122.4 ppm. The signals at δ = 127.3, 127.0 and 120.8 ppm can be assigned to the CH carbon atoms C13, C14 and C15. At δ = 112.2 ppm, the signal for the CH group ortho to the phenolic oxygen atom appears. The signals at δ = 126.5, 125.8, 125.7, 124.2 and 122.4 ppm can be assigned to the indenyl carbon atoms C7, C6, C5, C4 and C3, while the signal for C2 appears at δ = 99.2 ppm. The signals at δ = 66.8, 35.1 and 30.3 ppm can be assigned to the methylene group attached to the oxygen atom (C10) and the tertiary-butyl group (C17 and C18), while the signals at δ = 30.1 and 25.5 ppm can be assigned to the alkyl chain carbon atoms C8 and C9.

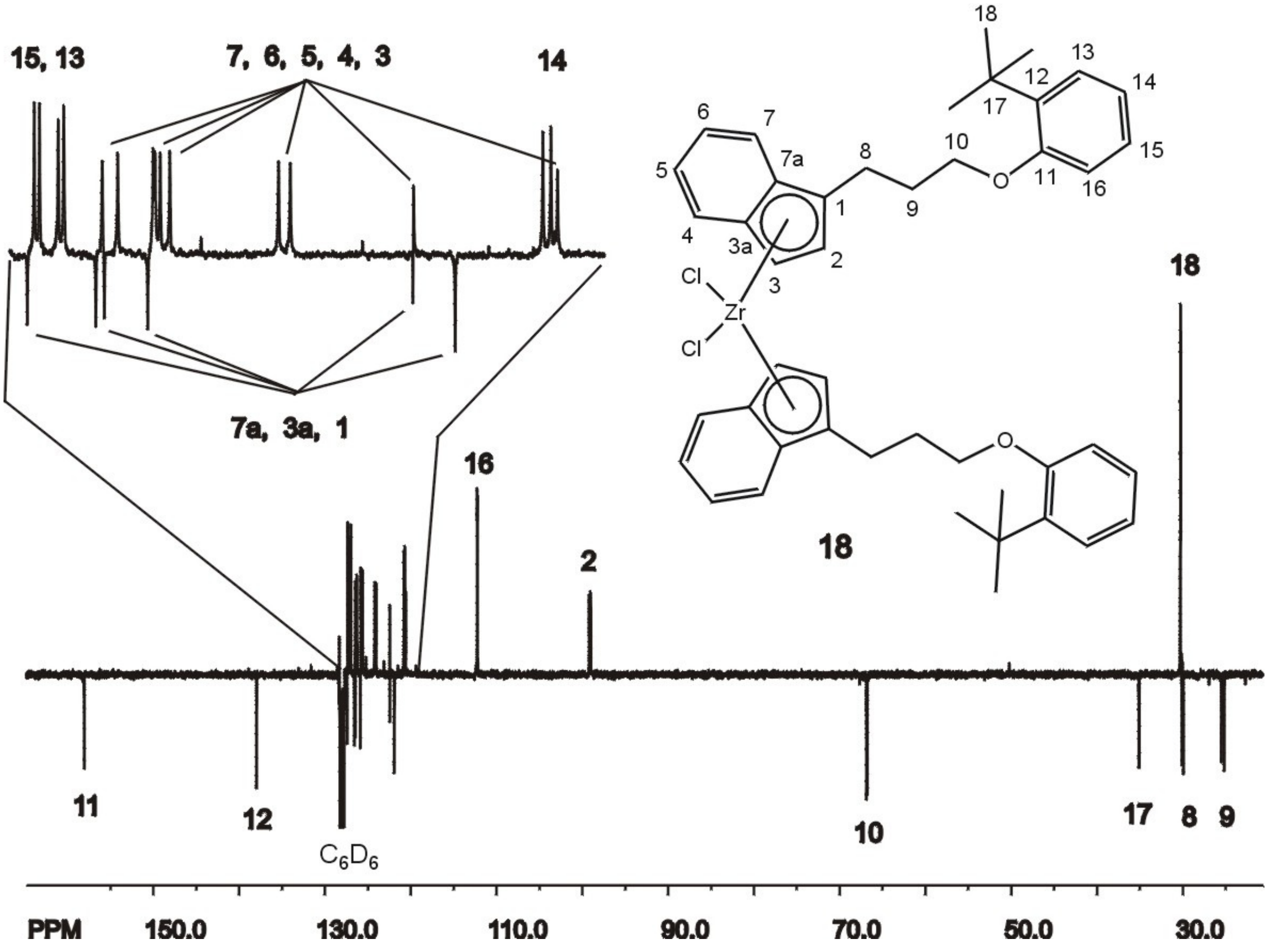

Scheme 21: ^{13}C-NMR spectrum of complex **18**.

The ^{1}H-NMR spectrum of complex **22** (Scheme 22) shows signals at δ = 7.58-7.36 (3m, 8H), 7.25-7.13 (m, 16H) and 6.76-6.70 (m, 8H) ppm for the aromatic CH groups H14, H13, H7, H6, H5 and H4 (rac and meso). Four signals appear at δ = 6.25 (d, J = 3.2 Hz, 2H), 5.98 (d, J = 3.2 Hz, 2H), 5.76 (d, J = 3.2 Hz, 2H) and 5.57 (d, J = 3.2 Hz, 2H) ppm for the indenyl protons H2 and H3 (rac and meso). The signal for the alkoxy protons (H11) appears at δ = 3.88-3.81 (m, 8H) ppm. The signal at δ = 3.00-2.60 (3m, 8H) ppm can be assigned to H8, the signal at δ = 1.80-1.55 (m, 16H) ppm to the methylene groups of the butyl chain (H9 and H10). The signal for the methyl protons of the tertiary butyl group appears at δ = 1.21 (br, 36H) ppm.

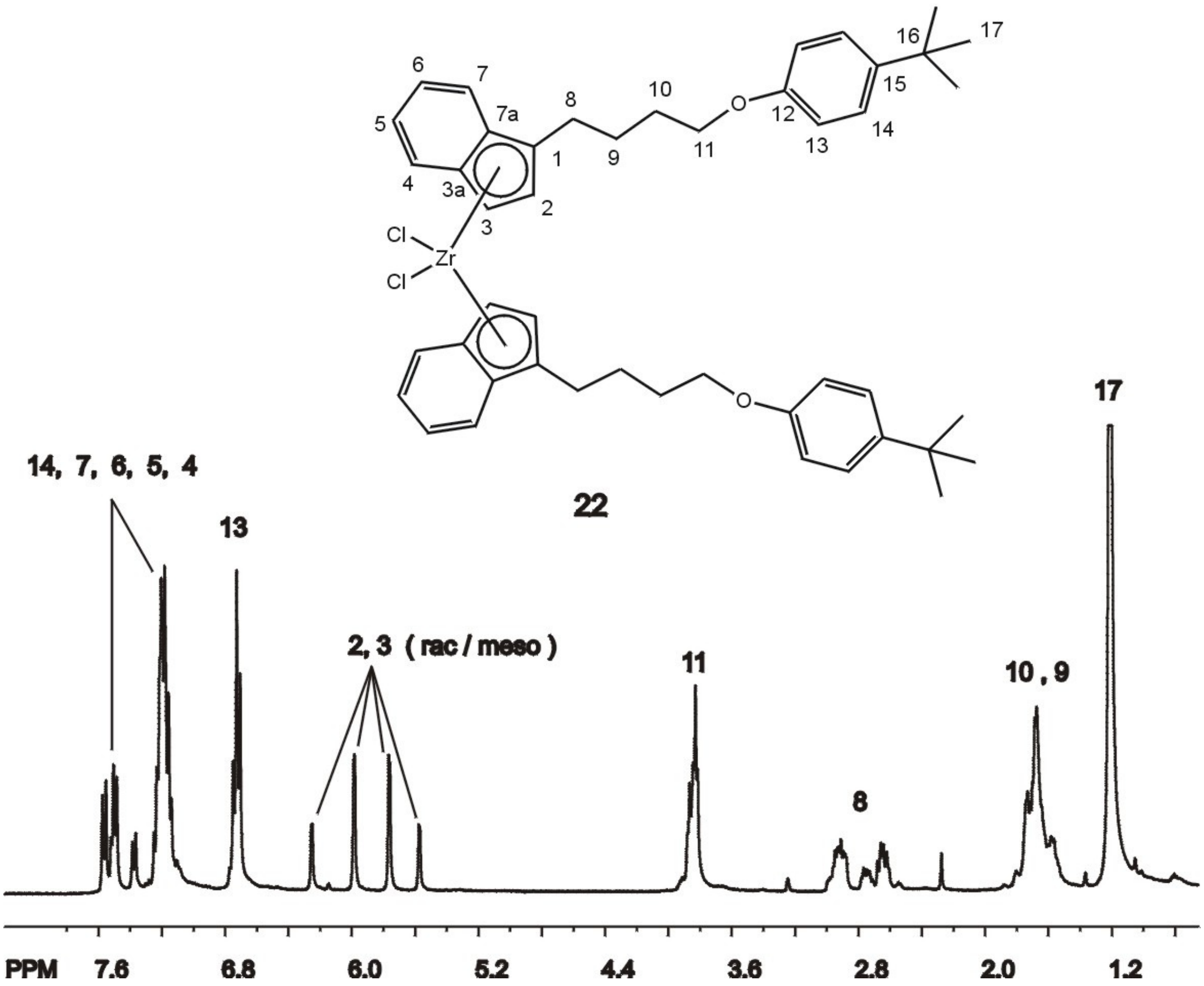

Scheme 22: ^{1}H-NMR spectrum of complex **22**.

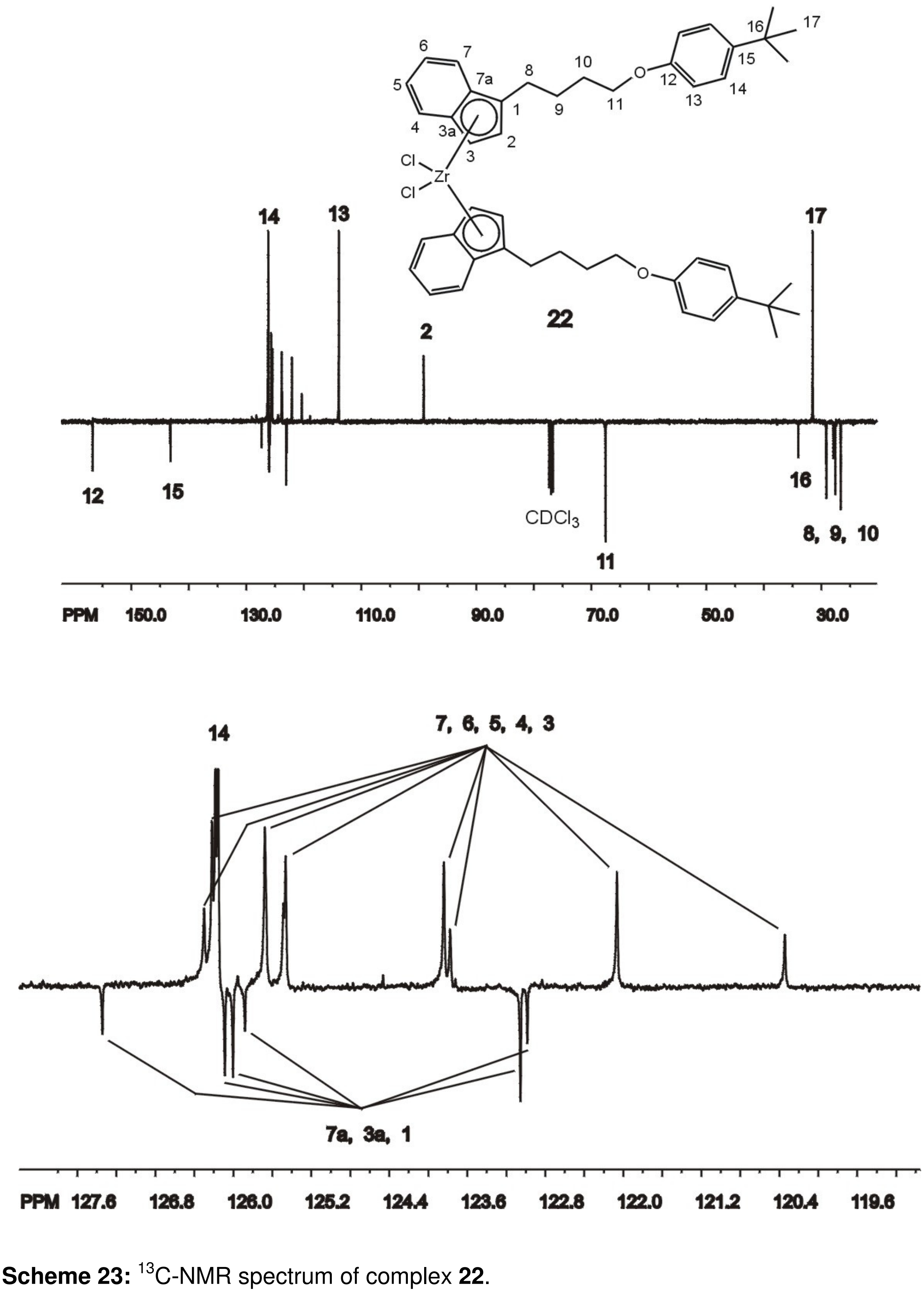

Scheme 23: ^{13}C-NMR spectrum of complex **22**.

The ^{13}C-NMR spectrum of complex **22** (Scheme 23) shows a signal for the quaternary carbon atom C12 at δ = 156.7 ppm. At δ = 143.2 ppm, the signal for the quaternary carbon atom C15 can be found. The signals at δ = 127.3, 125.9 and 123.0 ppm can be assigned to the indenyl quaternary carbon atoms C7a, C3a and C1 while the signals for the aromatic CH groups C14 and C13 appear at δ = 126.1 and 113.9 ppm. The signals at δ = 126.2, 125.7, 125.5, 123.8 and 122.1 ppm can be assigned to the indenyl CH carbon atoms C7, C6, C5, C4 and C3. The signal for the indenyl carbon atom C2 appears at δ = 99.2 ppm. The methylene carbon atom C11 shows a signal at δ = 67.5 ppm, while the signals for the tertiary carbon atom C16 and the methyl carbon atoms C17 of the tertiary butyl group appear at δ = 34.0 and 31.5 ppm respectively. The signals at δ = 29.2, 27.9 and 26.6 ppm can be assigned to the methylene groups C8, C10 and C9.

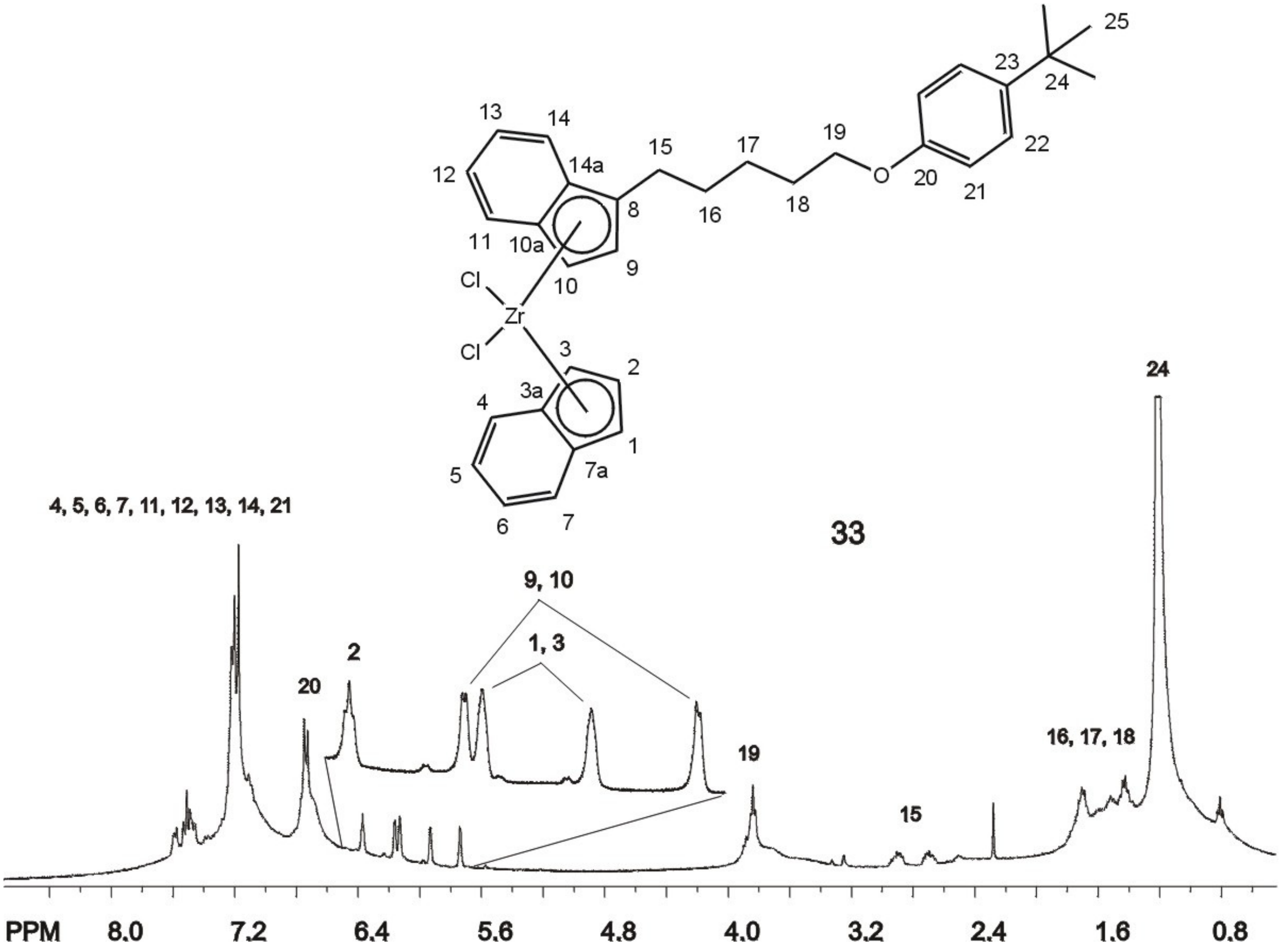

Scheme 24: ^{1}H-NMR spectrum of complex **33**.

The ^{1}H-NMR spectrum of complex **33** (Scheme 24) shows signals at δ = 7.67-7.53 (m, 2H) and 7.35-7.16 (m, 8H) ppm for the aromatic CH protons H22, H14, H13, H11, H10, H7, H6, H5 and H4, while the signal at δ = 6.83-6.77 (m, 2H) ppm can be assigned to CH protons H21. The signal of the indenyl proton H2 arises at δ = 6.43 (dd, J = 3.2 Hz, 1H), while the signals at δ = 6.20 (br, m, 1H) and 6.00 (br, m, 1H) ppm can be assigned to the indenyl protons H1 and H3. The signals at δ = 6.23 (d, J = 2.8 Hz, 1H) and 5.64 (d, J = 2.8 Hz, 1H) ppm belong to the indenyl protons H9 and H10 of the five membered substituted ring. The signal for the alkoxy protons H19 appears at δ = 3.91 (t, 2H) ppm. The signals at δ = 3.01-2.94 (m, 1H) and 2.80-2.73 (m, 1H) ppm can be assigned to the CH_2 protons H15 while the signals for the methylene protons H16, H17 and H18 appear as a multiplet at δ = 1.83-1.37 (m, 6H) ppm. The signal for the methyl protons of the tertiary butyl group appears at δ = 1.29 (s, 9H) ppm.

Table 3: ^{1}H- and ^{13}C-NMR data of complexes 15-36.

Complex No.	^{1}H-NMR [δ (ppm)]	^{13}C-NMR [δ (ppm)]
15$^{a)}$	7.63-7.60 m (2H) 7.58-7.53 m (4H) 7.43-7.40 m (2H) 7.30-7.16 m (16H) 6.94-6.81 m (12H) 6.29 d (J = 3.2 Hz, 2H, Ind-H) 6.04 d (J = 3.2 Hz, 2H, Ind-H) 5.81 d (J = 3.2 Hz, 2H, Ind-H) 5.66 d (J = 3.2 Hz, 2H, Ind-H) 3.97-3.83 m (8H) 3.20-3.07 m (4H) 2.98-2.81 m (4H) 2.19-1.92 m (8H)	158.8, 127.3, 126.2, 122.2 (C_q) 129.4, 126.4, 125.6, 124.6, 123.8, 122.2, 120.6, 114.5 (CH) 99.3 (Ind-CH) 66.7 29.4, 24.2 (CH_2)
16$^{a)}$	7.57-7.54 m (2H) 7.52-7.47 m (4H) 7.38-7.35 m (2H) 7.24-7.09 m (16H) 6.86-6.75 m (12H)	158.9, 127.3, 125.9, 123.0 (C_q) 129.4, 126.3, 125.6, 125.5, 123.8, 122.0, 120.5, 114.4 (CH) 99.1 (Ind-CH) 67.4 (OCH_2)

Complex No.	^{1}H-NMR [δ (ppm)]	^{13}C-NMR [δ (ppm)]
	6.25 d (J = 3.2 Hz, 2H, Ind-H) 5.97 d (J = 3.2 Hz, 2H, Ind-H) 5.77 d (J = 3.2 Hz, 2H, Ind-H) 5.57 d (J = 3.2 Hz, 2H, Ind-H) 3.90-3.80 m (8H) 3.00-2.60 m (8H) 1.82-1.56 m (16H)	29.1, 27.9, 26.6 (CH_2)
17[a)]	7.58-7.55 m (2H) 7.52-7.47 m (4H) 7.39-7.35 m (2H) 7.26-7.12 m (16H) 6.87-6.77 m (12H) 6.23 d (J = 3.2 Hz, 2H, Ind-H) 5.97 d (J = 3.2 Hz, 2H, Ind-H) 5.74 d (J = 3.2 Hz, 2H, Ind-H) 5.57 d (J = 3.2 Hz, 2H, Ind-H) 3.87-3.81 m (8H) 2.95-2.82 m (4H) 2.74-2.56 m (4H) 1.79-1.37 m (24H)	159.0, 127.3, 125.9, 123.2 (C_q) 129.4, 126.2, 125.7, 125.4, 123.8, 122.1, 120.5, 114.5 (CH) 99.2 (Ind-CH) 67.6 (OCH_2) 29.8, 29.0, 28.1, 26.0 (each CH_2)
18[b)]	7.55-7.51 m (4H) 7.35-7.30 m (6H) 7.20-7.07 m (6H) 7.02-6.88 m (12H) 6.62-6.55 (m, 4H) 6.14 d (J = 3.2 Hz, 2H, Ind-H) 5.92 d (J = 3.2 Hz, 2H, Ind-H) 5.50 d (J = 3.2 Hz, 2H, Ind-H) 5.47 d (J = 3.2 Hz, 2H, Ind-H) 3.60-3.50 m (8H, CH_2) 3.25-3.13 m (4H, CH_2) 3.05-2.93 m (4H, CH_2) 2.00-1.76 m (8H, CH_2)	158.0, 138.0, 127.4, 126.4, 122.4 (C_q) 127.3, 127.0, 126.5, 125.8, 125.7, 124.2, 122.1, 120.8, 112.2 (CH) 99.2 (Ind-CH) 66.8 (OCH_2) 35.1 (C_q) 30.3 (CH_3) 30.1, 25.5 (each CH_2)

Complex No.	**^{1}H-NMR [δ (ppm)]**	**^{13}C-NMR [δ (ppm)]**
	1.56 s (18H) 1.52 s (18H)	
19[a)]	7.60-7-56 m (2H) 7.53-7.47 m (4H) 7.39-7.35 m (2H) 7.24-7.02 m (16H) 6.81-6.69 m (8H) 6.26 d (J = 3.2 Hz, 2H, Ind-H) 5.98 d (J = 3.2 Hz, 2H, Ind-H) 5.76 d (J = 3.2 Hz, 2H, Ind-H) 5.56 d (J = 3.2 Hz, 2H, Ind-H) 3.93-3.82 m (8H, CH_2) 3.02-2.89 m (4H, CH_2) 2.81-2.61 m (4H, CH_2) 1.86-1.68 m (16H, CH_2) 1.28 s (18H) 1.26 s (18H)	157.7, 137.8, 127.3, 125.8, 123.0 (C_q) 126.9, 126.5, 126.3, 125.6, 125.5, 123.8, 122.2, 120.0, 111.7 (CH) 99.1 (Ind-CH) 67.2 (OCH_2) 34.8 (C_q) 29.8 (CH_3) 29.4, 28.0, 26.9 (each CH_2)
20[a)]	7.66-7.53 m (4H) 7.45-7.10 m (20H) 6.90-6.77 m (8H) 6.31 d (J = 3.2 Hz, 2H, Ind-H) 6.04 d (J = 3.2 Hz, 2H, Ind-H) 5.82 d (J = 3.2 Hz, 2H, Ind-H) 5.04 d (J = 3.2 Hz, 2H, Ind-H) 4.04-3.83 m (8H, CH_2) 3.04-2.87 m (4H, CH_2) 2.81-2.56 m (4H, CH_2) 1.88-1.44 m (24H, CH_2) 1.34 s (18H)	157.7, 137.9, 127.3, 125.9, 123.2 (C_q) 126.9, 126.5, 126.2, 125.7, 125.4, 123.8,122.1, 120.0, 111.7 (CH) 99.1 (Ind-CH) 67.4 (OCH_2) 34.8 (C_q) 29.8 (CH_3) 29.2, 28.1, 27.7, 26.3 (each CH_2)
21[a)]	7.63-7.53 m (6H) 7.44-7.40 m (2H) 7.30-7.18 m (16H) 6.83-6.75 m (8H)	156.6, 143.4, 127.3, 126.0, 122.2 (C_q) 126.4, 126.2, 125.7, 125.6, 123.8, 122.1, 114.0 (CH) 99.4 (Ind-CH)

Complex No.	^{1}H-NMR [δ (ppm)]	^{13}C-NMR [δ (ppm)]
	6.29 d (J = 3.2 Hz, 2H, Ind-H) 6.07 d (J = 3.2 Hz, 2H, Ind-H) 5.82 d (J = 3.2 Hz, 2H, Ind-H) 5.67 d (J = 3.2 Hz, 2H, Ind-H) 3.98-3.82 m (8H, CH_2) 3.19-3.06 m (4H, CH_2) 2.98-2.80 m (4H, CH_2) 2.18-1.90 m (8H, CH_2) 1.30 s (18H) 1.28 s (18H)	66.8 (OCH_2) 34.1 (C_q) 31.5 (CH_3) 29.4, 24.6 (each CH_2)
22[a)]	7.58-7.36 m (8H) 7.25-7.13 m (16H) 6.76-6.70 m (8H) 6.25 (d, J = 3.2 Hz, 2H, Ind-H) 5.98 (d, J = 3.2 Hz, 2H, Ind-H) 5.76 (d, J = 3.2 Hz, 2H, Ind-H) 5.57 (d, J = 3.2 Hz, 2H, Ind-H) 3.88-3.81 (m, 8H) 3.00-2.60 (m, 8H) 1.80-1.55 (m, 16H) 1.21 (s, 36H)	156.7, 143.2, 127.3, 125.9, 123.0 (C_q) 126.2, 126.1, 125.7, 125.5, 123.8, 122.1, 113.9 (CH) 99.2 (Ind-CH) 67.5 (OCH_2) 34.0 (C_q) 31.5 (CH_3) 129.2, 127.9, 126.6 (each CH_2)
23[a)]	7.67-7.57 m (6H) 7.49-7.45 m (2H) 7.34-7.22 m (16H) 6.86-6.79 m (8H) 6.33 d (J = 3.2 Hz, 2H, Ind-H) 6.07 d (J = 3.2 Hz, 2H, Ind-H) 5.85 d (J = 3.2 Hz, 2H, Ind-H) 5.67 d (J = 3.2 Hz, 2H, Ind-H) 3.96-3.88 m (8H, CH_2) 3.06-2.92 m (4H, CH_2) 2.84-2.66 m (4H, CH_2) 1.83-1.46 m (24H, CH_2)	156.7, 143.1, 127.3, 126.0, 123.2 (C_q) 126.2, 126.1, 125.7, 125.4, 123.8, 122.0, 113.9 (CH) 99.2 (Ind-CH) 67.6 (OCH_2) 34.0 (C_q) 31.5 (CH_3) 29.8, 29.1, 28.1, 26.0 (each CH_2)

Complex No.	^{1}H-NMR [δ (ppm)]	^{13}C-NMR [δ (ppm)]
	1.33 s (18H) 1.32 s (18H)	
24[a)]	7.62-7.51 m (8H) 7.45-7.37 m (12H) 7.36-7.11 m (24H) 7.04-6.98 m (4H) 6.91-6.85 m (4H) 6.10 d (J = 3.2 Hz, 2H, Ind-H) 5.95 d (J = 3.2 Hz, 2H, Ind-H) 5.72 d (J = 3.2 Hz, 2H, Ind-H) 5.47 d (J = 3.2 Hz, 2H, Ind-H) 3.97-3.81 m (8H, CH$_2$) 3.10-2.98 m (4H, CH$_2$) 2.80-2.64 m (4H, CH$_2$) 2.10-1.78 m (8H, CH$_2$)	155.6, 138.6, 130.8, 127.0, 126.0, 121.7 (C$_q$) 130.9, 129.6, 128.6, 128.0 126.8, 126.1, 125.6, 125.4, 123.7, 121.8, 120.8, 112.2 (CH) 99.6 (Ind-CH) 67.1 (OCH$_2$) 29.6, 24.6 (CH$_2$)
25[a)]	7.61-7.47 m (12H) 7.44-7.07 m (32H) 7.03-6.97 m (4H) 6.90-6.84 m (4H) 6.04 d (J = 3.2 Hz, 2H, Ind-H) 5.88 d (J = 3.2 Hz, 2H, Ind-H) 5.56 d (J = 3.2 Hz, 2H, Ind-H) 5.30 d (J = 3.2 Hz, 2H, Ind-H) 3.96-3.80 m (8H, CH$_2$) 3.12-3.00 m (4H, CH$_2$) 2.80-2.62 m (4H, CH$_2$) 2.07-1.76 m (8H, CH$_2$)	155.7, 138.6, 130.8, 125.8, 125.0, 118.9 (C$_q$) 130.9, 129.7, 128.6, 128.0, 126.8, 126.1, 125.5, 125.2, 123.7, 121.2, 120.9, 112.2 (CH) 96.6 (Ind-CH) 67.1 (OCH$_2$) 29.9, 24.5 (CH$_2$)
26[b)]	7.71-7.67 m (8H) 7.38-7.29 m (20H) 7.22-7.11 m (8H) 6.97-6.91 m (12H) 6.66-6.62 m (4H) 5.58 s (2H, Ind-H)	156.2, 139.4, 129.0, 116.4, 116.1, 113.2, 113.0 (C$_q$) 131.3, 130.1, 128.9, 128.4, 127.2, 125.5, 125.4, 124.4, 124.3, 121.4, 121.3, 112.5 (CH) 66.9 (OCH$_2$)

Complex No.	^{1}H-NMR [δ (ppm)]	^{13}C-NMR [δ (ppm)]
	5.52 s (2H, Ind-H) 3.53-3.43 m (8H, CH_2) 2.91-2.81 m (4H, CH_2) 2.58-2.46 m (4H, CH_2) 1.72-1.62 m (4H, CH_2) 1.60-1.51 m (4H, CH_2) 2.08 s (CH_3) 2.07 s (CH_3)	31.1, 24.6 (each CH_2) 13.0 (CH_3)
27$^{b)}$	7.33-7.27 m (8H) 7.15-7.10 m (2H) 7.06-6.93 m (14H) 6.91-6.81 m (12H) 6.73-6.59 m (12H) 6.43-6.36 m (4H) 5.76 d (J = 3.2 Hz, 2H, Ind-H) 5.58 d (J = 3.2 Hz, 2H, Ind-H) 5.20 d (J = 3.2 Hz, 2H, Ind-H) 5.07 d (J = 3.2 Hz, 2H, Ind-H) 3.28-3.16 m (8H, CH_2) 2.62-2.50 m (4H, CH_2) 2.46-2.36 m (4H, CH_2) 1.35-1.05 m (16H, CH_2)	156.5, 139.4, 131.5, 127.5, 126.6, 123.3 (C_q) 131.3, 130.1, 128.8, 128.2, 127.0, 126.4, 125.8, 125.5, 124.3, 122.4, 121.2, 112.9 (CH) 99.0 (Ind-CH) 68.0 (OCH_2) 29.3, 28.2, 26.8 (each CH_2)
28$^{b)}$	7.35-7.28 m (8H) 7.20-7.16 m (2H) 7.10-6.83 m (28H) 6.75-6.60 m (10H) 6.47-6.39 m (4H) 5.81 d (J = 3.2 Hz, 2H, Ind-H) 5.61 d (J = 3.2 Hz, 2H, Ind-H) 5.24 d (J = 3.2 Hz, 2H, Ind-H) 5.13 d (J = 3.2 Hz, 2H, Ind-H) 3.33-3.21 m (8H, CH_2) 2.67-2.55 m (4H, CH_2)	156.5, 139.3, 131.5, 127.4, 126.6, 123.4 (C_q) 131.2, 130.0, 128.8, 128.1, 127.0, 126.3, 125.8, 125.5, 124.3, 122.4, 121.2, 112.9 (CH) 99.0 (Ind-CH) 68.2 (OCH_2) 29.8, 29.2, 28.5, 26.2 (each CH_2)

Complex No.	^{1}H-NMR [δ (ppm)]	^{13}C-NMR [δ (ppm)]
	2.50-2.41 m (4H, CH$_2$) 1.23-0.81 m (24H, CH$_2$)	
29a)	8.28-8.18 m (4H) 7.78-7.73 m (4H) 7.59-7.50 m (4H) 7.47-7.09 m (28) 6.69-6.62 m (4H) 6.25 d (J = 3.2 Hz, 2H, Ind-H) 5.99 d (J = 3.2 Hz, 2H, Ind-H) 5.80 d (J = 3.2 Hz, 2H, Ind-H) 5.58 d (J = 3.2 Hz, 2H, Ind-H) 4.12-3.93 m (8H, CH$_2$) 3.28-3.14 m (4H, CH$_2$) 3.08-2.90 m (4H, CH$_2$) 2.29-2.04 m (8H, CH$_2$)	154.5, 134.5, 127.4, 126.2, 125.9, 122.2 (C$_q$) 127.5, 127.4, 126.4, 126.3, 125.9, 125.6, 125.2, 123.8, 122.2, 122.0, 120.2, 104.6 (CH) 99.3 (Ind-CH) 66.9 (OCH$_2$) 29.3, 24.8 (CH$_2$)
30b)	8.52-8.38 m (4H) 7.99-7.91 m (4H) 7.74-7.26 m (32H) 6.91-6.76 m (4H) 6.39 d (J = 3.2 Hz, 2H, Ind-H) 6.13 d (J = 3.2 Hz, 2H, Ind-H) 5.84 d (J = 3.2 Hz, 2H, Ind-H) 5.60d (J = 3.2 Hz, 2H, Ind-H) 4.28-4.11 m (8H, CH$_2$) 3.48-3.12 m (8H, CH$_2$) 2.46-2.00 m (8H, CH$_2$)	155.1, 135.2, 127.5, 126.4, 125.4, 119.6 (C$_q$) 128.3, 126.8, 126.5, 126.2, 125.7, 125.6, 125.4, 124.2, 122.6, 121.6, 120.5, 105.1, (CH) 96.2 (Ind-CH) 66.9 (OCH$_2$) 29.6, 25.0 (each CH$_2$)
31b)	7.50-7.44 m (2H) 7.32-7.19 m (6H) 6.96-6.90 m (2H) 6.86-6.81 m (2H) 6.06 dd (J = 3.3 Hz, 1H) 5.91d (J = 3.1 Hz, 1H) 5.86 br (m, 1H)	157.4, 143.3, 127.4, 126.7, 126.1, 122.2 , 122.1(C$_q$) 126.5, 126.4, 126.3, 126.2, 125.8, 125.7, 125.6, 125.5, 124.2, 124.1, 122.3, 121.5, 114.4 (CH) 104.0 (Ind-CH) 99.1 (Ind-CH)

Complex No.	^{1}H-NMR [δ (ppm)]	^{13}C-NMR [δ (ppm)]
	5.72 br (m, 1H) 5.46 d (J = 3.1 Hz, 1H) 3.61 t (2H) 3.19-3.10 (m, 1H) 3.04-2.94 (m, 1H) 1.92-1.79 (m, 2H) 1.25 s (9H)	66.8 (OCH_2) 34.1 (C_q) 31.7 (CH_3) 29.7, 24.8 (CH_2)
32b)	7.50-7.42 m (2H) 7.36-7.29 m (2H) 7.25-7.20 m (4H) 6.97-6.92 m (2H) 6.89-6.84 m (2H) 6.10 br (m, 1H) 6.05 d (1H) 5.91 dd (1H) 5.74 br (m, 1H) 5.45 d (1H) 3.64 t (2H) 3.02-2.92 m (1H) 2.87-2.77 m (1H) 1.69-1.54 m (4H) 1.25 s (9H)	156.8, 143.4, 127.4, 126.6, 126.3, 123.3, 123.1 (C_q) 126.5, 126.4, 126.1, 126.0, 125.9, 125.8, 125.6, 125.4, 124.0, 123.8, 122.0, 121.8, 113.9 (CH) 104.2 (Ind-CH) 99.3 (Ind-CH) 67.6 (OCH_2) 34.1(C_q) 31.6 (CH_3) 29.2, 127.8, 126.6 (CH_2)
33a)	7.67-7.53 (m, 2H) 7.35-7.16 (m, 8H) 6.83-6.77 (m, 2H) 6.43 dd (J = 3.2 Hz, 1H) 6.23 d (J = 2.8 Hz, 1H) 6.20 (br, m, 1H) 6.00 (br, m, 1H) 5.64 d (J = 2.8 Hz, 1H) 3.91 (t, 2H) 3.01-2.94 (m, 1H) 2.80-2.73 (m, 1H)	156.8, 143.1, 127.3, 126.5, 125.9, 123.4, 123.2 (C_q) 126.4, 126.3, 126.2, 125.7, 125.6, 125.5, 125.4, 124.4, 123.8, 122.0, 121.6, 121.0, 113.9 (CH) 104.0 (Ind-CH) 99.2 (Ind-CH) 67.6 (OCH_2) 34.0 (C_q) 31.5 (CH_3)

Complex No.	^{1}H-NMR [δ (ppm)]	^{13}C-NMR [δ (ppm)]
	1.83-1.37 (m, 6H) 1.29 s (9H)	129.7, 129.1, 127.7, 126.0 (CH_2)
34[b]	7.69-7.65 m (2H) 7.42-7.28 m (5H) 7.20-7.11 m (4H) 6.96-6.90 m (4H) 6.67-6.61 m (2H) 6.04 dd (J = 3.3 Hz, 1H) 6.00 d (J = 3.2 Hz, 1H) 5.87 br (m, 1H) 5.83 d (J = 3.2 Hz, 1H) 5.71 br (m, 1H) 3.48 t (2H) 3.09-3.01 m (1H) 2.84-2.74 m (1H) 1.72-1.56 m (2H)	156.2, 139.3, 131.4, 127.4, 126.7, 126.6, 126.3, 122.0 (C_q) 131.3, 130.1, 128.8, 128.4, 127.1, 127.0, 126.6, 126.5, 126.2, 125.8, 125.6, 125.5, 124.2, 124.1, 122.4, 121.3, 121.2, 112.6 (CH) 104.1 (Ind-CH) 99.5 (Ind-CH) 67.1 (OCH_2) 29.9, 24.8 (CH_2)
35[a]	7.49-7.39 m (4H) 7.31-7.09 m (9H) 6.95-6.81 m (4H) 6.32 dd (J = 3.3 Hz, 1H) 6.09 d (J = 3.2 Hz, 1H) 6.06 br (m, 1H) 5.88 br (m, 1H) 5.70 d (J = 3.2 Hz, 1H) 3.82 t (2H) 2.87-2.74 m (1H) 2.66-2.51 m (1H) 1.69-1.22 m (6H)	155.9, 138.5, 130.9, 127.2, 126.2, 126.0, 125.8, 123.2 (C_q) 130.8, 129.5, 128.5, 127.8, 126.7, 126.4, 126.2, 126.1, 125.9, 125.6, 125.5, 125.4, 125.3, 124.4, 123.8, 122.0, 120.8, 112.5 (CH) 104.0 (Ind-CH) 99.0 (Ind-CH) 68.1 (OCH_2) 28.9, 27.6, 27.5, 25.9 (CH_2)
36[b]	8.57-8.51 m (1H) 7.70-7.65 m (1H) 7.48-7.44 m (1H) 7.40-7.20 m (9H) 6.97-6.86 m (2H)	155.1, 135.2, 127.6, 126.6, 126.4, 126.3, 122.3, 122.2 (C_q) 126.8, 126.7, 126.5, 126.4, 126.3, 126.2 126.1, 125.8, 125.7, 125.6, 125.5, 125.5, 124.2, 122.6, 122.4, 120.6,

Complex No.	^{1}H-NMR [δ (ppm)]	^{13}C-NMR [δ (ppm)]
	6.48-6.41 m (1H) 6.08 dd (J = 3.3 Hz, 1H) 6.00 d (J = 3.1 Hz, 1H) 5.86 br (m, 1H) 5.72 br (m, 1H) 5.47 d (J = 3.1 Hz, 1H) 3.61 t (2H) 3.22-3.15 m (1H) 3.10-2.98 m (1H) 1.98-1.84 m (2H)	120.5, 105.0 (CH) 104.2 (Ind-CH) 98.9 (Ind-CH) 66.9 (OCH_2) 29.4, 24.9 (CH_2)

[a] δ (ppm) rel. $CHCl_3$ (7.24 ppm, ^{1}H-NMR) and rel. $CDCl_3$ (77.0 ppm, ^{13}C-NMR) at 298 K

[b] δ (ppm) rel. benzene (7.16 ppm, ^{1}H-NMR) and rel. C_6D_6 (128.0 ppm, ^{13}C-NMR) at 298 K

2.1.4 Polymerization experiments and polymer analysis

2.1.4.1 General

The olefin polymerization reaction with metallocene catalysts can be explained by the Cossee-Arlman[14-16] mechanism. This mechanism involves the following steps:

a) Activation of the metallocene complex

Methylaluminoxane (MAO) activates the metallocene complex by replacing a chloride ligand with a methyl group and abstracting the remaining chloride ligand to generate a metallocene cation with a vacant coordination site. An olefin molecule can coordinate to this vacant site.

a)

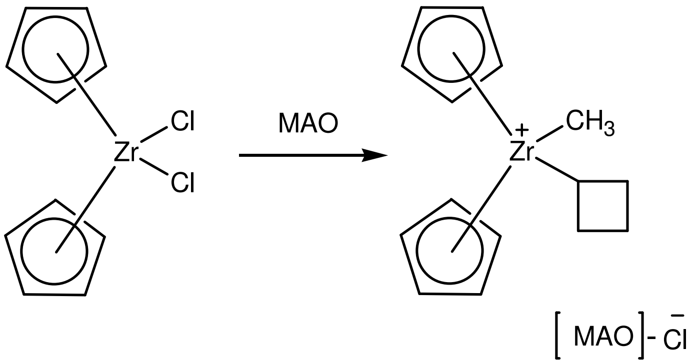

b) Chain propagation step

In the chain propagation step the olefin molecule inserts into the metal-carbon δ-bond generating a new vacant coordination site at the metal center. The next olefin molecule can coordinate to this vacant site to repeat the insertion process.

b)

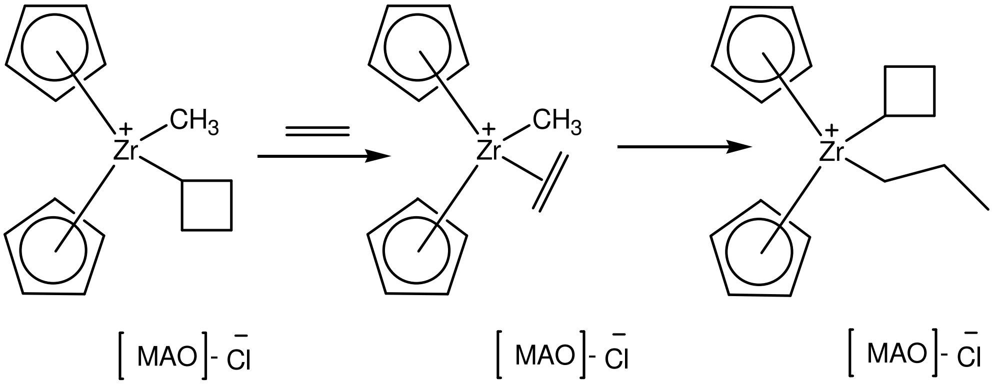

c) Chain termination step

Finally the chain growth is terminated by β-hydrogen elimination.

c)

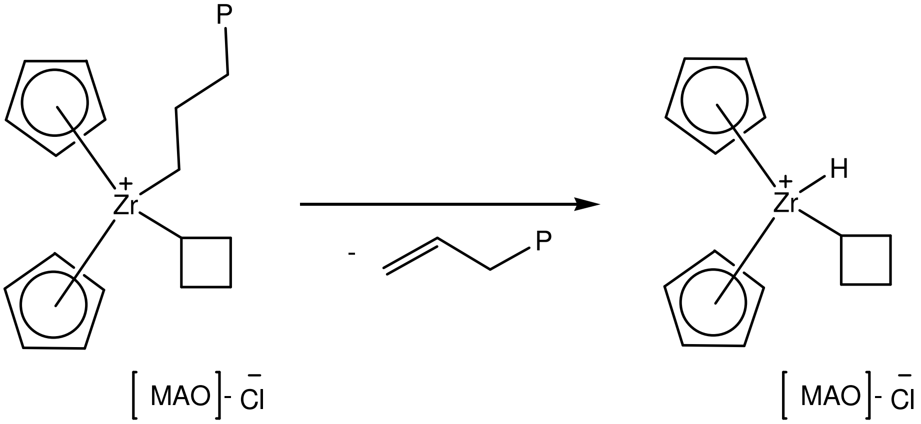

Scheme 25: Cossee-Arlman mechanism: a) activation of the metallocene complex with MAO; b) chain propagation; c) chain termination

2.1.4.1.1 Ethylene polymerization activities of complexes 15-23

Complexes **15**-**23** bear ω-phenoxy alkyl groups on the indenyl rings. They vary by the nature and position of substituents on the phenyl ring of the phenoxy group as well as the chain length between the indenyl and the phenoxy group.

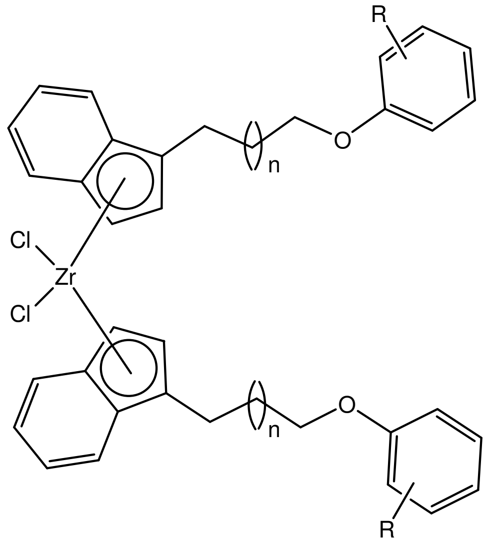

Scheme 26: General structure of complexes **15-23**.

Table 4: Ethylene polymerization activities[a] of complexes 15-23.

Complex No.	n	R	Activity (kg PE/mol cat. h)
15	1	H	3860
16	2	H	9449
17	3	H	3382
18	1	2-t-butyl	16333
19	2	2-t-butyl	27467
20	3	2-t-butyl	7666
21	1	4-t-butyl	6666
22	2	4-t-butyl	16667
23	3	4-t-butyl	9433

[a] Polymerization conditions: M:Al = 1:2000, 250 mL n-pentane, 65 ℃, 10 bar ethylene, 1 h

In the series of complexes **15-23** bearing ω-phenoxy alkyl substituents on the indenyl groups, catalyst **19** showed the maximum activity for ethylene polymerization while catalyst **17** showed the minimum activity. A comparison of catalysts **15**, **18** and **21** with equal separation between indenyl and phenoxy groups showed that the catalysts **18** and **21** bearing tertiary butyl groups on the phenoxy substituent were more active than catalyst **15**. This can be attributed to the fact that the bulky alkyl group protects the cationic metal centre from the approaching oxygen atom of the phenoxy group. Catalyst **18** shows higher activity than catalyst **21** because the tertiary butyl group at the ortho position to the donor oxygen atom of the phenoxy group provides more protection than a tertiary butyl group at the para position. The same trend is obvious for catalysts **16**, **19** and **22** as well as for **17**, **20** and **23**. A comparison of the activities of catalysts **15, 16** and **17** (Scheme 27) differing in chain length between the indenyl and the phenoxy groups showed that catalyst **16** with four methylene bridging units was more active (9449 kg PE/mol cat. h) than catalyst **15** with three methylene bridging units (3860 kg PE/mol cat. h) and catalyst **17** with five methylene bridging units (3382 kg PE/mol cat. h). The same trend could be observed for catalysts **18**-**20** and **21**-**23**.

This can be explained by the fact that the 1-substituted metallocene complexes are able to exist in different conformations[87]. The reason for the higher activity of catalysts **16**, **19** and **21** may be that the conformation obtained with four methylene bridging units prevents bimolecular deactivation of the active species.

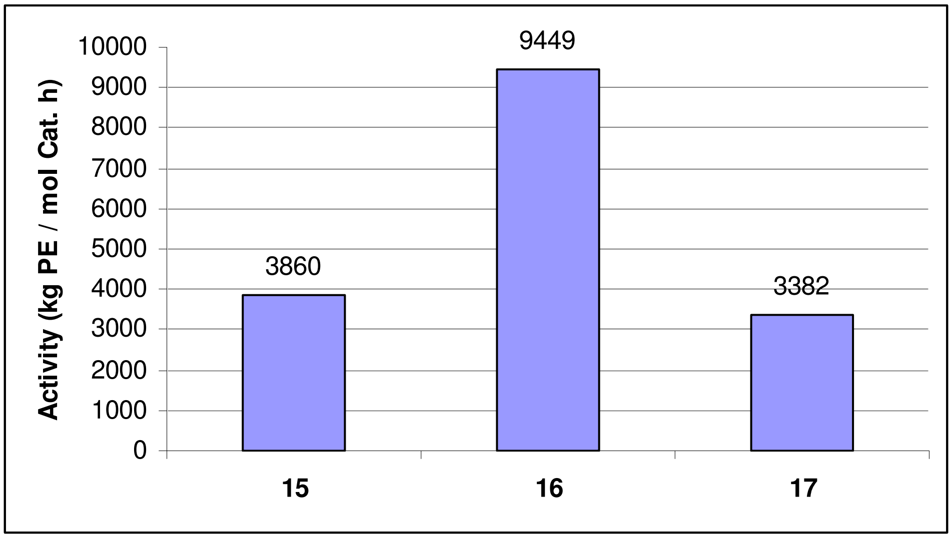

Scheme 27: Ethylene polymerization activities of complexes **15**, **16** and **17**.

The ethylene polymerization activity of catalyst **19** was investigated at different temperatures (Scheme 27). By increasing the polymerization temperature from 55 to 65 ℃ the activity increased. Further increase of the temperature resulted in a sharp decrease of activity. This may be due to decomposition reaction of the active species at higher temperatures.

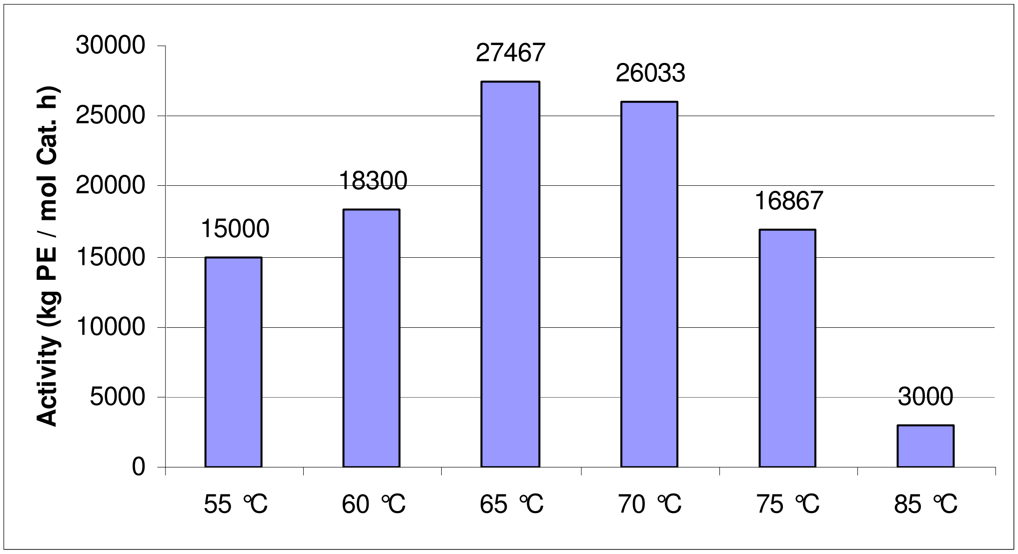

Scheme 28: Ethylene polymerization activities of catalyst **19** at different temperatures.

2.1.4.1.2 Ethylene polymerization activities of complexes 24-30

Catalysts **24**-**28** bearing an ω-(2-phenyl) phenoxy alkyl group on the indenyl rings and catalysts **29** and **30** bearing an ω-naphthoxy alkyl group were also tested for ethylene polymerization.

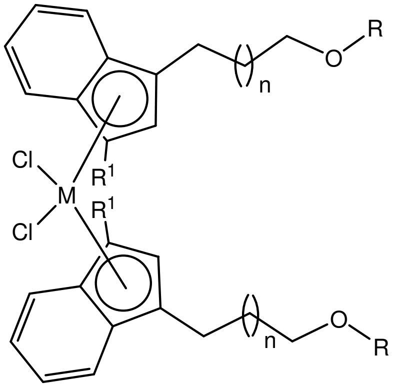

Scheme 29: General structure of complexes **24**-**30**.

Table 5: Ethylene polymerization activities of complexes 24-30.

Complex No.	M	n	R^1	R	Activity[a] (kg PE/mol cat. h)
24	Zr	1	H	2-phenyl phenyl	15500
25	Hf	1	H	2-phenyl phenyl	833
26	Zr	1	CH_3	2-phenyl phenyl	2400

27	Zr	2	H	2-phenyl phenyl	9000
28	Zr	3	H	2-phenyl phenyl	2200
29	Zr	1	H	1-naphthyl	3167
30	Hf	1	H	1-naphthyl	0

[a] Polymerization conditions: M:Al = 1:2000, 250 mL n-pentane, 65 ℃, 10 bar ethylene, 1 h

In the catalyst series **24**, **27** and **28** with three, four and five bridging methylene groups between the phenoxy and the indenyl groups, catalyst **24** showed the highest activity (15500 kg PE/mol cat. h) for ethylene polymerization while catalyst **28** showed the lowest (2200 kg PE/mol cat. h). This trend may be explained by a stronger interaction of the oxygen atom of one catalyst species and a cationic metal centre of the neighbouring catalyst species. Compared to catalyst **24** catalyst **26** bearing a methyl substituent on position 3 of the indenyl group showed very low activity. The reason may be that the methyl group blocks the active centre of the catalyst quite effectively.

The hafnium catalyst **30** was inactive while catalyst **25** showed very low activity compared to the similar zirconium catalyst **24**.

2.1.4.1.3 Ethylene polymerization activities of complexes 31-36

Complexes **31**-**36** are asymmetric bearing a substituted and an unsubstituted indenyl ligand (Scheme 30).

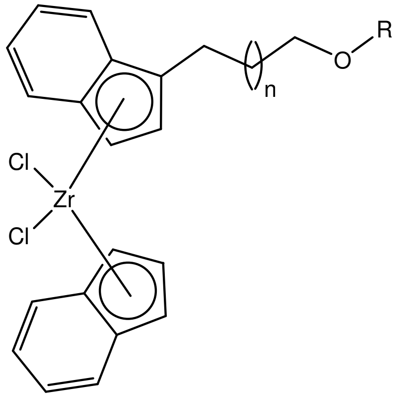

Scheme 30: General structure of complexes **31**-**36**.

Table 6: Ethylene polymerization activities of complexes 31-36.

Complex No.	n	R	Activity[a] (kg PE/mol cat. h)
31	1	4-t-butyl phenyl	7800
32	2	4-t-butyl phenyl	11666
33	3	4-t-butyl phenyl	3600
34	1	2-phenyl phenyl	26233
35	3	2-phenyl phenyl	1400
36	1	1-naphthyl	5333

[a] Polymerization conditions: M:Al = 1:2000, 250 mL n-pentane, 65 ℃, 10 bar ethylene, 1 h

In the asymmetric catalyst series **31**-**33**, catalyst **32** containing four methylene bridging units between the indenyl and the phenoxy groups is the most active one for ethylene polymerization (11666 kg PE/mol cat. h). This trend is similar to the symmetric analogues in the series **21**-**23**.

The asymmetric catalyst **34** with three methylene bridging units between the indenyl and the phenoxy group shows a very high activity as compared to catalyst **35** with five methylene bridging units. This trend is also similar to the symmetric analogues **24** and **28**.

Asymmetric catalysts with three separating CH_2 units **31**, **34** and **36** showed higher activities as compared to their symmetric analogues **21**, **24** and **29** while those with longer alkyl chains showed lower activities than their symmetric analogues.

2.1.4.2 Polymer analysis

Polymers were analyzed by DSC and viscometry analysis.

Table 7: DSC and molecular weight analyses of the polyethylenes produced with complexes 18-36.

Complex No.	ΔH_m [J/g]	T_m [℃]	Crystallinity (α)	M_η [g/mol]
18	121.9	126.3	0.42	230000
19	134.3	127.7	0.46	280000
20	131.2	127.2	0.45	260000
21	135.1	133.2	0.46	310000
22	130.7	126.3	0.45	n.d.

23	112.9	126.0	0.39	270000
24	141.3	134.3	0.49	n.d.
25	103.8	134.5	0.36	n.d.
26	142.3	134.0	0.49	n.d.
27	143.4	133.3	0.49	330000
28	118.1	134.8	0.41	360000
29	148.3	138.3	0.51	n.d.
30	n.d.	n.d.	n.d.	n.d.
31	137.3	135.7	0.47	420000
32	145.8	138.8	0.50	n.d.
33	155.3	137.2	0.54	420000
34	116.7	127.2	0.40	410000
35	150.7	139.0	0.52	n.d.
36	n.d.	n.d.	n.d.	n.d.

DSC and molecular weight analyses showed that polyethylene samples produced with the symmetric catalysts **18**-**23** have low melting points and comparatively low molecular weights. This is in accordance with the results observed by Piccolrovazzi et. al.[51] that electron withdrawing groups on the indenyl moiety result in a decrease of the molecular weight of the produced polymers. The asymmetric catalysts **31**-**35** bearing phenoxy substituent on only one indenyl moiety produced polyethylene samples with relatively higher melting points and molecular weights.

2.2 9-Methylfluorenyl substituted bis (indenyl) zirconium dichloride complexes

2.2.1 General

The nature and size of substituents on metallocene complexes greatly affects the activity of a catalyst as well as the quality of the polyolefin resin produced. When an indenyl moiety of the non bridged bis (indenyl) zirconium dichloride complex is substituted with bulky groups the free rotation of the indenyl moiety is hindered resulting in a mixture of rac and meso isomers. Such chiral non bridged bis (indenyl) zirconium dichloride/MAO systems have been investigated by several research groups for the production of elastomeric polypropylene with specific tacticity[75-89]. Kravchenko et. al. investigated this system for ethylene-propylene copolymerization[90] and Schmidt et. al. for ethylene polymerization[89]. Coville et. al. reported a systematic investigation of effects of H, Me, Et, $SiMe_3$, Ph, benzyl and 1-naphthyl substitutions on the ethylene polymerization behaviour of bis (indenyl) zirconium dichloride/MAO system[91]. Herein zirconium complexes with bulky 9-methylfluorenyl substituted indenyl ligand are reported for ethylene polymerization after activation with MAO.

2.2.1.1 Synthesis and characterization of 9-methylfluorenyl substituted indenyl compounds

9-Methylfluorenyl substituted indenyl compounds were prepared by deprotonating 9-methyl fluorene with n-butyllithium and subsequent reaction with one equivalent of ω-bromo-1-indenylalkanes (Scheme 31).

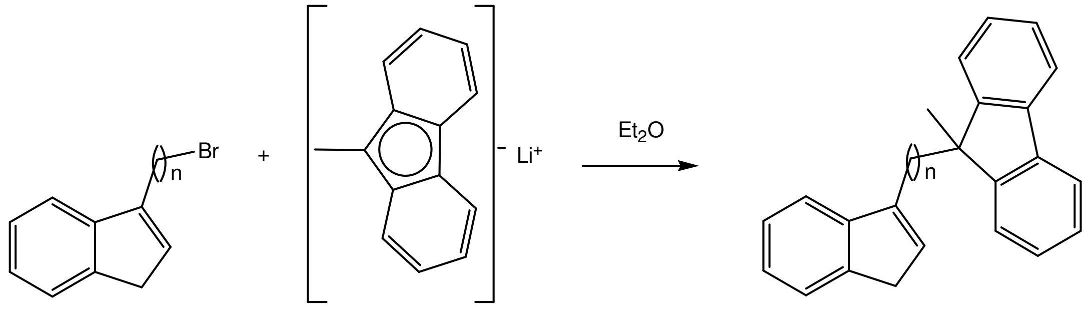

No.	37	38	39
n	2	3	4

Scheme 31: Synthesis of compounds **37-39**.

Compounds **37**-**39** were characterized by ^{1}H- and ^{13}C-NMR spectroscopy and GC/MS. The mass and NMR spectra of compounds **37**-**39** are given in Table 8. Mass and NMR spectra of compound **38** are discussed as an example.

The ^{1}H-NMR spectrum of compound **38** (Scheme 32) shows signals at δ = 7.71-7.68 (m, 2H), 7.38-7.25 (m, 7H), 7.20-7.10 (m, 2H) and 7.07-7.04 (m, 1H) ppm for the aromatic protons H15, H14, H13, H12, H7, H6, H5 and H4. The signal for the indenyl proton H2 appears at δ = 5.92 (br, 1H) ppm. At δ = 3.19 (br, 2H) ppm, the signal of the indenyl methylene group can be observed. The signal at δ = 2.31-2.25 (m, 2H) ppm can be assigned to the CH_2 protons H10, the signal at δ = 2.11-2.07 (m, 2H) ppm to the CH_2 protons H8. The fluorenyl methyl group gives the signal at δ = 1.46 (s, 3H) ppm, while the signal at δ = 1.11-1.03 (m, 2H) ppm is assigned to the residual CH_2 group (H9).

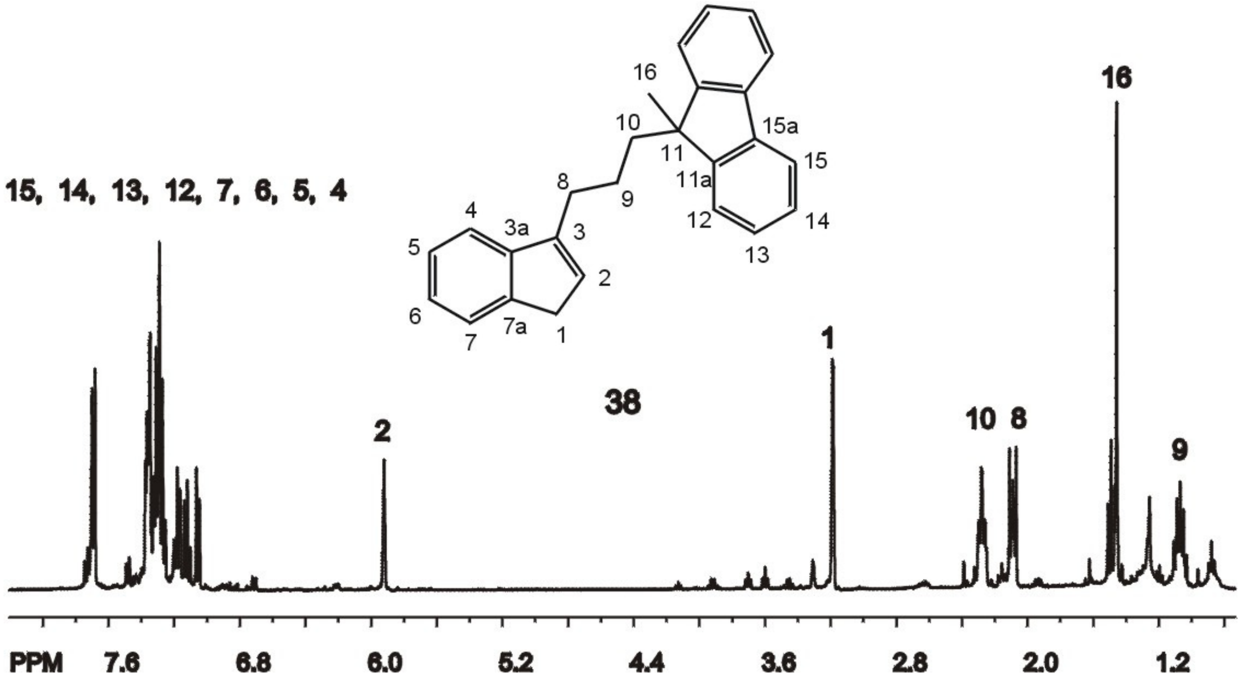

Scheme 32: ^{1}H-NMR spectrum of compound **38**.

The ^{13}C-NMR spectrum of compound **38** (Scheme 33) shows the signals for the quaternary carbon atoms C11a and C15a at δ = 151.8 and 140.1 ppm, while the signals for the quaternary carbon atoms C7a, C3a and C3 arise at δ = 145.4, 144.3 and 144.0 ppm. The signals for the aromatic CH groups C15, C14, C13 and C12 of the fluorenyl ring appear at δ = 127.1, 126.9, 122.7 and 119.9 ppm while the signals for the indenyl CH groups C7, C6, C5, C4 and C2 appear at δ = 127.5, 125.8, 124.3, 123.5, and 118.8 ppm. The signal at δ = 50.7 ppm is assigned to the quaternary carbon atom C11 of the fluorenyl ring, while the signals at δ = 40.4, 37.5 and 27.9 ppm can be assigned to the indenyl methylene group C1 and the alkyl chain methylene groups C10 and C8. The signal at δ = 26.8 ppm belongs to the methyl group C16, while the signal at δ = 22.6 ppm results from the methylene group C9.

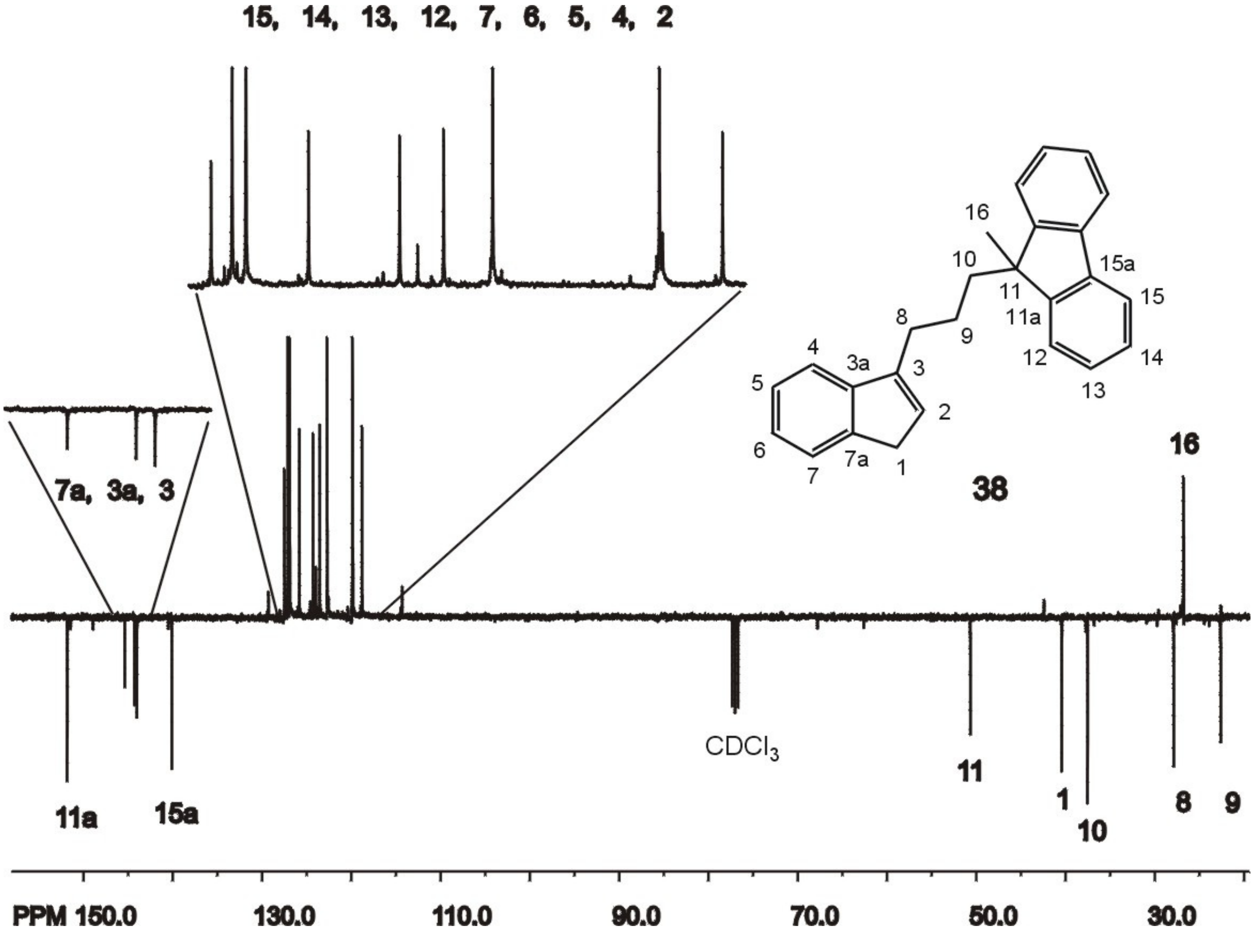

Scheme 33: ^{13}C-NMR spectrum of compound **38**.

The mass spectrum of compound **38** (Scheme 34) shows the molecular ion peak at m/z = 336 with 6% intensity relative to the base peak. Fragmentation at the C8-C9 bond and further loss of one proton gives a peak at m/z = 206 with 42% intensity relative to the base peak while the fragmentation at the C10-C11 bond gives the molecular ion peak at m/z = 179.

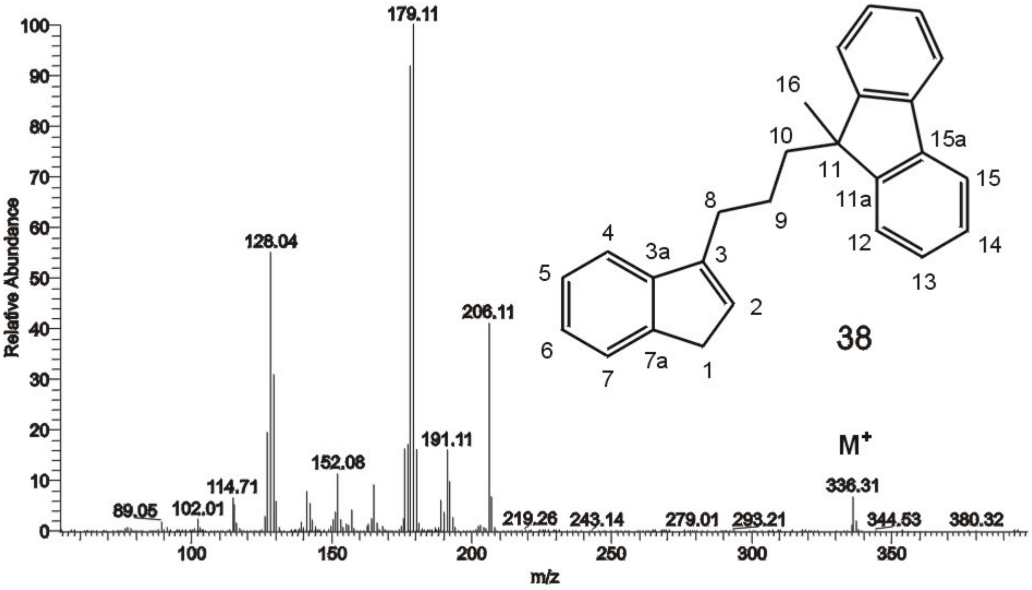

Scheme 34: Mass spectrum of compound **38**.

Table 8: NMR[a)] and MS data of compounds 37-39.

No.	^{1}H-NMR	^{13}C-NMR	MS [m/z (%)]
37	7.74-7.70 m (2H)	151.4, 147.2, 144.4, 140.2 (C_q)	322 [M^+] (10)
	7.39-7.29 m (6H)	139.0, 131.0, 127.2, 127.0,	179 (100)
	7.26-7.22 m (2H)	126.3, 124.5, 122.7, 120.8,	128 (45)
	7.13-7.10 m (2H)	119.9, 119.8 (CH)	
	6.76 d (J = 5.4 Hz, 1H)	50.5 (C_q)	
	6.36 d (J = 5.4 Hz, 1H)	50.0 (CH-Ind)	
	3.21 s (br, 1H, Ind-H1)	36.4 (CH_2)	
	2.04-1.95 m (2H, CH_2)	26.8 (CH_3)	
	1.40 s (3H, CH_3)	25.3 (CH_2)	
	1.89-1.77 m (2H, CH_2)		
38	7.62-7.69 m (2H)	151.8, 145.4, 144.3, 144.0,	336 [M^+] (6)
	7.30-7.16 m (7H)	140.1 (C_q)	206 (42)
	7.11-7.07 m (1H)	127.5, 127.1, 126.9, 125.8,	179 (100)

No.	^{1}H-NMR	^{13}C-NMR	MS [m/z (%)]
	7.06-7.01 m (1H) 6.98-6.95 m (1H) 5.83 m (br, 1H, Ind-H2) 3.10 br (2H, Ind-H1) 2.22-2.16 m (2H, CH_2) 2.03-1.98 m (2H, CH_2) 1.37 s (3H, CH_3) 1.02-0.95 m (2H, CH_2)	124.3, 123.5, 122.7, 119.9, 118.8 (CH) 50.7 (C_q) 40.4 (CH_2) 37.5 (CH_2-Ind) 27.9 (CH_2) 26.8 (CH_3) 22.6 (CH_2)	
39	7.75-7.69 m (2H) 7.42-7.16 m (10H) 6.63 d (J = 5.4 Hz, 1H) 6.48 d (J = 5.4 Hz, 1H) 3.23 br (1H, Ind-H1) 2.10-1.81 m (4H, CH_2) 1.49 s (3H, CH_3) 1.33-1.23 m (2H, CH_2) 0.88-0.76 m (2H, CH_2)	152.0, 145.4, 144.4, 140.1 (C_q) 145.0, 127.4, 127.1, 126.8, 126.3, 124.3, 122.7, 120.9, 119.8, 118.8 (CH) 50.7 (C_q) 50.3 (CH-Ind) 40.5 (CH_2) 35.6 (CH_2) 28.2 (CH_2) 26.7 (CH_3) 26.0 (CH_2)	350 [M^+] (8) 179 (100) 129 (12)

[a] δ (ppm) rel. $CHCl_3$ (7.24 ppm, ^{1}H-NMR) and rel. $CDCl_3$ (77.0 ppm, ^{13}C-NMR) at 298 K

2.2.1.2 Synthesis and characterization of the transition metal complexes

For the synthesis of the transition metal complexes from the compounds **37**-**39**, two equivalents of the substituted indenes were deprotonated by the addition of two equivalents of n-butyllithium (n-BuLi) followed by the addition of one equivalent of zirconium tetrachloride to yield the desired zirconocene dichloride complexes. The general synthesis equation of the prepared complexes is given in Scheme 35.

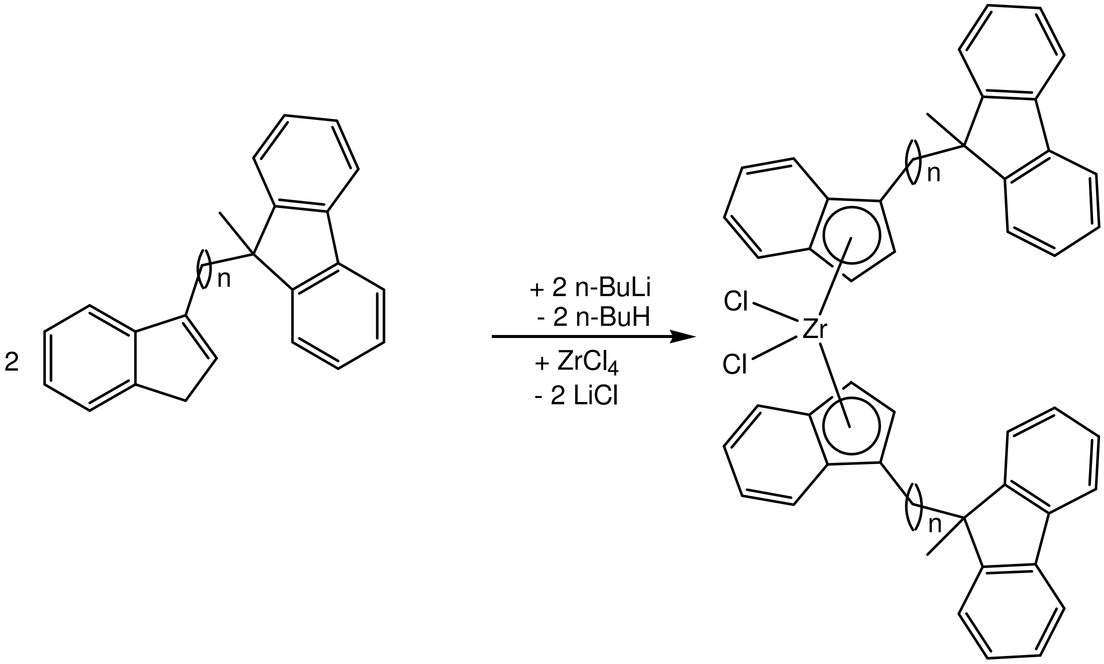

No.	40	41	42
n	2	3	4

Scheme 35: Synthesis of complexes **40**-**42**.

Complexes **40**-**42** were characterized by ^{1}H- and ^{13}C-NMR spectroscopy (Table 9) and elemental analysis (see experimental part). All complexes show two sets of signals for the rac and meso isomers. The ^{1}H-NMR spectrum of **40** and the ^{13}C-NMR spectrum of **42** will be discussed here as an example.

The ^{1}H-NMR spectrum of complex **40** (Scheme 36) shows signals at δ = 7.66-7.59 (m, 8H) and δ = 7.32-6.92 (m, 40H) ppm which can be assigned to the aromatic CH protons of the indenyl and fluorenyl rings (H16, H15, H14, H13, H7, H6, H5 and H4). The signals for the indenyl protons H2 and H3 arise at δ = 5.74 (d, J = 3.2 Hz, 2H), δ = 5.55 (d, J = 3.2 Hz, 2H), δ = 5.53 (d, J = 3.2 Hz, 2H) and δ = 5.21 (d, J = 3.2 Hz, 2H) ppm. The multiplet at δ = 2.16-2.02 (16H) ppm can be assigned to the methylene groups H8 and H9 while the signals of the fluorenyl methyl groups (H15) arise at δ = 1.38 (s, 6H) and δ = 1.34 (s, 6H) ppm.

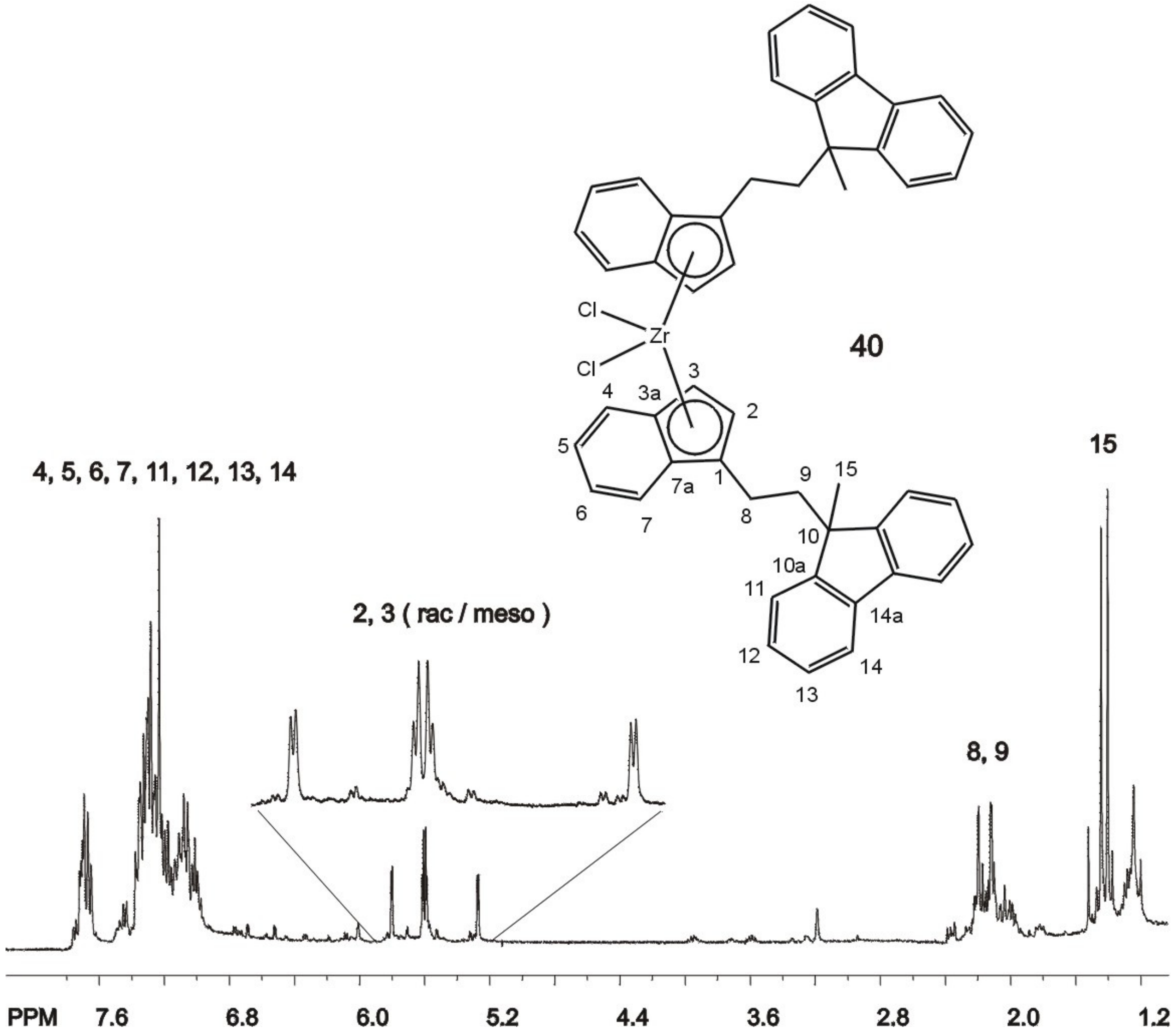

Scheme 36: ^{1}H-NMR spectrum of complex **40**.

The ^{13}C-NMR spectrum of complex **42** (Scheme 37) shows signals for the quaternary carbon atoms C16a and C12a at δ = 151.9 and δ = 140.0 ppm while the signals for the quaternary carbon atoms C7a, C3a and C1 arise at δ = 125.9, 125.7 and 123.2 ppm. The signals at δ = 127.1, 126.9, 122.7 and 119.8 ppm are assigned to the fluorenyl CH groups C16, C15, C14 and C13, while the signals at δ = 126.0, 125.6, 125.2, 123.7 and 121.8 ppm can be assigned to the indenyl CH carbon atoms C7, C6, C5, C4 and C3. The signal at δ = 99.1 ppm can be assigned to the CH carbon atom C2. At δ = 50.6 ppm, the signal for the quaternary carbon atom C12 shows up, while the signal at δ = 40.3 ppm is assigned to the methylene carbon atom C11. The signals at δ = 30.2, 27.4 and 24.3 ppm derive from the residual alkyl chain carbon atoms C8, C9 and C10 while the signal at δ = 26.6 ppm is assigned to the methyl group C17.

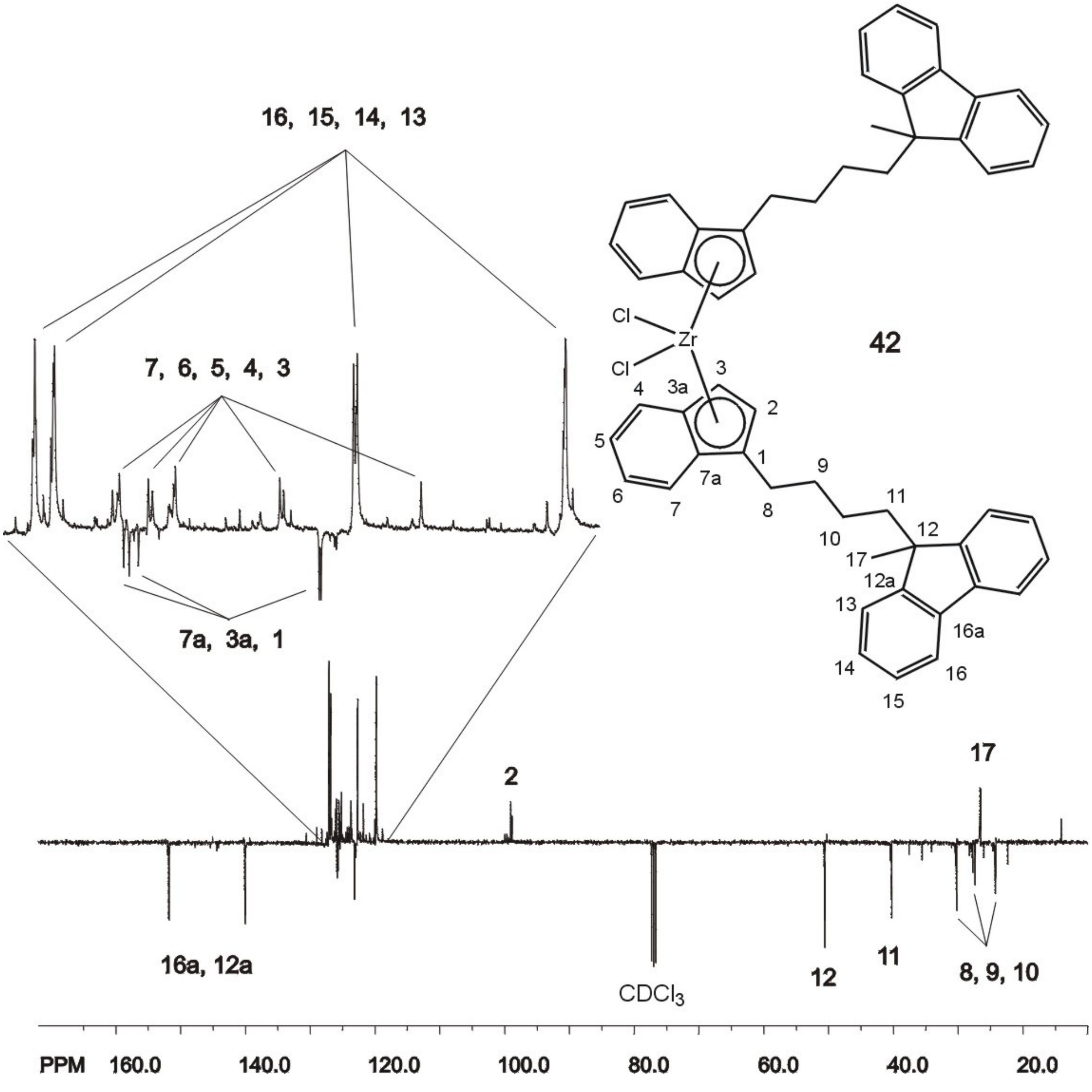

Scheme 37: ^{13}C-NMR spectrum of complex **42**.

Table 9: ^{1}H- and ^{13}C-NMR$^{a)}$ data of complexes 40-42

No.	^{1}H-NMR	^{13}C-NMR
40	7.66-7.59 m (8H) 7.32-6.92 m (40H) 5.74 d (J = 3.2 Hz, 2H) 5.55 d (J = 3.2 Hz, 2H) 5.53 d (J = 3.2 Hz, 2H) 5.21 d (J = 3.2 Hz, 2H) 2.16-2.02 m (16H, CH_2) 1.38 s (6H, CH_3), 1.34 s (6H, CH_3)	151.2, 140.3, 126.2,125.7, 123.2 (C_q) 127.3, 127.1, 126.0, 125.3, 125.0, 123.1, 122.7, 120.9, 120.0, 98.3 (CH) 50.6 (C_q) 39.7 (CH_2) 23.0 (CH_3) 22.7 (CH_2)
41	7.74-7.62 m (8H) 7.39-7.04 m (40H) 5.68 d (J = 3.2 Hz, 2H) 5.62 d (J = 3.2 Hz, 2H) 5.56 d (J = 3.2 Hz, 2H) 5.30 d (J = 3.2 Hz, 2H) 2.59-2.42 m (4H, CH_2) 2.40-2.26 m (4H, CH_2) 2.11-1.93 m (8H, CH_2) 1.43 s (6H, CH_3), 1.40 s (6H, CH_3) 1.36-1.17 m (8H, CH_2)	151.9, 140.2, 126.7, 125.7, 123.2 (C_q) 127.2, 127.0, 126.1, 125.4, 125.2, 123.6, 122.7, 120.9, 119.9, 99.4 (CH) 50.7(C_q) 40.2 (CH_2) 28.0 (CH_2) 27.0 (CH_3) 24.8 (CH_2)
42	7.64-7.59 m (8H) 7.31-7.05 m (40H) 5.95 d (J = 3.2 Hz, 2H) 5.72 d (J = 3.2 Hz, 2H) 5.55 d (J = 3.2 Hz, 2H) 5.37 d (J = 3.2 Hz, 2H) 2.63-2.49 m (4H, CH_2) 2.41-2.20 m (4H, CH_2) 1.92-1.83 m (8H, CH_2) 1.35 s (6H, CH_3), 1.37 s (6H, CH_3) 1.25-1.10 m (8H, CH_2) 0.68-0.55 m (8H, CH_2)	151.9, 140.1, 125.9, 125.8, 123.2 (C_q) 127.1, 126.9, 126.0, 125.6, 125.2, 123.7, 122.7, 121.8, 119.8, 99.1 (CH) 50.6 (C_q) 40.3 (CH_2) 30.2 (CH_2) 27.4 (CH_2) 26.6 (CH_3) 24.3 (CH_2)

$^{a)}$ δ (ppm) rel. $CHCl_3$ (7.24 ppm, ^{1}H-NMR) and rel. $CDCl_3$ (77.0 ppm, ^{13}C-NMR) at 298 K

2.2.2 Polymerization experiments and polymer analysis

Complexes **40**-**42** were activated with methylaluminoxane (MAO) and tested for ethylene polymerization. The produced polymers were analyzed by DSC. The ethylene polymerization activities and DSC results are given in Table 10.

Table 10: Ethylene polymerization results of complexes 40-42.

Complex No.	Activity[a] (kg PE/mol cat. h)	ΔH_m [J/mol]	T_m [°C]	Crystallinity (α)
40	9573	122.0	131.83	0.42
41	12333	n.d.	n.d.	n.d.
42	15786	142.1	129.33	0.49

[a] Polymerization conditions: M:Al = 1:2000, 250 mL n-pentane, 65 °C, 10 bar ethylene, 1 h

2.3 Asymmetric chelating diamide complexes of titanium and zirconium

2.3.1 General

Chelating diamide complexes of group (IV) metals are precursors of a promising catalyst system for olefin polymerization[25, 26, 92-104]. Scollard et. al. found that chelating diamide complexes of titanium after activation with MAO show very high activity for 1-hexene polymerization[25]. Uozumi et. al. investigated such systems for propylene polymerization[103, 104] and ethylene/2-butene copolymerization[102]. These chelating diamide systems are of great interest because they can act as precursors for living α-olefin polymerization catalysts[26]. A new chelating diamine ligand system containing an aniline moiety and a tertiary butyl amine moiety bridged with an ethylidene or propylidene group was prepared, the corresponding titanium and zirconium complexes were investigated for their ethylene polymerization potential after activation with MAO.

.

2.3.1.1 Synthesis and characterization of asymmetric diamine compounds

To synthesize asymmetric diamines, an excess of the respective dibromoalkane was heated at 100-105 °C with the desired aniline in DMF in the presence of potassium carbonate. The resulting mixture was distilled to give the N-substituted bromoalkyl aniline derivative. These N-substituted bromoalkyl aniline derivatives were refluxed in THF with tertiary butylamine in the presence of potassium carbonate to give the required asymmetric diamine compounds (Scheme 38).

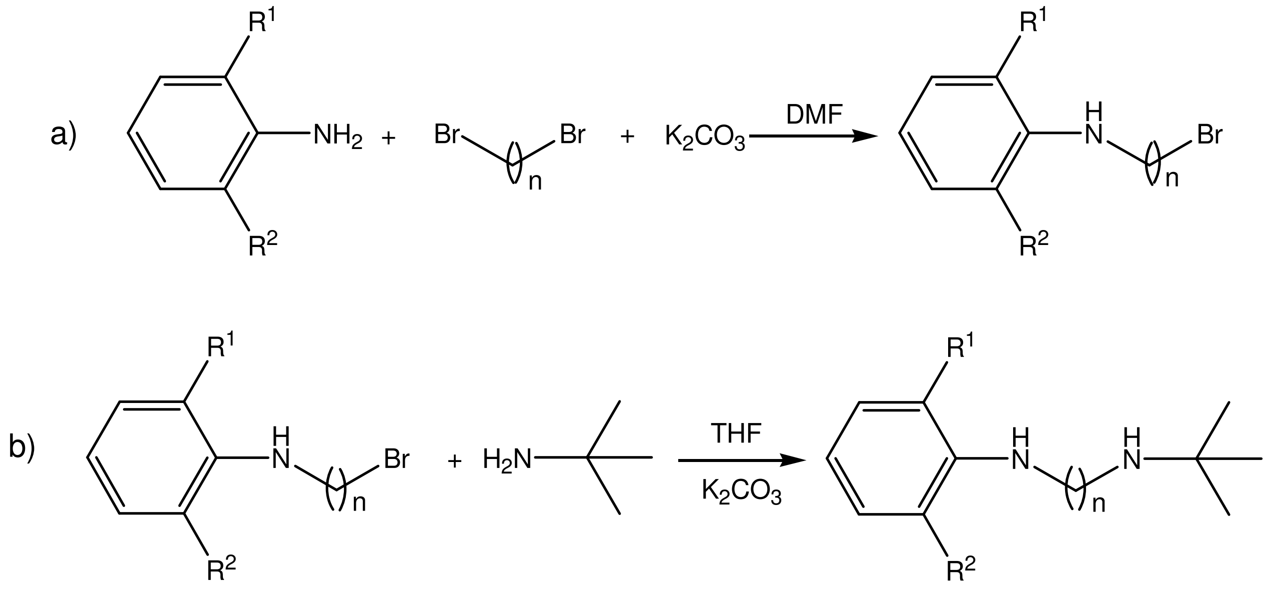

Compound No.	n	R^1	R^2
43	2	Me	i-Pr
44	2	i-Pr	i-Pr
45	3	Me	Me
46	3	i-Pr	i-Pr

Scheme 38: Synthesis of the asymmetric diamine compounds **43**-**46**.

Compounds **43**-**46** were characterized by GC/MS and ^{1}H- and ^{13}C-NMR spectroscopy (Table 11). The mass and NMR spectra of compounds **44** and **45** will be discussed as examples.

The ^{1}H-NMR spectrum of compound **44** (Scheme 39) shows a multiplet for the aryl protons H5 and H6 at δ = 7.08-6.98 (m, 3H) ppm. A septet for the CH protons H7 appears at δ = 3.32 (septet, 2 H) ppm. Two triplets at δ = 2.93 t (2H) ppm and at δ = 2.79 t (2H) can be assigned to the CH$_2$ protons H2 and H1. At δ = 1.21 (d, J = 6.8 Hz, 12H) ppm a doublet appears for the methyl protons of the isopropyl groups (H8) while the signal at δ = 1.11 (s, 9H) ppm is assigned to the tertiary butyl groups (H10). The signals for the NH protons are not visible.

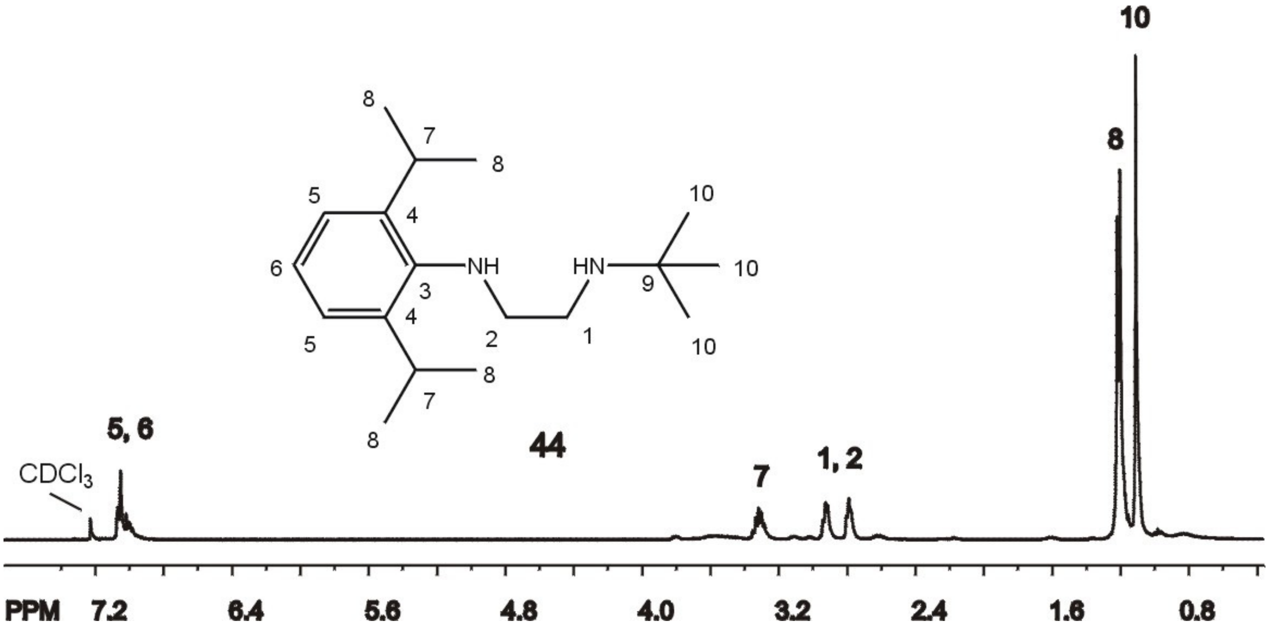

Scheme 39: ^{1}H-NMR spectrum of compound **44**.

The ^{13}C-NMR spectrum of compound **44** (Scheme 40) shows a signal for the quaternary carbon atoms C4 at δ = 143.9 ppm, while the signal at δ = 142.1 ppm can be assigned to the quaternary carbon atom C3. At δ = 123.4 and 123.3 ppm, the signals for the aromatic CH groups C5 and C6 can be located. The signal at δ = 52.5 ppm is assigned to the methylene group C2, while the signals at δ = 50.2 and 42.7 ppm derive from the quaternary carbon atom C9 and the methylene group C1. The signals at δ = 29.2, 27.6 and 24.2 ppm can be assigned to the tertiary butyl C10 and the isopropyl groups C7 and C8.

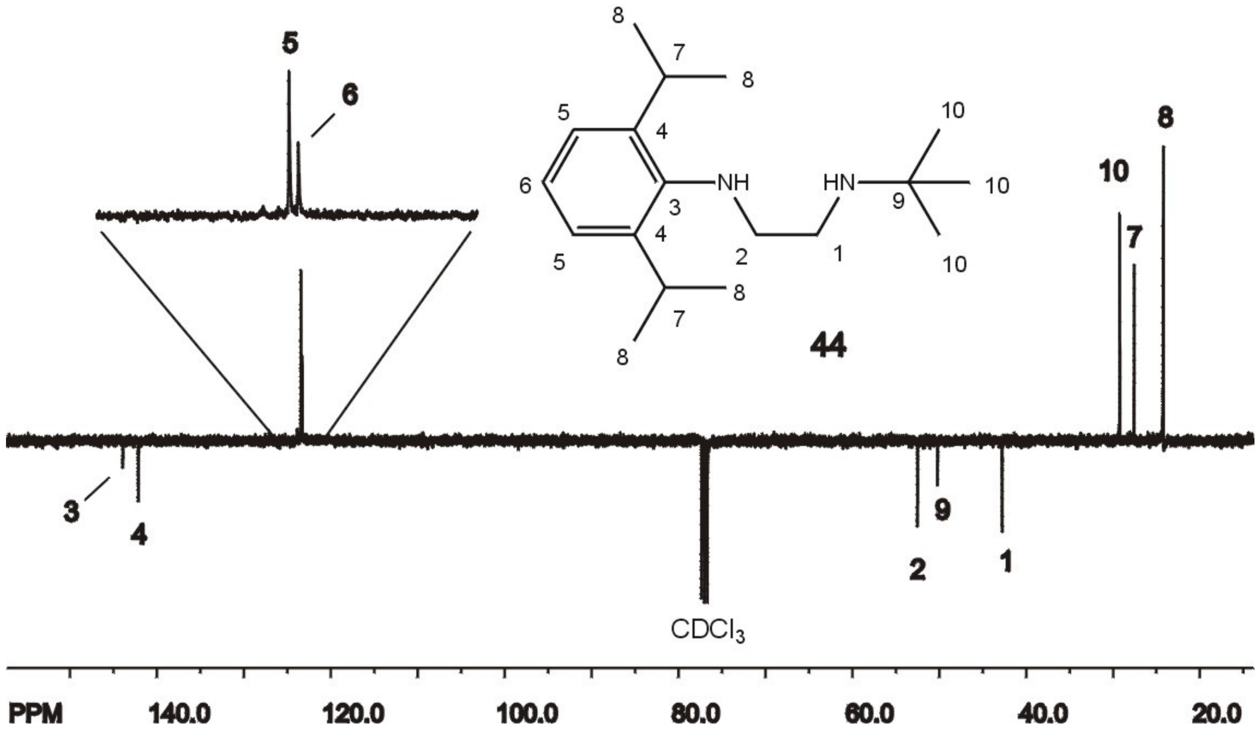

Scheme 40: ^{13}C-NMR spectrum of compound **44**.

The mass spectrum of compound **44** (Scheme 41) shows the molecular ion peak at m/z = 276 with 6% intensity relative to the base peak. Cleavage of the C1-C2 bond results in the fragments at m/z = 190 as the base peak and the fragment at m/z = 86 with 83% intensity relative to the base peak.

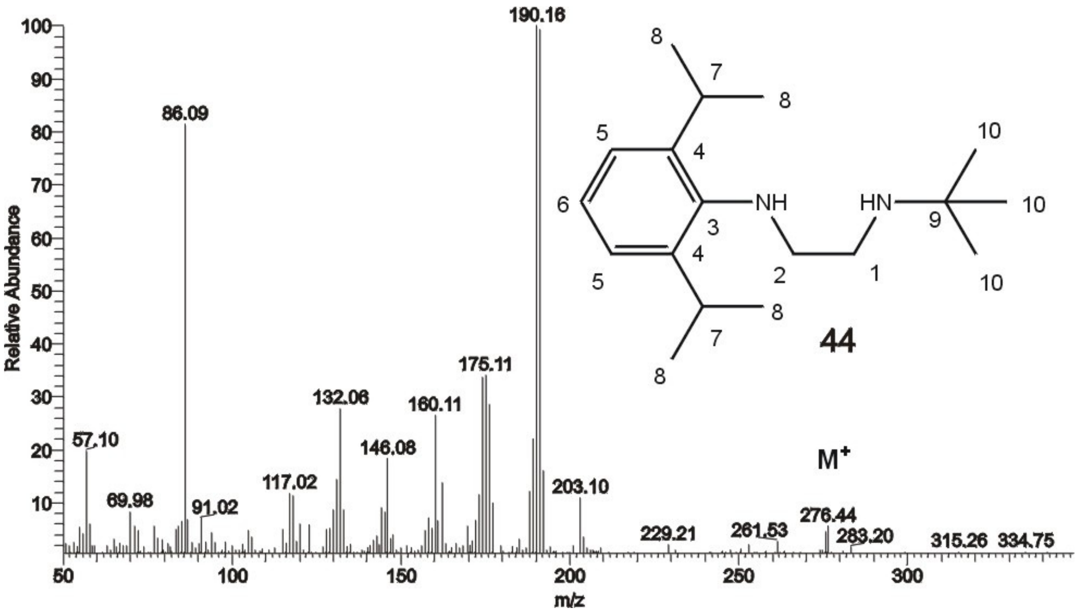

Scheme 41: Mass spectrum of compound **44**.

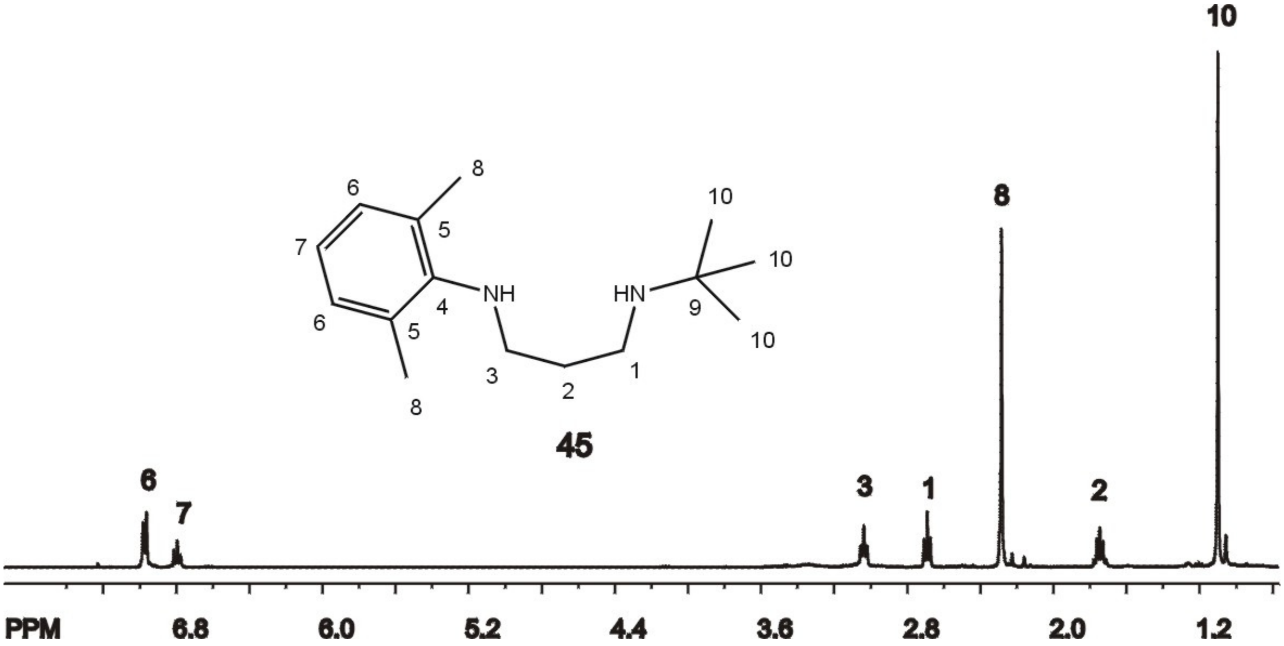

Scheme 42: ^{1}H-NMR spectrum of compound **45**.

The ^{1}H-NMR spectrum of compound **45** (Scheme 42) shows a doublet for the aryl protons H6 at δ = 6.97 (2H) ppm. The corresponding triplet for the aryl proton H7 appears at δ = 6.79 (J = 7.4 Hz, 1H) ppm. The triplets at δ = 3.04 (t, J = 6.6 Hz, 2H) and 2.69 (t, J = 6.6

Hz, 2H) ppm can be assigned to the methylene groups H3 and H1. The singlet at δ = 2.28 (s, 6H) ppm is assigned to the methyl protons at the aromatic ring (H8), while the signal at δ = 1.79-1.69 (m, 2H) ppm belongs to the methylene protons H2. At δ = 1.10 (s, 9 H) ppm, the signal for the methyl protons of the tertiary butyl group can be found. The signals for the NH protons are again not visible.

The ^{13}C-NMR spectrum of compound **45** (Scheme 43) shows the signal for the quaternary, amino substituted carbon atom C4 at δ = 146.3 ppm. The signal for the quaternary methyl substituted carbon atom C5 appears at δ = 129.2 ppm. At δ = 128.6 and 121.6 ppm, the signals for the aryl CH groups C6 and C7 can be observed. The signal at δ = 50.1 ppm is assigned to the quaternary carbon atom of the tertiary butyl group (C9) while the signals at δ = 47.3, 40.9 and 32.1 ppm derive from the methylene groups C3, C1 and C2. At δ = 29.0 ppm the methyl groups of the tertiary butyl group show up. The aryl methyl groups C8 give the signal at δ = 18.6 ppm.

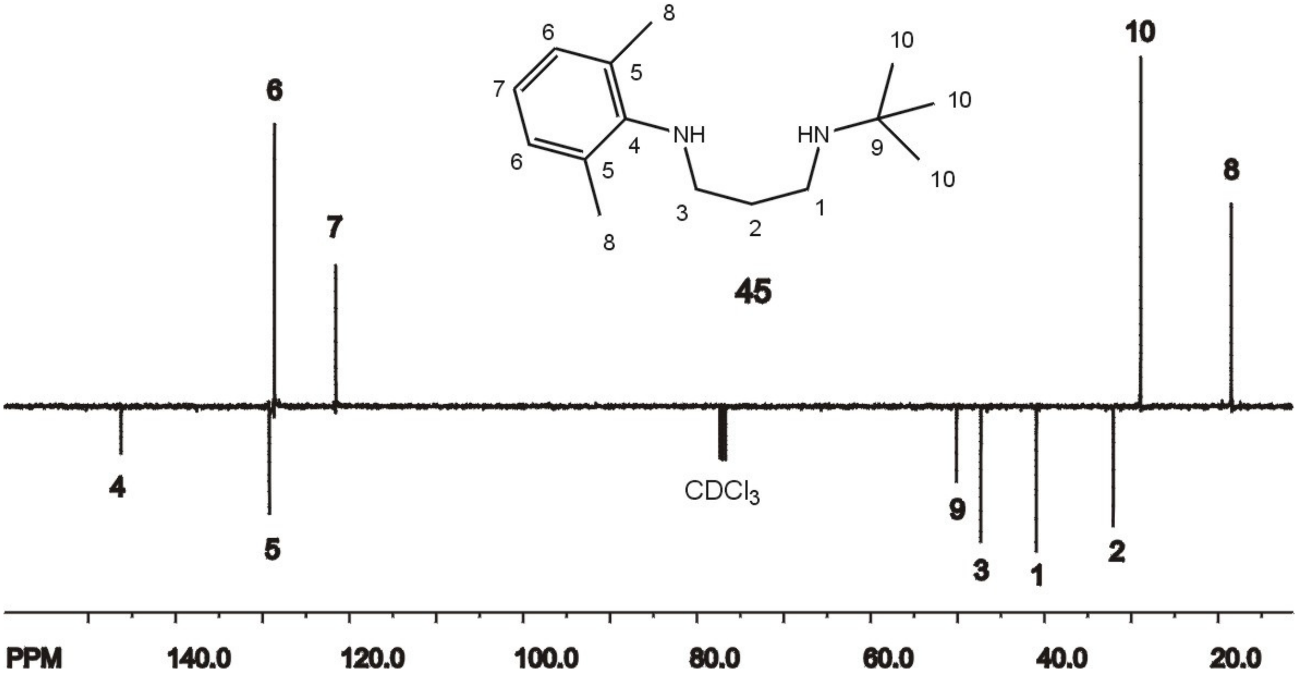

Scheme 43: ^{13}C-NMR spectrum of compound **45**.

The mass spectrum of compound **45** (Scheme 44) shows the molecular ion peak at m/z = 234 with 38% intensity relative to the base peak. Cleavage of the C1-C2 bond gives the fragment at m/z = 148 with 65% intensity relative to the base peak while the cleavage of the C2-C3 bond gives the base peak at m/z = 134.

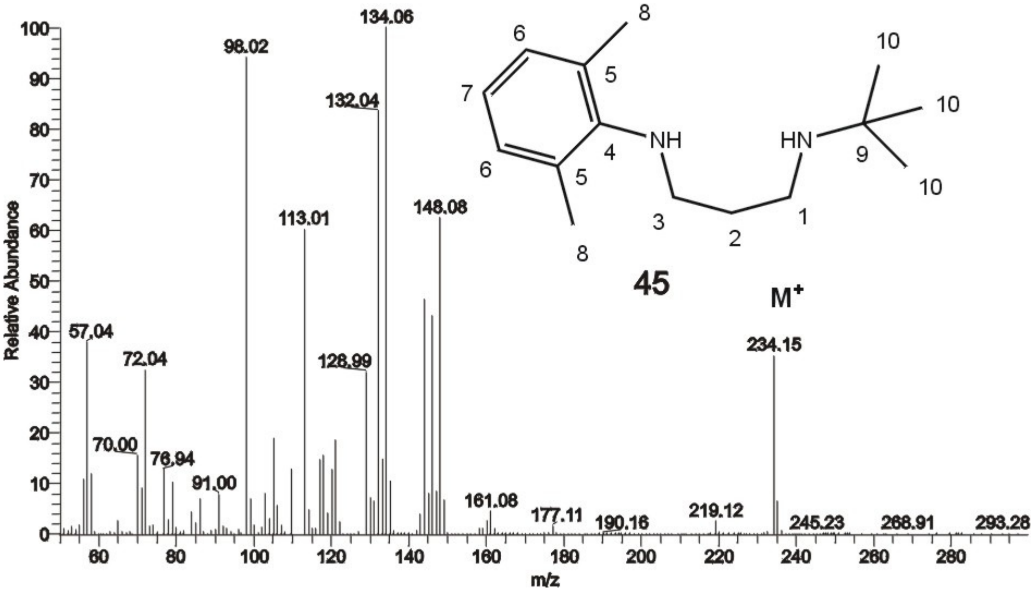

Scheme 44: Mass spectrum of compound **45**.

Table 11: NMR[a)] and MS data of compounds 43-46.

No.	^{1}H-NMR	^{13}C-NMR	MS [m/z (%)]
43	7.09-7.04 m (1H) 6.98-6.94 m (1H) 6.89 dd (J = 7.4 Hz, 1H) 3.28 sep (1H, CH) 2.99 t (J = 5.7 Hz, 2H, CH_2) 2.79 t (J = 5.7 Hz, 2H, CH_2) 2.31 s (3 H, CH_3) 1.22 d (J = 6.9 Hz, 6 H, CH_3) 1.12 s (9 H, CH_3) NH n.a.	145.2, 140.6, 130.5 (C_q) 128.4, 123.6, 122.2 (CH) 50.6 (CH_2) 50.2 (C_q) 42.8 (CH_2) 29.2 (CH_3) 27.5 (CH) 24.0 (CH_3) 18.9 (CH_3)	248 [M^+] (12) 163 (100) 146 (40) 86 (60)
44	7.08-6.98 m (3H) 3.32 septet (2 H, CH) 2.93 t (2H, CH_2)	143.9, 142.1 (C_q) 123.4, 123.3 (CH) 52.5 (CH_2)	276 [M^+] (6) 191 (100) 86 (70)

No.	^{1}H-NMR	^{13}C-NMR	MS [m/z (%)]
	2.79 t (2H, CH_2) 1.21 d (J = 6.8 Hz, 12H, CH_3) 1.11 s (9H, CH_3) NH n.a.	50.2 (C_q) 42.7 (CH_2) 29.2 (CH_3) 27.6 (CH) 24.2 (CH_3)	
45	6.99-6.95 m (2 H) 6.79 dd (J = 7.4 Hz , 1H) 3.04 t (J = 6.6 Hz, 2H, CH_2) 2.69 t (J = 6.6 Hz, 2H, CH_2) 2.28 s (6H, CH_3) 1.79-1.69 m (2H, CH_2) 1.10 s (9 H, CH_3) NH n.a.	146.3, 129.2 (C_q) 128.6, 121.6 (CH) 50.1 (C_q) 47.3, 40.9, 32.1 (each CH_2) 29 (CH_3) 18.6 (CH_3)	234 [M^+] (38) 148 (65) 134 (100)
46	7.09-6.98 m (3H) 3.28 septet (2 H, $CH(CH_3)_2$) 2.92 t (2H, CH_2) 2.72 t (J = 6.6 Hz, 2H, CH_2) 1.83-1.73 m (2H, CH_2) 1.22 d (J = 6.8 Hz, 12H, CH_3) 1.09 s (9H, CH_3) NH n.a.	143.6, 142.5 (C_q) 123.6, 123.5 (CH) 51.1 (CH_2) 50.2(C_q) 41.3 (CH_2) 31.9 (CH_2) 29.0 (CH_3) 27.6 (CH) 24.3 (CH_3)	290 [M^+] (20) 204 (40) 190 (45) 174 (75) 146 (50) 113 (52)

[a] δ (ppm) rel. $CHCl_3$ (7.24 ppm, ^{1}H-NMR) and rel. $CDCl_3$ (77.0 ppm, ^{13}C-NMR) at 298 K

2.3.1.2 Synthesis and characterization of the transition metal complexes

For the synthesis of asymmetric diamide complexes, the corresponding diamine compounds were deprotonated with two equivalents of n-butyllithium followed by the addition of one equivalent of titanium tetrachloride or zirconium tetrachloride to synthesize the diamide complexes **47**-**54** (Scheme 45).

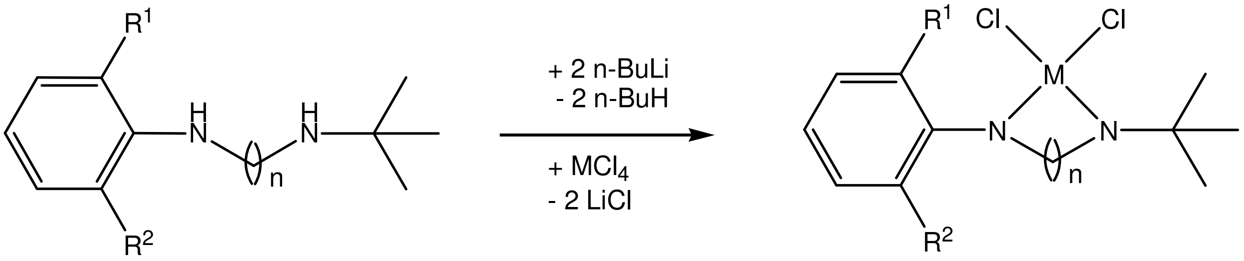

Complex No.	M	n	R^1	R^2
47	Ti	2	Me	i-Pr
48	Ti	2	i-Pr	i-Pr
49	Ti	3	Me	Me
50	Ti	3	i-Pr	i-Pr
51	Zr	2	Me	i-Pr
52	Zr	2	i-Pr	i-Pr
53	Zr	3	Me	Me
54	Zr	3	i-Pr	i-Pr

Scheme 45: Synthesis of complexes **47**-**54**.

Complexes **47**-**54** were characterized by ^{1}H- and ^{13}C-NMR spectroscopy (Table 12) and elemental analysis (see experimental part). NMR spectra of complex **53** are discussed as an example.

The ^{1}H-NMR spectrum of complex **53** (Scheme 46) shows the signals for the arylic protons H7 and H6 at δ = 7.12-7.07 (m, 1H) and 7.05-6.98 (m, 2H) ppm. The signals for the three methylene groups C3, C2 and C1 appear at δ = 3.32-2.85 (m, 6H,) ppm. At δ = 2.66 (s, 6H) ppm, the signal for the aryl methyl protons H8 is found, while the singlet for the tertiary butyl group appears at δ = 1.47 (s, 9H) ppm.

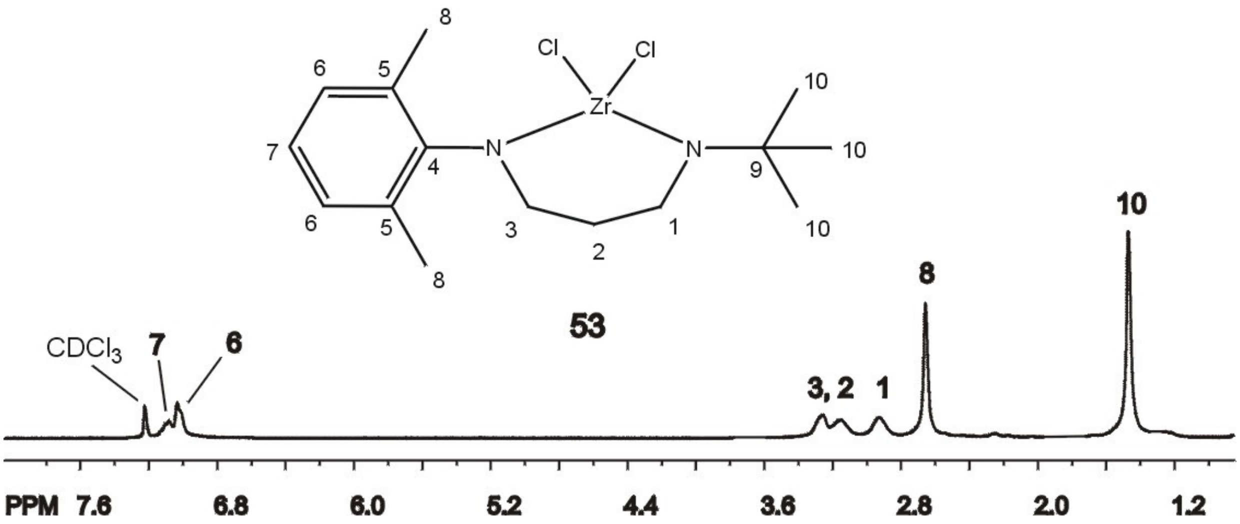

Scheme 46: ^{1}H-NMR spectrum of complex **53**.

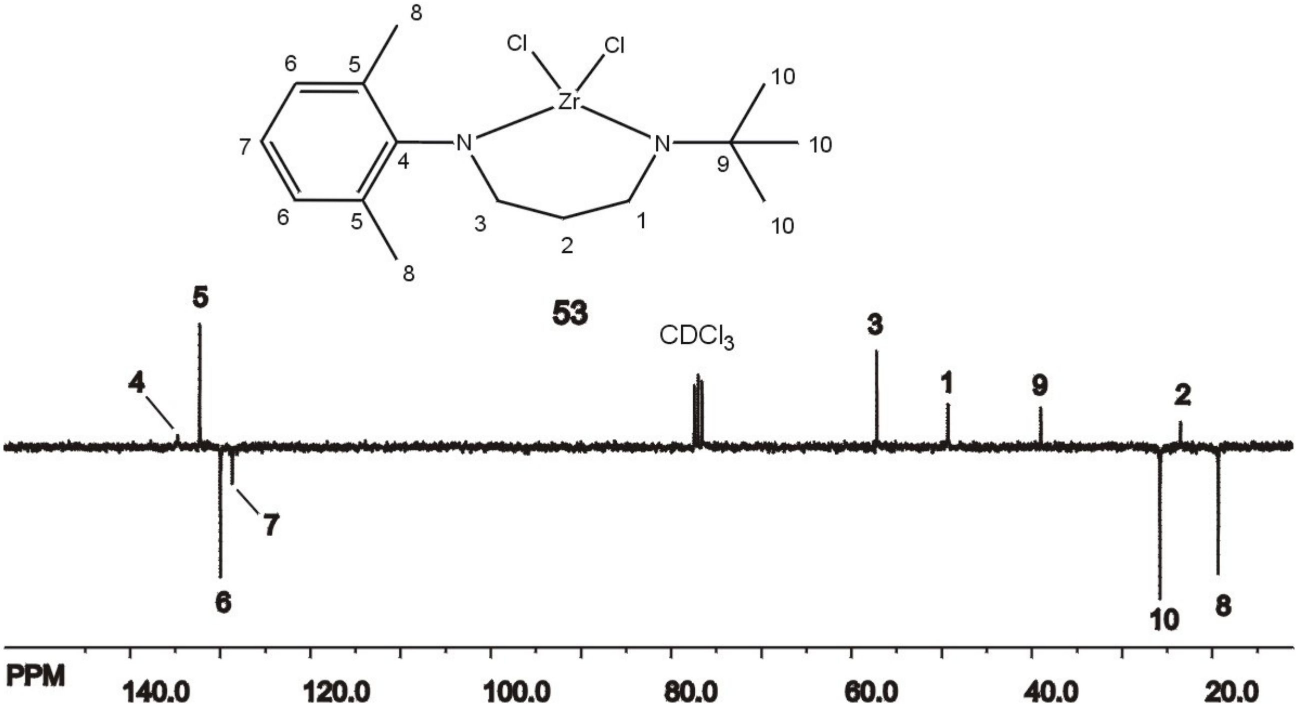

Scheme 47: ^{13}C-NMR spectrum of complex **53**.

The ^{13}C-NMR spectrum of complex **53** (Scheme 47) shows a signal at δ =134.7 ppm which can be assigned to the quaternary amino substituted carbon atom C4. In the free ligand the corresponding carbon atom appears at δ = 146.3 ppm. The signal at δ = 132.3 ppm can be assigned to the quaternary carbon atoms C5, while in the free ligand these carbon atoms appear at δ = 129.2 ppm. At δ = 130.0 ppm, the signal for the arylic carbon atoms C6 appears which is 1.4 ppm at higher field than the signal for the corresponding atoms in the free ligand. The signal for the aryl CH carbon C7 arises at δ = 128.7 ppm. The signals at δ = 57.2 and 49.3 ppm can be assigned to the methylene groups C3 and C1, the signal at δ = 39.0 ppm to the quaternary carbon atom C9. At δ = 25.8 ppm, the signal for the methyl carbons of the tertiary butyl group can be found. The signal for the residual methylene group C2 arises at δ = 23.5 ppm. At δ = 19.3 ppm, the signal for the aryl methyl groups C8 appears.

Table12: ^{1}H- and ^{13}C-NMR data of complexes 47-53.

No.	^{1}H-NMR	^{13}C-NMR
47$^{c)}$	7.33-7.05 m (3H) 4.02 m (br, 2H, CH_2) 3.73 m (br, 2H, CH_2) 3.57 septet (CH) 2.69 s (3H, CH_3) 1.36 s (9H, CH_3) 1.25 d (J = 6.6 Hz, 6 H, CH_3)	144.0, 132.9, 131.7 (C_q) 130.7, 130.6, 126.7 (CH) 58.3 (CH_2), 49.8 (C_q) 38.4 (CH_2) 28.7 (CH) 26.1, 25.3, 20.1 (each CH_3)
48$^{a)}$	7.28-7.24 m (1H) 7.17-7.13 m (2H) 4.34-3.14 m (6H) 1.52 s (9H, CH_3) 1.47 d (3H, CH_3) 1.22 d (3H, CH_3)	159.7, 138.7 (C_q) 128.5, 124.2 (CH) 64.1 (CH_2), 58.9 (C_q) 44.6 (CH_2) 28.7 (CH_3) 28.3 (CH) 24.1 (CH_3)
49$^{c)}$	6.96-6.93 m (2H) 6.80 dd (1H) 3.17-3.03 m (4H, CH_2) 2.40-2.33 m (2H, CH_2) 2.27 s (6H, CH_3) 1.46 s (9H, CH_3)	133.9, 132.9 (C_q) 130.7, 130.0 (CH) 58.0, 50.1 (each CH_2) 39.5 (C_q), 26.2 (CH_3) 23.7 (CH_2) 19.4 (CH_3)

No.	^{1}H-NMR	^{13}C-NMR
50$^{c)}$	7.22-7.02 m (3H) 3.22 septet (2H, CH) 2.99-2.88 m (4H, CH_2) 2.44-2.36 m (2H, CH_2) 1.50 s (CH_3) 1.20 d (CH_3)	143.7, 143.1 (C_q) 124.1, 123.2 (CH) 57.9 (CH_2), 51.4 (C_q) 42.5 (CH_2) 28.2 (CH) 26.7, 24.8 (each CH_3)
51$^{a)}$	7.06-7.01 m, 6.95-6.89 m (3H) 3.56-3.09 m (1H, CH, 2H, CH_2) 2.28 s (3H, CH_3) 1.43 s (9H, CH_3) 1.16 d (6H, CH_3)	143.7, 141.8, 131.6 (C_q) 128.6, 123.7, 123.4 (CH) 58.1 (C_q) 45.7, 43.1 (each CH_2) 27.6 (CH) 26.2, 24.1, 19.6 (each CH_3)
52$^{a)}$	7.10-7.00 m (3H) 3.52-3.00 m (6H (2H, CH + 4H, CH_2)) 1.44 s (9H, CH_3) 1.18 d (12H, CH_3)	143.0, 142.4 (C_q) 124.3, 123.6 (CH) 57.2 (Cq) 47.5, 43.0 (each CH_2) 27.9 (CH) 26.0, 24.4 (each CH_3)
53$^{a)}$	7.12- 7.07 m (1H) 7.05-6.98 m (2H) 3.32-2.85 m (6H, CH_2) 2.66 s (5H, CH_3) 1.47s (9H, CH_3)	134.7, 132.3 (C_q) 130.0, 128.7 (CH) 57.2, 49.3 (each CH_2) 39.0 (C_q), 25.8 (CH_3) 23.5 (CH_2), 19.3 (CH_3)
54$^{c)}$	7.45-7.15 m (3H) 3.68-2.96 m (8H) 1.47 s (9H, CH_3) 1.29 d (br, 12H, CH_3)	143.5, 129.9 (C_q) 130.9, 126.4 (CH) 58.5 (CH_2), 52.8 (C_q) 39.8 (CH_2), 28.9 (CH) 26.3, 25.4 (each CH_3) 24.2 (CH_2)

[a)] δ (ppm) rel. $CHCl_3$ (7.24 ppm, ^{1}H-NMR) and rel. $CDCl_3$ (77.0 ppm, ^{13}C-NMR) at 298 K

[c)] δ (ppm) rel. methylene chloride (5.30 ppm, ^{1}H-NMR and 54.0 ppm, ^{13}C-NMR) at 298 K

2.3.2 Ethylene polymerization experiments and polymer analysis

Asymmetric diamide complexes of titanium and zirconium were studied for ethylene polymerization after activation with MAO. Polymerization activities, polymerization conditions and DSC results are summarized in Table 13.

Table 13: Ethylene polymerization results of complexes 47-54.

No.	structure	Activity[a] (Kg PE/mol cat. h)	ΔH_m [J/mol]	T_m [°C]	Crystallinity (α)
47	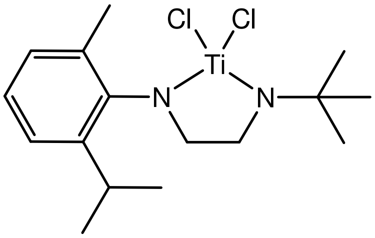	205	107.2	135.33	0.37
48	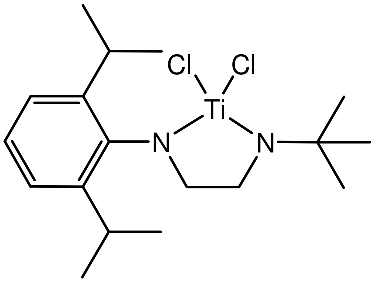	263	n.d.	n.d.	n.d.
49	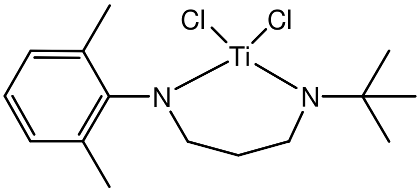	106	125.1	138.17	0.43
50	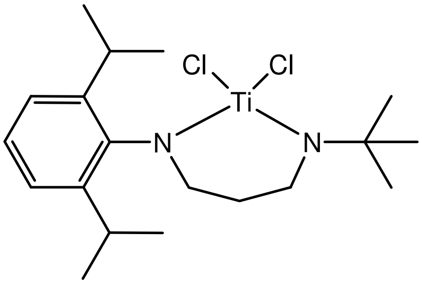	190	114.1	139.83	0.39
51	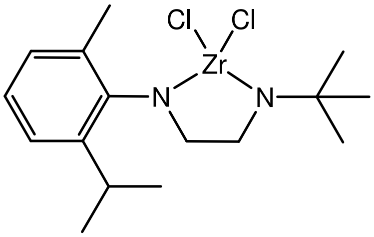	110	113.8	139.17	0.39

No.	structure	Activity[a] (Kg PE/mol cat. h)	ΔH_m [J/mol]	T_m [℃]	Crystallinity (α)
52	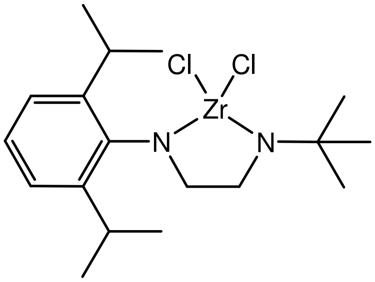	116.5	128.1	137.83	0.44
53	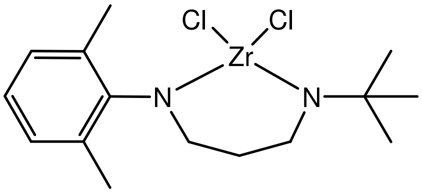	172	130.5	138.67	0.45
54	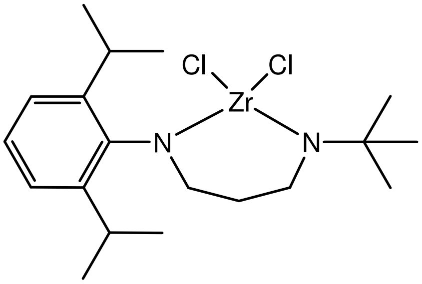	209	n.d.	n.d.	n.d.

[a] Polymerization conditions: M:Al = 1:1000, 250 mL n-pentane, 60 ℃, 10 bar ethylene, 1 h

2.4 Schiff base derivatives of 2-(2-aminophenyl)benzothiazole and their titanium and zirconium complexes

2.4.1 General

Schiff base derivatives of 2-(2-aminophenyl)benzimidazole with aromatic aldehydes are a promising ligand system for transition metal complexes. Iron, cobalt, nickel and copper complexes with these Schiff base compounds have been synthesized and their biological activities have been studied by different research groups[105-109]. The synthesis and catalytic ethylene polymerization potential of early transition metal complexes of these Schiff base compounds is of interest. A Schiff base compound derived from 2-(2-aminophenyl) benzothiazole and benzaldehyde, its complexes with titanium and zirconium and the activities of these complexes towards ethylene polymerization after activation with MAO were investigated.

2.4.2 Synthesis and characterization of Schiff base derivatives of 2-(2-aminophenyl)benzothiazole

2-(2-Aminophenyl)benzothiazole was prepared according to the reported procedures[110-113]. Its Schiff base compound was synthesized by reacting it with one equivalent of benzaldehyde in ethanol at room temperature (Scheme 48).

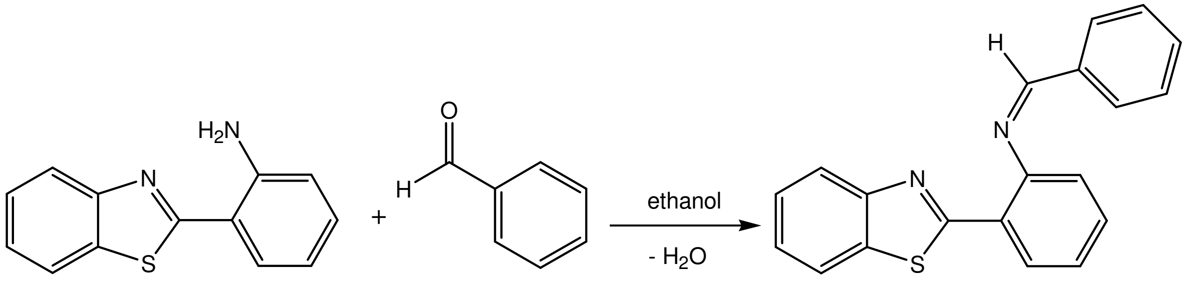

55

Scheme 48: Synthesis of compound **55**.

Compound **55** was characterized by GC/MS and ^{1}H- and ^{13}C-NMR spectroscopy (Table 14). Its MS and ^{13}C-NMR spectra will be discussed here.

The ^{13}C-NMR spectrum of compound **55** (Scheme 49) shows the signal for the quaternary carbon atom C2' at δ = 164.3 ppm. At δ = 160.9 ppm the signal for the imino group (C7) can be found, while the signal for the quaternary carbon atom C2a' appears at δ = 153.2 ppm. The signals for the residual quaternary carbon atoms C6, C8, C6a' and C1 arise at δ = 150.2, 138.2, 136.5 and 127.9 ppm. The signals for the aromatic CH groups C9 and C10 appear at δ = 130.0 and 129.0 ppm, while the signals for the residual aromatic CH groups (C11, C5, C4, C3, C2, C6', C5', C4' and C3') can be located at δ = 131.9, 131.4, 129.5, 126.4, 126.1, 124.8, 123.6, 121.5 and 118.8 ppm.

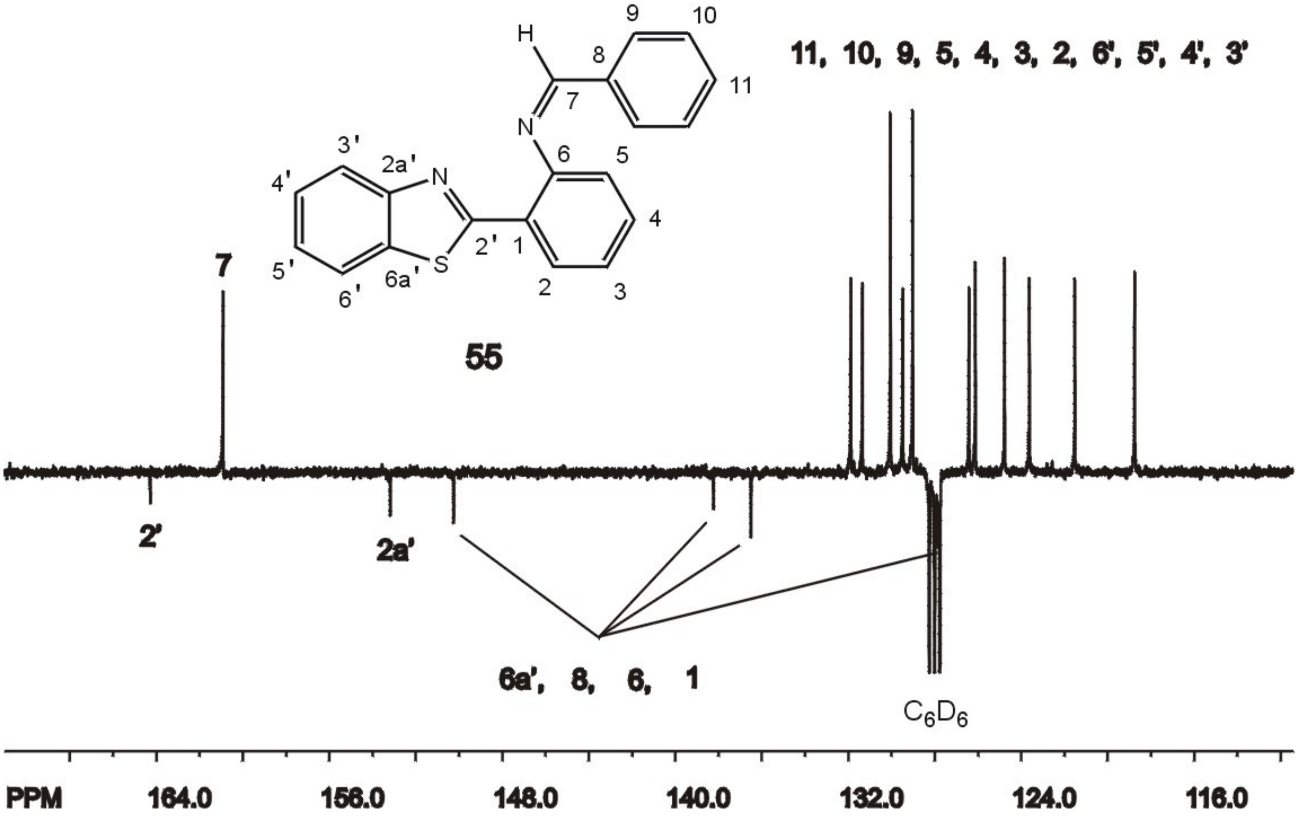

Scheme 49: ^{13}C-NMR spectrum of compound **55.**

The mass spectrum of compound **55** (Scheme 50) shows the molecular ion peak at m/z = 314 with 24% intensity relative to the base peak. Fragmentation at the C8-C7 bond results in a peak at m/z = 237 with 35% intensity relative to the base peak while the fragmentation at the C6-N bond results in the base peak at m/z = 211.

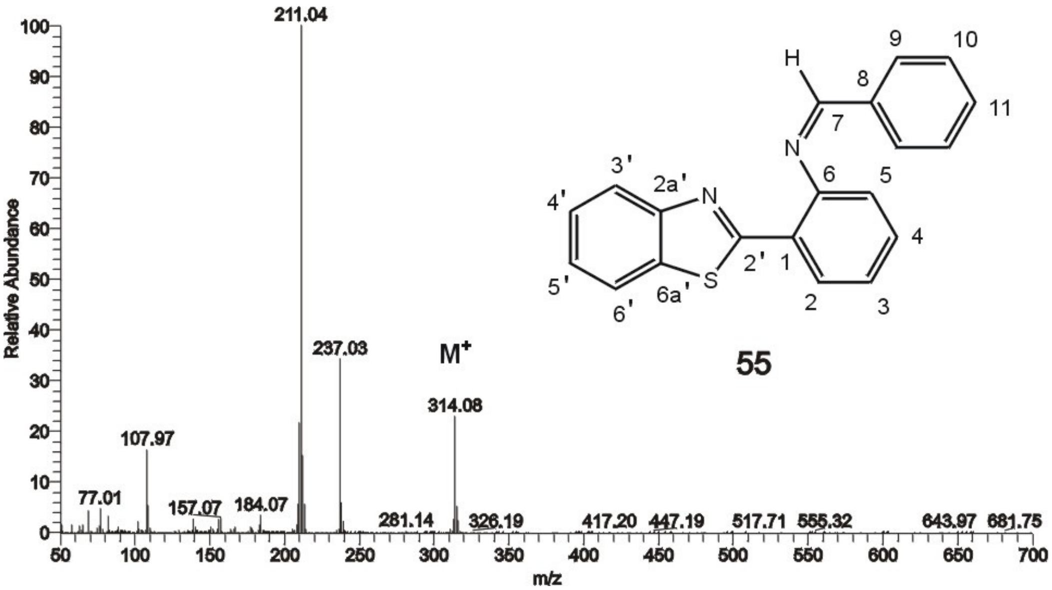

Scheme 50: Mass spectrum of compound **55.**

2.4.3 Synthesis and characterization of the titanium and zirconium complexes

For the synthesis of titanium and zirconium complexes, one equivalent of the Schiff base derivative of 2-(2-aminophenyl)benzothiazole was added to one equivalent of titanium tetrachloride or zirconium tetrachloride in toluene (Scheme 51).

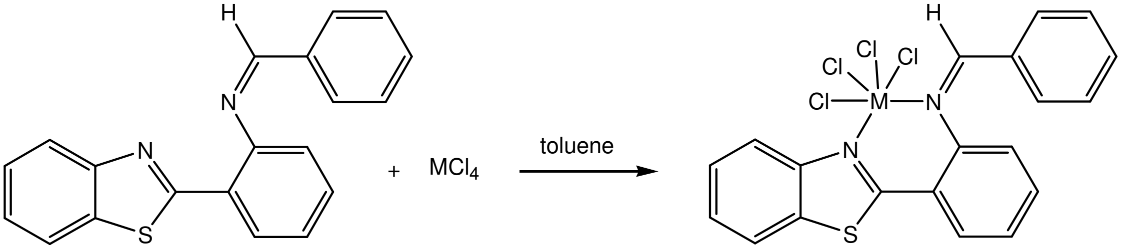

56: M = Ti

57: M = Zr

Scheme 51: Synthesis of complexes **56** and **57**.

Complexes **56** and **57** were characterized by ^{1}H- and ^{13}C-NMR spectrocopy (Table 14) and elemental analysis (see experimental part). The ^{13}C-NMR spectrum of complex **56** is discussed as an example.

In the ^{13}C-NMR spectrum of complex **56** (Scheme 52), the signal for the imino group (C7) arises at δ = 193.5 ppm. The signals for the quaternary carbon atoms C2$^{'}$ and C2a$^{'}$ appear at δ = 168.3 and 153.2 ppm while the signals for the residual quaternary carbon atoms C6a$^{'}$, C8, C6, and C1 can be found at δ = 136.4, 136.2, 132.7 and 115.4 ppm. The signals at δ = 134.6, 131.8 and 130.0 ppm can be assigned to the aromatic CH groups C5, C4 and C3, while the signals for the aromatic CH groups C11, C10 and C9 can be located at δ = 129.5, 129.2 and 129.1 ppm. The signals at δ = 128.1, 126.6, 125.3, 122.3 and 121.9 ppm result from the residual CH groups C2, C6$^{'}$, C5$^{'}$, C4$^{'}$ and C3$^{'}$.

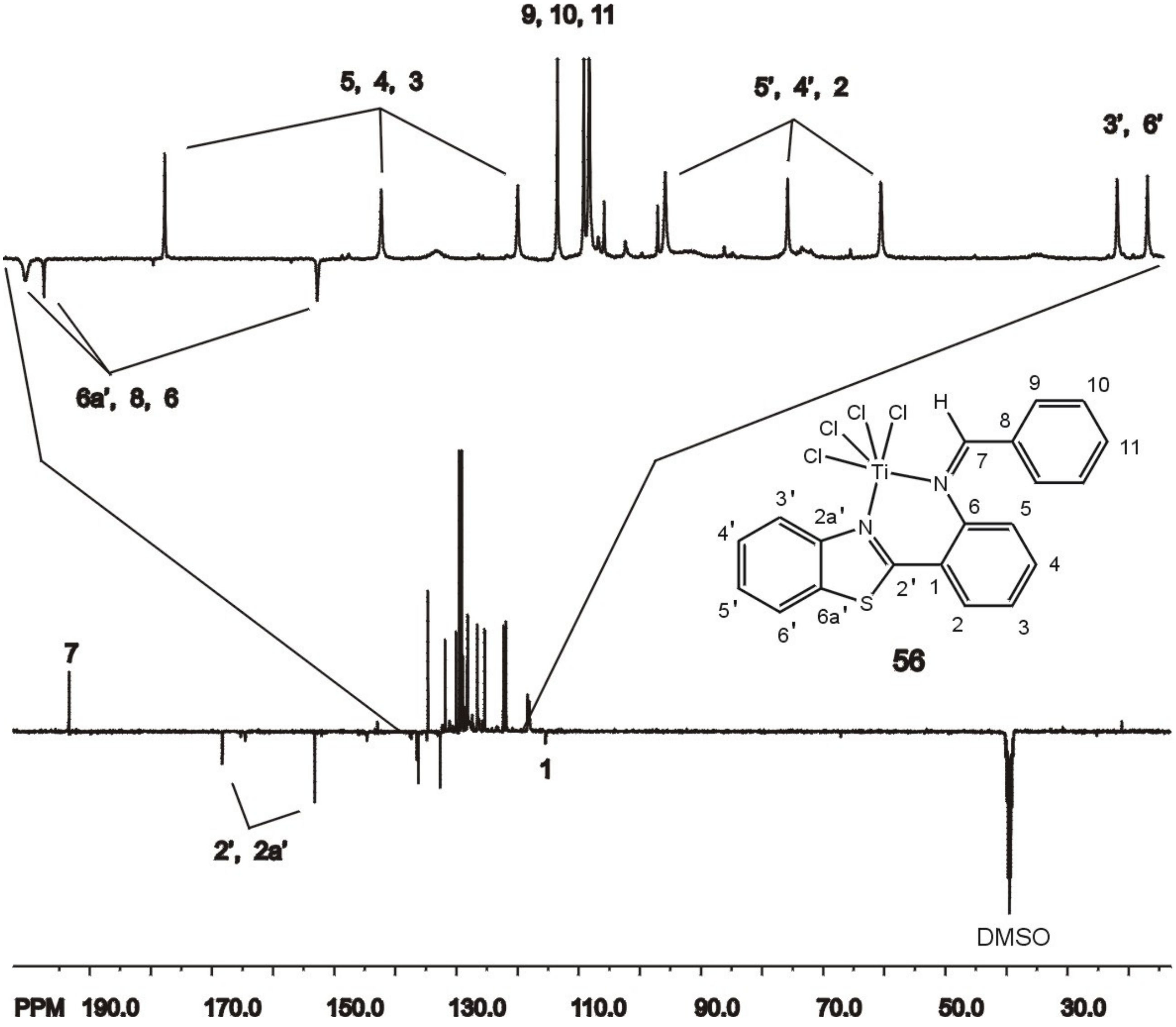

Scheme 52: ^{13}C-NMR spectrum of complex **56**.

Table 14: ^{1}H- and ^{13}C-NMR data of compound 55 and its complexes 56 and 57.

No.	^{1}H-NMR	^{13}C-NMR
55[b]	8.71-8.68 m (1H) 8.46 s (1H) 8.15-8.12 m (1H) 8.09-8.04 m (2H) 7.90-7.86 m (1H) 7.56-7.52 m (3H) 7.50-7.43 m (2H) 7.41-7.31 m (2H) 7.09-7.05 m (1H)	164.3 (C_q) 160.9 (CH) 153.2, 150.2, 138.2, 136.5 (C_q) 131.9, 131.4, 130.0, 129.5, 129.0 (CH) 127.9 (C_q) 126.4, 126.1, 124.8, 123.6, 121.5, 118.8 (CH)
56[d]	10.02 s (1H) 8.54-8.16 m (3H) 8.08-7.73 m (5H) 7.70-7.37 m (2H) 7.32-7.06 m (2H) 6.83-6.75 m (1H)	193.5 (CH) 168.3, 153.2, 136.4, 136.2, 132.7, 115.4 (C_q) 134.6, 131.8, 130.0, 129.5, 129.2, 129.1, 128.1, 126.6, 125.3, 122.3, 121.9 (CH)
57[d]	10.00 s (1H) 8.55-8.13 m (3H) 8.09-7.38 m (7H) 7.32-7.03 m (2H) 6.82-6.74 m (1H)	193.3 (CH) 168.8, 153.3, 136.2, 136.1, 132.5, 113.6 (C_q) 134.6, 131.8, 130.0, 129.6, 129.2, 129.1, 128.2, 126.5, 125.2, 122.1, 121.8 (CH)

[b] δ (ppm) rel. benzene (7.16 ppm, ^{1}H-NMR and 128.0 ppm, ^{13}C-NMR) at 298 K

[d] δ (ppm) rel. DMSO (2.50 ppm, ^{1}H-NMR and 39.5 ppm, ^{13}C-NMR) at 298 K

2.4.4 Ethylene polymerization studies

Complexes **56** and **57** were activated with methylaluminoxane (MAO) and tested for ethylene polymerization. Ethylene polymerization activities and polymerization conditions are given in Table 15.

Table 15: Ethylene polymerization activities of complexes 56 and 57.

No.	M:Al	Activity[a] (Kg PE/mol cat. h)
56	1:2000	432
57	1:2000	276

[a] Polymerization conditions: 250 mL n-pentane, 65 °C, 10 bar ethylene, 1 h

2.5 Indene-phenoxyimine and indene/fluorene-amidine bridged compounds as potential ligands for group (IV) metal complexes

2.5.1 General

Non bridged half sandwich-phenoxyimine complexes of group (IV) metals have been considered as promising candidates for olefin polymerization because of their relatively easy synthesis and ligand modifications. When activated with MAO, these complexes show very high activities for ethylene polymerization[114-117]. Similarly, non bridged half sandwich-benzamidinato complexes of group (IV) metals also show very good activities for ethylene polymerization[118, 119]. Bridged half sandwich-phenoxyimine and bridged half sandwich-benzamidinato complexes of group (IV) metals are interesting as the bridge is expected to render more rigidity to the complexes and hence the catalytically active species. Some indene-phenoxyimine and indene/fluorene-amidine bridged compounds and attempts to synthesize their titanium and zirconium complexes are reported.

2.5.2 Synthesis of indene-phenoxyimine and indene/fluorene-amidine bridged compounds

1-(3-Aminopropyl) indene and 9-(3-aminopropyl) fluorene were synthesized according to reported methods[120, 121]. 1-(3-Aminopropyl) indene was refluxed with 2-hydroxy aldehydes or ketones in ethanol to give indene-phenoxyimine bridged compounds (Scheme 53).

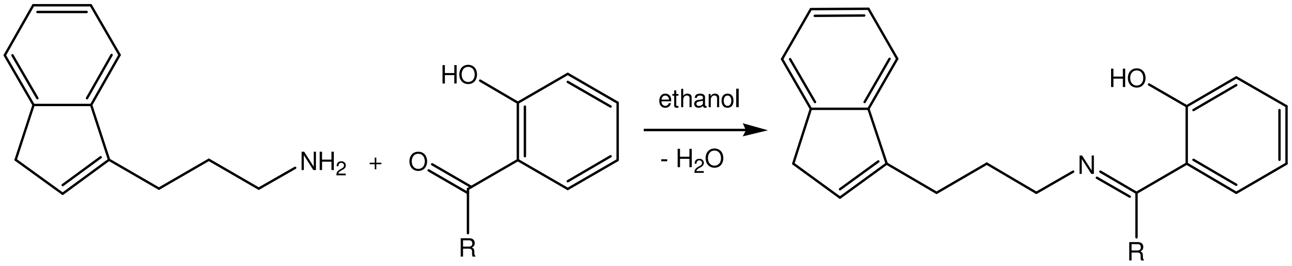

No.	R
58	H
59	CH_3

Scheme 53: Synthesis of indenyl compounds **58** and **59**.

Indene-amidine and fluorene-amidine bridged compounds were synthesized by refluxing 1-(3-aminopropyl) indene or 9-(3-aminopropyl) fluorene and benzoylchloride in dichloromethane in the presence of triethylamine (Scheme 54).

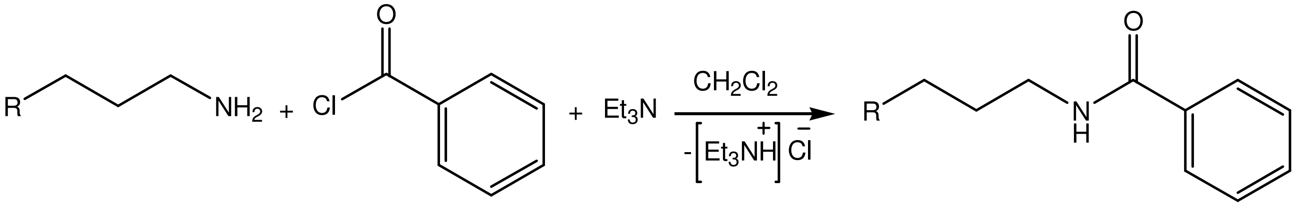

No.	R
60	-1-indenyl
61	-9-fluorenyl

Scheme 54: Synthesis of compounds **60** and **61**.

Compounds **58**-**61** were characterized by GC/MS and ^{1}H- and ^{13}C-NMR spectroscopy (Table 16). MS and ^{1}H- and ^{13}C-NMR spectra of compound **58** are discussed as an example.

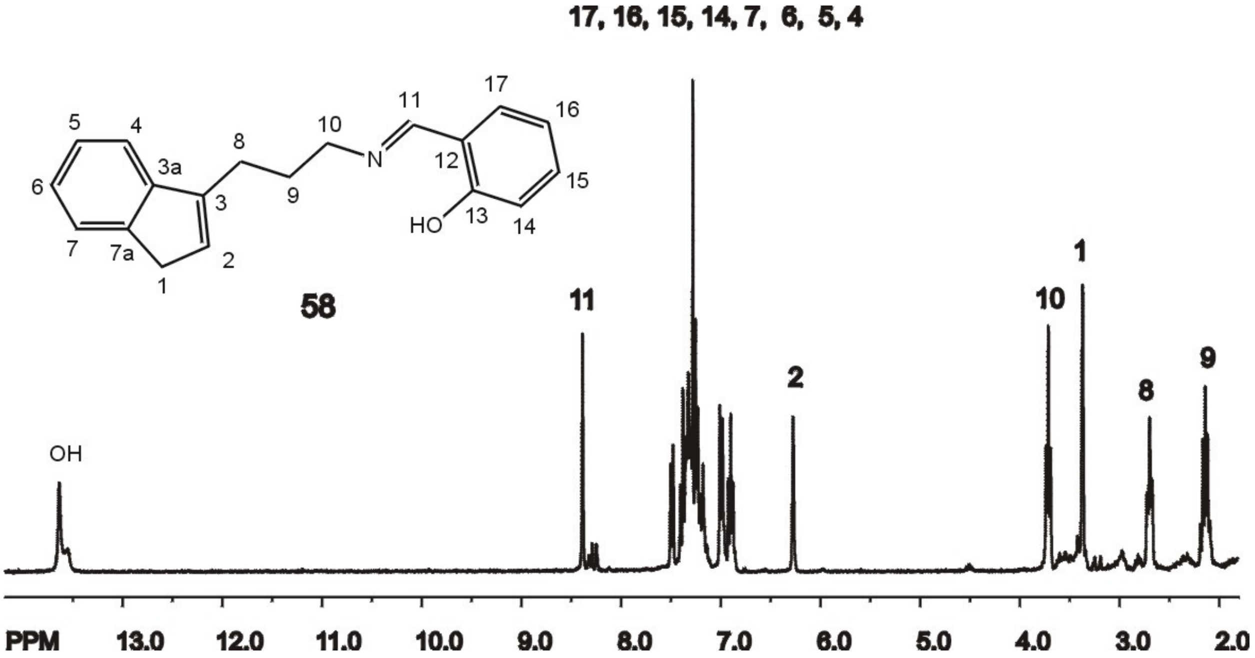

Scheme 55: ^{1}H-NMR spectrum of compound **58**.

In the ^{1}H-NMR spectrum of compound **58** (Scheme 55), the signal of the hydroxyl group appears at δ =13.63 (br, 1H) ppm, while the signal for the imino group can be found at δ = 8.38 (s, 1H) ppm. The aromatic CH groups (H17, H16, H15, H14, H7, H6, H5 and H4) give signals at δ = 7.51-7.47 (m, 1H), 7.40-7.18 (m, 5H), 7.01-6.97 (m, 1H) and 6.97-6.87 (m, 1H) ppm. The signal at δ = 6.27 (br, 1H) ppm results from the indenyl CH group (H2). The triplet at δ = 3.71 (J = 7.7 Hz, 2H) ppm is assigned to the methylene group adjacent to the N atom (H10), while the signal for the indenyl methylene group (H1) arises at δ = 3.37 (br, 2H) ppm. The multiplets at δ = 2.73-2.65 (2H) and 2.20-2.06 (2H) ppm are assigned to the residual methylene groups of the alkyl chain (H8 and H9).

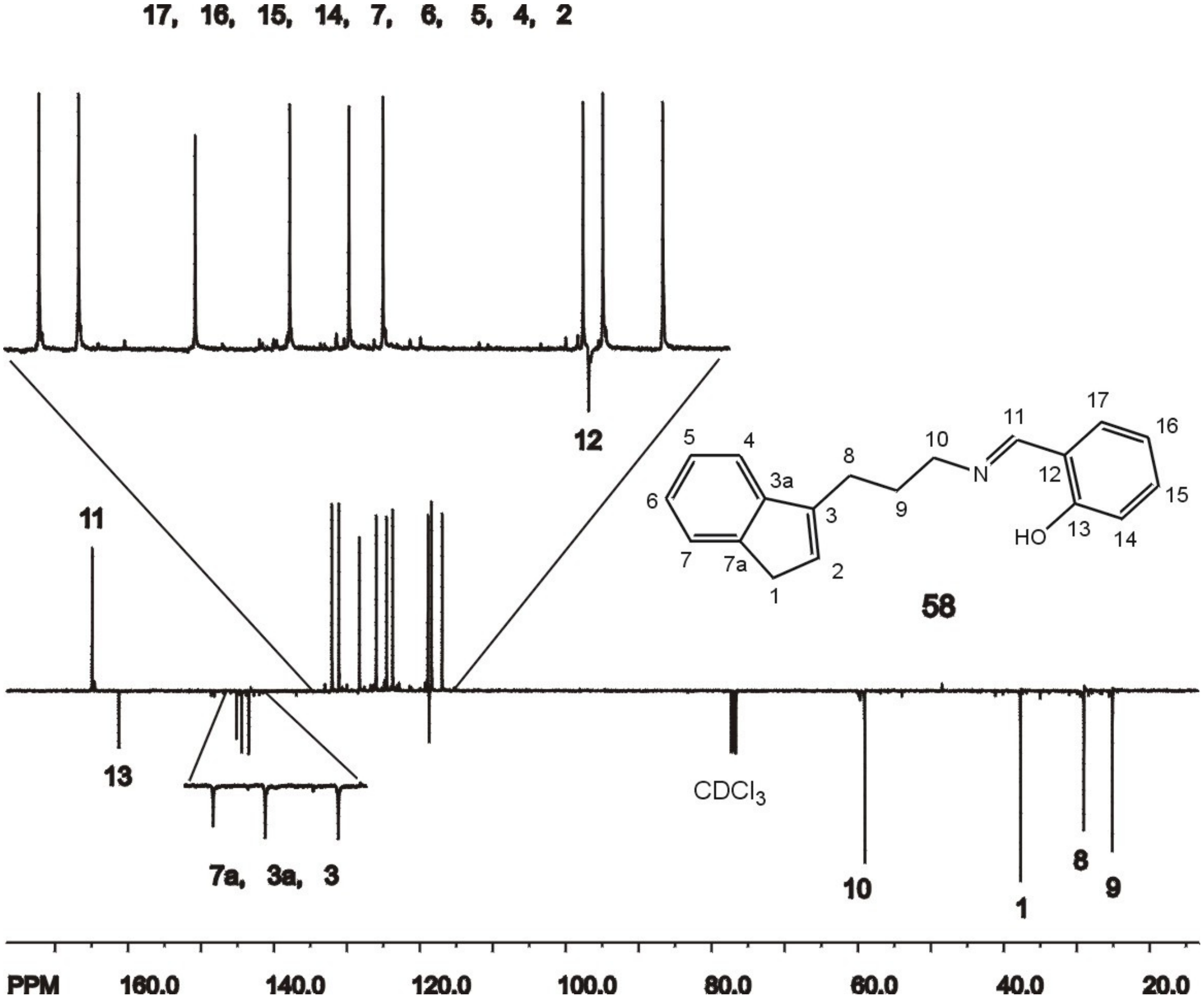

Scheme 56: ^{13}C-NMR spectrum of compound **58**.

The ^{13}C-NMR spectrum of compound **58** (Scheme 56) shows the signal for the imino group (C11) at δ = 165.0 ppm. The signal for the quaternary carbon atom C13 arises at δ = 161.2 ppm, while the signals for the quaternary carbon atoms C7a, C3a and C3 can be located at δ = 145.1, 144.4 and 143.4 ppm. At δ = 118.7 ppm, the signal for the quaternary carbon atom C12 appears. The signals for the aromatic CH groups (C17, C16, C15, C14, C7, C6, C5, C4 and C2) can be found at δ = 132.0, 131.1, 128.3, 126.0, 124.6, 123.7, 118.9, 118.4 and 117.0 ppm. The signal of the methylene group attached to the nitrogen atom (C10) appears at δ = 59.0 ppm, while the signal at δ = 37.7 ppm is assigned to the indenyl methylene group C1. The signals at δ = 29.0 and 25.1 ppm result from the residual methylene groups (C8 and C9) of the alkyl chain.

In the MS spectrum of compound **58** (Scheme 57), the molecular ion peak can be found at m/z = 277 with 64% intensity relative to the base peak. Loss of the hydroxyl group results in the peak at m/z = 260 with 9% intensity relative to the base peak, while the fragmentation at the C9-C10 bond results in the base peak at m/z = 134.

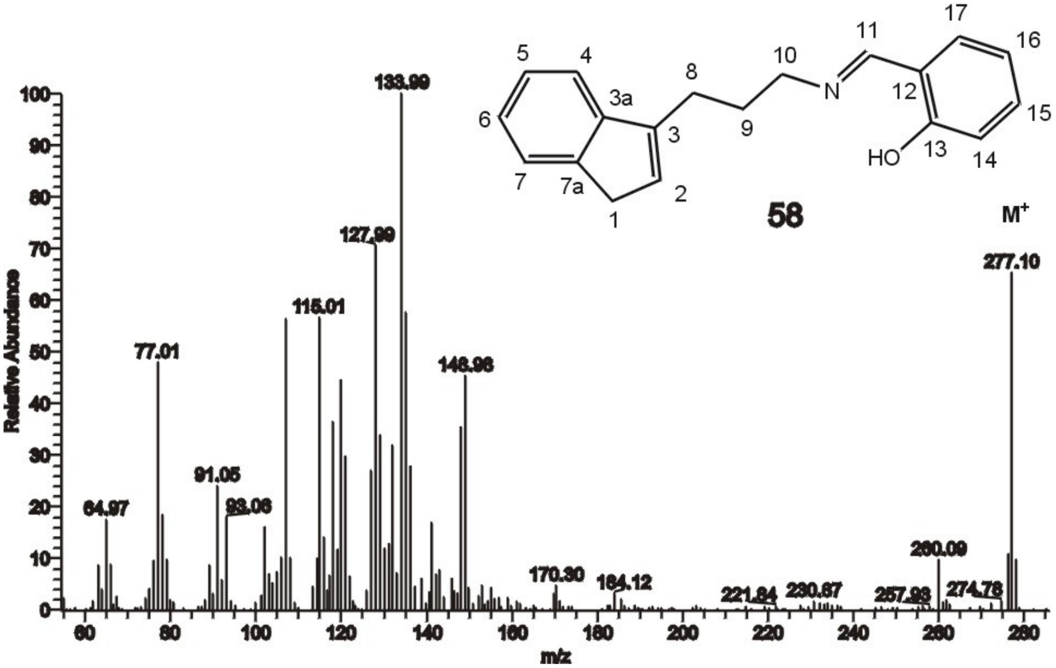

Scheme 57: MS spectrum of compound **58**.

Table16: NMR and MS data of compounds 58-61.

No.	^{1}H-NMR$^{a)}$	^{13}C-NMR$^{a)}$	MS [m/z (%)]
58	13.63 br (1H, OH) 8.38 s (1H, HC=N) 7.51-7.47 m (1H) 7.40-7.18 m (5H) 7.01-6.97 m (1H) 6.97-6.87 m (1H) 6.27 br (1H, Ind-H2) 3.71 t (2H, CH$_2$) 3.37 br (2H, Ind-H1) 2.73-2.65 m (2H, CH$_2$) 2.20-2.06 m (2H, CH$_2$)	165.0 (C=N) 161.2, 145.1, 144.4, 143.4, 118.7 (C$_q$) 132.0, 131.1, 128.3, 126.0, 124.6, 123.7, 118.9, 118.4, 117.0 (CH) 59.0 (CH$_2$) 37.7 (CH$_2$-Ind) 29.0, 25.1 (CH$_2$)	277 [M$^+$] (64) 260 (9) 149 (33) 134 (100) 128 (78) 115 (71) 77 (50)
59	16.76 br (1H, OH) 7.47-7.41 m (2H) 7.36-7.33 m (1H) 7.29-7.23 m (2H) 7.20-7.15 m (1H) 6.93-6.90 m (1H) 6.74-6.70 m (1H) 6.22 br (1H, Ind-H2) 3.56 t (2H, CH$_2$) 3.30 br (2H, Ind-H1) 2.73-2.68 m (2H, CH$_2$) 2.24 s (3H, CH$_3$) 2.16-2.09 m (2H, CH$_2$)	171.6 (C=N) 164.8, 145.0,144.4, 143.2 (C$_q$) 132.5, 128.3, 127.8, 125.9, 124.5, 123.6, 119.0, 118.8, 116.5 (CH) 48.3 (CH$_2$) 37.6 (Ind-CH$_2$) 28.4 (CH$_2$) 25.2 (CH$_2$) 14.1 (CH$_3$)	n.d.
60	7.67-6.64 m (2H) 7.45-7.42 m (2H) 7.38-7.33 m (3H) 7.29-7.25 m (1H) 7.21-7.17 m (1H) 6.26 br (1H, NH) 6.24 br (1H, Ind-H2) 3.53 m (2H, CH$_2$)	167.7 (O=C-N) 145.2, 144.7, 143.6, 134.9 (C$_q$) 131.5, 128.7, 127.0, 126.9, 126.3, 124.9, 124.0, 119.1 (CH) 40.2 (CH$_2$) 37.9 (Ind-CH$_2$) 28.0 (CH$_2$)	277 [M$^+$] (6) 156 (100) 105 (65) 77 (26)

No.	^{1}H-NMR$^{a)}$	^{13}C-NMR$^{a)}$	MS [m/z (%)]
	3.30 br (2H, CH_2) 2.64 m (2H, CH_2) 2.01 m (2H, CH_2)	25.5 (CH_2)	
61	7.75-7.72 m (2H) 7.68-7.65 m (2H) 7.50-7.47 m (2H) 7.45-7.42 m (1H) 7.39-7.33 m (4H) 7.31-7.26 m (2H) 6.00 br (1H, NH) 4.05-4.01 m (1H, Flu-H9) 3.33-3.28 m (2H, CH_2) 2.17-2.12 m (2H, CH_2) 1.34-1.27 m (2H, CH_2)	167.4 (O=C-N) 146.7, 141.2, 134.6 (C_q) 131.3, 128.4, 127.1, 127.0, 126.8, 124.2, 119.8 (CH) 46.8 (CH, Flu-C9) 40.0 (CH_2) 29.8 (CH_2) 25.2 (CH_2)	n.d.

a) δ (ppm) rel. $CHCl_3$ (7.24 ppm, ^{1}H-NMR) and rel. $CDCl_3$ (77.0 ppm, ^{13}C-NMR) at 298 K

2.5.3 Attempted synthesis of titanium and zirconium complexes of indene-phenoxyimine and indene-amidine bridged compounds

Deprotonation of the indene-phenoxyimine and indene-amidine bridged compounds with two equivalents of n-butyllithium followed by the addition of one equivalent of titanium tetrachloride or zirconium tetrachloride did not yield the desired complexes but gave unidentified residues. The dilithium salts of compounds **58**-**61** could not be characterized by NMR spectroscopy because of their insolubility in common deuterated solvents. However, the NMR spectra of their bis (trimethylsilyl) derivatives show that deprotonation does not occur at the indenyl or fluorenyl moiety. Instead, deprotonation occurs at the hydroxyl group and the imino CH (-N=CH) or imino methyl (-N=C-CH_3) group of the indene-phenoxyimine bridged compounds. In case of indene-amidine and fluorene-amidine bridged compounds, n-butyllithium reacts with the amido NH group and the carbonyl group instead of deprotonating the indenyl or fluorenyl groups.

3. Experimental

3.1 General

Schlenk technique was used to carry out the experimental work. Argon was purified before its use as an inert gas. Methylene chloride was distilled over phosphorus pentoxide. Toluene, tetrahydrofuran, diethyl ether and n-pentane were purified by distillation over Na/K alloy. Diethyl ether was additionally distilled over lithium aluminum hydride, while toluene was additionally distilled over phosphorus pentoxide. Deuterated solvents ($CDCl_3$, CD_2Cl_2, C_6D_6 and DMSO) were purchased from Eurisotop and stored over molecular sieves (3 Å). Argon (5.0) and ethylene (3.5) were purchased from Rieβner Company. Methylaluminoxane (10% in toluene) was purchased from Chemtura Europe Limited. All other starting materials were commercially available and used as received.

3.2 NMR spectroscopy

NMR spectra were recorded with Varian Inova (300 MHz) and Varian Inova (400 MHz) spectrometers. All spectra were recorded at 298 K. In the ^1H-NMR spectra the chemical shift of the residual proton signal of the solvent was used as a reference (δ = 7.24 ppm for chloroform, δ = 5.30 ppm for methylene chloride, δ = 7.16 ppm for benzene and δ = 2.50 ppm for DMSO), while in the ^{13}C-NMR spectra the chemical shift of the solvent was used as a reference (δ = 77.0 ppm for chloroform-d_1, δ = 54.0 ppm for methylene chloride-d_2, δ = 128.0 ppm for benzene-d_6 and δ = 39.50 for DMSO-d_6).

3.3 GC/MS

GC/MS spectra were recorded with a FOCUS Thermo gas chromatograph combined with a DSQ mass detector. A 30 m HP-5 fused silica column (internal diameter 0.32 mm, film 0.25 µm and flow 1 mL/min) was used and helium (4.6) was applied as carrier gas. The measurements were recorded using the following temperature program:

Starting temperature: 50 °C, duration: 2 minutes;
Heating rate: 20 °C/minute, duration: 12 minutes;
Final temperature: 290 °C, duration: 27 minutes.

3.4 Mass spectrometry

Mass spectra were recorded with a VARIAN MAT CH-7 instrument (direct inlet, EI, E = 70 Ev) and a VARIAN MAT 8500 spectrometer at the Zentrale Analytik of the University of Bayreuth.

3.5 Elemental analysis

Elemental analyses were performed with a Vario EL III CHN instrument. Into a standard tin pan, 4-6 mg of the complex was weighed, the pan was carefully closed and introduced into the auto sampler of the instrument. The values of C, H and N were calibrated using acetamide as a standard.

3.6 DSC analysis

DSC analyses were performed on a Mettler Toledo DSC/SDTA 821e instrument. The polymer samples were prepared by enclosing 4-6 mg of the polymers in standard aluminum pans. The samples were introduced into the auto sampler of the instrument and the measurements were recorded using the following temperature program:

First heating phase: from 50 °C to 160 °C (10 °C/minute);

Cooling phase: 160 °C to 50 °C (10 °C/minute);

Second heating phase: from 50 °C to 160 °C (10 °C/minute).

Nitrogen was used as a cooling medium. Melting enthalpies and melting points were taken from the second heating phase. The values were calibrated using indium as a standard (m.p. 429.78 K, H_m = 28.45 J/g).

3.7 Viscometry analysis

Viscometry analyses for the determination of the viscosity average molecular weights of the polyethylene samples were performed on an Ubbelohde precision capillary viscometer in cis/trans-decalin at 135 ± 0.1 °C. For the preparation of the sample solutions, 50 mg polymer was dissolved in 45 mL decalin by heating at 135 °C overnight. M_η were determined by comparing the obtained values with calibration curves available for different polymer concentrations.

3.8 Polymerization of ethylene

For the homogeneous polymerization of ethylene, few milligrams of the complexes were dissolved in toluene (5-10 mL) and activated with methylaluminoxane (MAO). The activated complexes were suspended in pentane (250 mL) and transferred to a 1l Büchi autoclave under inert atmosphere. The temperature of the thermostat was adjusted to the desired value and an ethylene pressure of 10 bar was applied for one hour. After releasing the pressure, the obtained polymer was filtered over a frit, washed with dilute hydrochloric acid, water and finally with acetone and dried under vacuum.

3.9 Syntheses

3.9.1 General synthesis procedure for ω-bromo-1-indenylalkanes

An amount of 10 mmol of n-butyllithium (1.6 M in hexanes) was added to 10 mmol of indene dissolved in 100 mL diethyl ether at -78 °C. After warming up to room temperature and stirring for further 3 hours, the solution was cooled to -78 °C and 10 mmol of the appropriate dibromoalkane was added. The solution was allowed to warm up to room temperature and stirred for further 12 hours. Distilled water was added to the solution, the organic layer was separated and dried over sodium sulphate. After removing the solvent, the residue was distilled to obtain oily compound in 60-70% yield.

3.9.2 General synthesis procedure for ω-bromo-1-phenoxyalkanes

An amount of 10 mmol of an appropriate phenol, 10 mmol of potassium carbonate, 30 mmol of the desired dibromoalkane and catalytic amounts of 18-crown-6 were refluxed in acetone for 24-72 hours. The reaction mixture was cooled, the solvent was removed followed by the addition of distilled water and extraction with diethyl ether (2×100 mL). After passing over sodium sulphate and removing the solvent, the residue was distilled to obtain the required compound in 80-90% yield.

3.9.3 General synthesis procedure for indenyl compounds with phenoxy and naphthoxy substituents (1-14)

Method 1: The appropriate phenol (5 mmol), an ω-bromo-1-indenylalkane (5 mmol), potassium carbonate (5 mmol) and catalytic amounts of 18-crown-6 were refluxed in acetone for 24-72 hours. After cooling the mixture, acetone was removed and 100 mL of distilled water was added. The mixture was extracted with diethyl ether (2×100 mL) and dried over sodium sulphate. After removing diethyl ether, the residue was distilled to obtain the desired compound in 60-70% yield.

Method 2: An amount of 5 mmol of n-butyllithium (1.6 M in n-hexane) was added to 5 mmol of indene dissolved in 100 mL of diethyl ether at -78 °C. After warming up to room temperature and stirring for further 3 hours, the solution was cooled to -78 °C and 5 mmol of the ω-bromo-1-phenoxyalkane was added. The solution was allowed to warm up to room temperature and stirred for further 12 hours. The solution was washed with distilled water and dried over sodium sulphate. Removal of the solvent provided the desired compound in almost quantitative yield.

3.9.4 General synthesis procedure for symmetric phenoxy and naphthoxy substituted zirconocene and hafnocene dichloride complexes (15-30)

An amount of 2 mmol of the appropriate substituted indenyl compound was dissolved in 50 mL of diethyl ether. To this solution, 2 mmol of n-butyllithium (1.6 M in hexanes) was added at -78 °C. This solution was allowed to come to room temperature and stirred for further 3 hours. Then it was added to 1 mmol of zirconium tetrachloride or hafnium tetrachloride suspended in 50 mL of diethyl ether at -78 °C. The mixture was slowly allowed to come to room temperature and stirred for further 24 hours**.** Diethyl ether was removed and 100 mL of toluene was added. The toluene suspension was filtered, the volume of the filtrate was reduced and the complexes were precipitated by the addition of n-pentane. After filtration, the precipitate was washed several times with n-pentane and dried by evacuation to obtain the desired complexes as yellow powders in 50-60% yield.

Table 17: Elemental analysis data of the complexes 15-30.

No.	C_{exp}%	C_{theor}%	H_{exp}%	H_{theor}%
15	65.75	65.44	5.95	5.19
16	65.37	66.26	5.50	5.56
17	67.03	67.02	6.20	5.91
18	68.34	68.37	6.82	6.52
19	68.79	68.97	6.94	6.79
20	69.94	69.53	6.80	7.05
21	68.46	68.37	6.79	6.52

No.	C_{exp}%	C_{theor}%	H_{exp}%	H_{theor}%
22	68.71	68.97	7.04	6.79
23	69.75	69.53	7.18	7.05
24	71.68	70.91	6.14	5.21
25	64.15	64.04	5.62	4.70
26	70.93	70.92	6.18	6.51
27	71.90	71.40	5.50	5.51
28	71.42	71.86	6.49	5.80
29	69.71	69.45	6.17	5.03
30	62.87	62.31	4.96	4.52

3.9.5 General synthesis procedure for asymmetric phenoxy and naphthoxy substituted zirconocene dichloride complexes (31-36)

An amount of 1 mmol of n-butyllithium (1.6 M in hexanes) was added to 1 mmol of the appropriate substituted indenyl compound dissolved in 50 mL of diethyl ether at -78 °C. The solution was allowed to come to room temperature and stirred for further 3 hours. Then this solution was transferred to a suspension of indenyl zirconium trichloride (1 mmol) in 50 mL diethyl ether at -78 °C. The reaction mixture was allowed to come to room temperature and it was stirred for two days. Diethyl ether was removed, toluene (100 mL) was added and the mixture was filtered. The volume of the filtrate was reduced and pentane was added to precipitate the complex. After filtration, the residue was washed several times with pentane and dried under vacuum to obtain the desired complex as yellow powder in 40-50% yield.

Table 18: Elemental analysis data of complexes 31-36.

No.	C_{exp}%	C_{theor}%	H_{exp}%	H_{theor}%
31	63.65	63.90	6.01	5.54
32	64.51	64.41	5.79	5.74
33	64.55	65.89	6.09	5.94
34	65.34	65.76	4.86	4.68
35	65.76	66.65	4.95	5.11
36	64.71	64.57	6.04	4.54

3.9.6 General synthesis procedure for 9-methylfluorenyl substituted indenyl compounds (37-39)

An amount of 5 mmol of n-butyllithium (1.6 M in hexanes) was added to 5 mmol of 9-methylfluorene dissolved in 50 mL of diethyl ether at -78 °C. The mixture was stirred for three hours at room temperature. It was then again cooled to -78 °C and 5 mmol of the desired ω-bromo-1-indenylalkane was added. The mixture was stirred for 6 hours at room temperature, distilled water was added and the organic layer was separated and dried over sodium sulphate. The solvent was removed to obtain the desired compound as an oil.

3.9.7 General synthesis procedure for 9-methylfluorenyl substituted zirconocene dichloride complexes (40-42)

n-Butyllithium (2 mmol, 1.6 M in hexanes) was added to 2 mmol of the appropriate 9-methylfluorenyl substituted indenyl compound dissolved in 50 mL of diethyl ether at -78 °C. The mixture was stirred for three hours at room temperature. Then this mixture was transferred to a zirconium tetrachloride suspension (1 mmol) in 50 mL of diethyl ether at -78 °C and was stirred for 24 hours at room temperature. Diethyl ether was removed and toluene (100 mL) was added. The mixture was filtered to remove the insoluble lithium chloride and the volume of the filtrate was reduced. The complex was precipitated by adding pentane.. The precipitate was filtered, washed with pentane and dried under vacuum to obtain the desired complex as yellow powder in 40-50% yield.

Table 19: Elemental analysis data of complexes 40, 42.

No.	C_{exp}%	C_{theor}%	H_{exp}%	H_{theor}%
40	73.59	74.79	6.41	5.79
42	74.59	75.47	6.61	6.33

3.9.8 General synthesis procedure for asymmetric diamine compounds (43-46)

A mixture of 20 mmol of a dibromoalkane compound, 10 mmol of the appropriate aniline, 10 mmol of potassium carbonate and DMF (10 mL), was heated at 100-105 °C for 5 hours. After cooling to room temperature, distilled water (100 mL) was added and the mixture was extracted with diethyl ether (2×100 mL). The ether phase was dried over sodium sulphate, the solvent was removed by rotary evaporation and the residue was distilled to give the N-substituted bromoalkyl aniline derivative in 70-80% yield. 5 mmol of the appropriate N-substituted bromoalkyl aniline derivative, 5 mmol of potassium carbonate and an excess of tertiary butylamine were refluxed in 100 mL THF for 6-8 hours. After cooling to room temperature, 50 mL of distilled water and 100 mL of diethyl ether were added, the organic phase was separated and dried over sodium sulphate. The solvent was removed and the residue was distilled to give the required asymmetric diamine compound as an oil in 70-80% yield.

3.9.9 General synthesis procedure for the titanium and zirconium complexes containing asymmetric diamide ligands (47-54)

n-Butyllithium (2 mmol, 1.6 M in hexanes) was added to 1 mmol of the appropriate asymmetric diamine compound dissolved in 50 mL diethyl ether at -78 °C and the reaction mixture was stirred for 2 hours at room temperature. Then it was transferred to a metal salt suspension (1 mmol) in 50 mL diethyl ether at -78 °C and the reaction mixture was stirred for 24 hours at room temperature. Diethyl ether was removed and toluene (100 mL) was added. The mixture was filtered and the volume of the filtrate was reduced. The complexes were precipitated by adding pentane. The residue was filtered, washed with pentane and dried under vacuum to obtain the desired complex in 30-40% yield.

Table 20: Elemental analysis data of complexes 47-54.

No.	C_{exp}%	C_{theor}%	H_{exp}%	H_{theor}%	N_{exp}%	N_{theor}%
47	52.63	52.63	8.66	7.18	6.78	7.67
48	54.89	54.98	9.07	7.69	7.03	7.12
49	51.09	51.31	8.32	6.89	6.45	7.98
50	56.10	56.04	8.60	7.92	7.25	6.88
51	47.18	47.04	6.03	6.41	5.99	6.86
52	49.54	49.52	7.85	6.93	6.34	6.42
53	45.63	45.67	6.08	6.13	5.81	7.10
54	50.43	50.64	7.95	7.16	6.51	6.22

3.9.10 Synthesis procedure for the Schiff base derivative of 2-(2-aminophenyl) benzothiazole (55)

A mixture of 10 mmol 2-aminobenzoic acid, 11 mmol 2-aminothiophenol and polyphosphoric acid (10 g) was heated at 140 °C for 24 hours. After cooling, 100 mL of distilled water was added and the mixture was filtered. The precipitate was dried and recrystallized from methylene chloride to obtain 2-(2-aminophenyl)benzothiazole. An amount of 2 mmol of benzaldehyde was added to a solution of 2-(2-aminophenyl)benzothiazole (2 mmol) in ethanol (20 mL) at room temperature and stirred overnight. The reaction mixture was filtered and the precipitate was dried to obtain the desired compound in almost quantitative yield.

3.9.11 General synthesis procedure for the titanium and zirconium complexes of the Schiff base derivative 55

The Schiff base compound **55** (1 mmol), dissolved in 25 mL of toluene, was added to 1 mmol of a metal salt suspended in 25 mL of toluene at 0 °C. The mixture was stirred at room temperature for 4 hours and filtered. The precipitate was washed with pentane and dried under vacuum to obtain the desired complex in 60-70% yield.

Table 21: Elemental analysis data of complexes 56-57.

No.	C_{exp}%	C_{theor}%	H_{exp}%	H_{theor}%	N_{exp}%	N_{theor}%
56	48.60	47.65	3.37	2.80	5.63	5.56
57	44.82	43.88	3.35	2.58	5.22	5.12

3.9.12 General synthesis procedure for the indene-phenoxyimine bridged compounds 58 and 59

Triethylamine (60 mmol) and chlorotrimethylsilane (40 mmol) were added to 3-bromopropylamine hydrobromide (20 mmol) dissolved in 100 mL of methylene chloride at 0 °C. The reaction mixture was stirred overnight at room temperature. Methylene chloride was removed, pentane (100 mL) was added and the mixture was filtered. The solvent was removed from the filtrate to obtain N,N-bis(trimethylsilyl)-3-bromopropylamine in almost quantitative yield. Indenyllithium (10 mmol), dissolved in 50 mL of THF, was added dropwise to N,N-bis(trimethylsilyl)-3-bromopropylamine (10 mmol) dissolved in 50 mL of THF at room temperature and the reaction mixture was stirred overnight. THF was removed, pentane was added and the mixture was filtered. After removing the solvent, N,N-bis(trimethylsilyl)-3-indenylpropylamine was obtained in almost quantitative yield. 50 mL of a HBr solution (1M) was added to the above N,N-bis(trimethylsilyl)-3-

indenylpropylamine and the mixture was stirred at 50 ℃ for 2 hours. Then sodium hydroxide solution (1M) was added dropwise until the mixture was slightly alkaline and extracted with pentane (3×100 mL). Pentane was removed to afford 1-(3-aminopropyl) indene as yellow oil in 80% yield. An amount of 2 mmol of the appropriate 2-hydroxy aldehyde or ketone was added to 2 mmol of 1-(3-aminopropyl) indene in 50 mL of methanol and refluxed for 4 hours. The solution was kept at -24 ℃ for 24 hours, the solvent was decanted, the residual thick oil was washed with little methanol and dried under vacuum to obtain the indene-phenoxyimine bridged compound as yellow thick oil.

3.9.13 General synthesis procedure for the indene-amidine and fluorene-amidine bridged compounds 60 and 61

Benzoyl chloride (2 mmol) in 25 mL of methylene chloride was added dropwise to 1-(3-aminopropyl) indene (2 mmol) and triethylamine (3 mmol) dissolved in 25 mL of methylene chloride at room temperature. The mixture was refluxed for 6 hours, cooled to room temperature, washed with 50 mL of distilled water and dried over sodium sulphate. The solvent was removed to obtain an indene-amidine bridged compound as a light brown powder. Fluorene-amidine bridged compounds were prepared in the same way.

4. Summary

The aim of the project included the synthesis and characterization of new group (IV) metal complexes and their applications as catalysts in homogeneous ethylene polymerization reactions. For this purpose, different types of organic compounds and their group (IV) metal complexes were synthesized and tested for ethylene polymerization after activation with MAO.

The first part of this work describes the synthesis of symmetric and asymmetric metallocene dichloride complexes bearing bulky alkoxy substituents on indenyl moieties and the investigation of their potential as ethylene polymerization catalysts.

Indenyl compounds bearing bulky alkoxy substituents can be prepared by refluxing phenol or naphthol derivatives with ω-bromo-1-indenylalkanes and potassium carbonate in the presence of catalytic amounts of 18-crown-6 in acetone. They can be prepared in better yields by the reaction of ω-bromo-1-phenoxyalkanes with indenyl lithium.

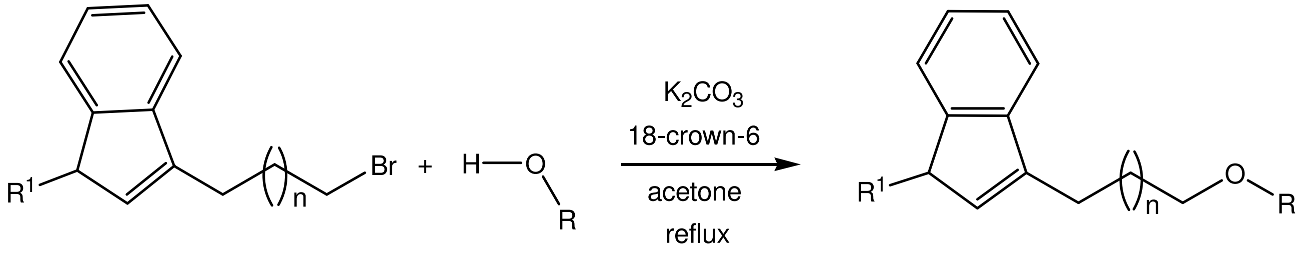

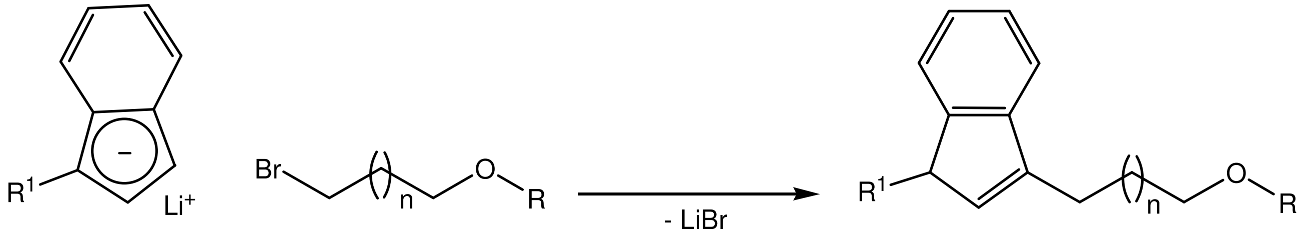

n = 1, 2, 3; R^1 = H, Me; R = substituted phenyl

Symmetric metallocene dichloride complexes were synthesized by deprotonating the alkoxy substituted indenyl compounds with n-butyllithium followed by the reaction with metal tetrachlorides.

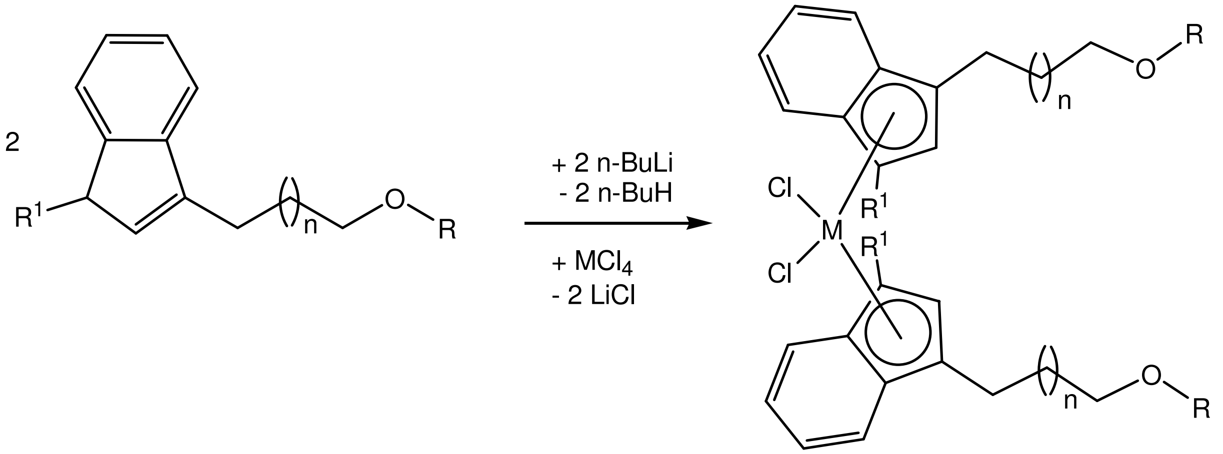

M = Zr, Hf; n = 1, 2, 3; R^1 = H, Me; R = substituted phenyl

Asymmetric metallocene dichloride complexes were synthesized by deprotonating alkoxy substituted indenyl compounds with n-butyllithium followed by the reaction with indenyl zirconium trichloride.

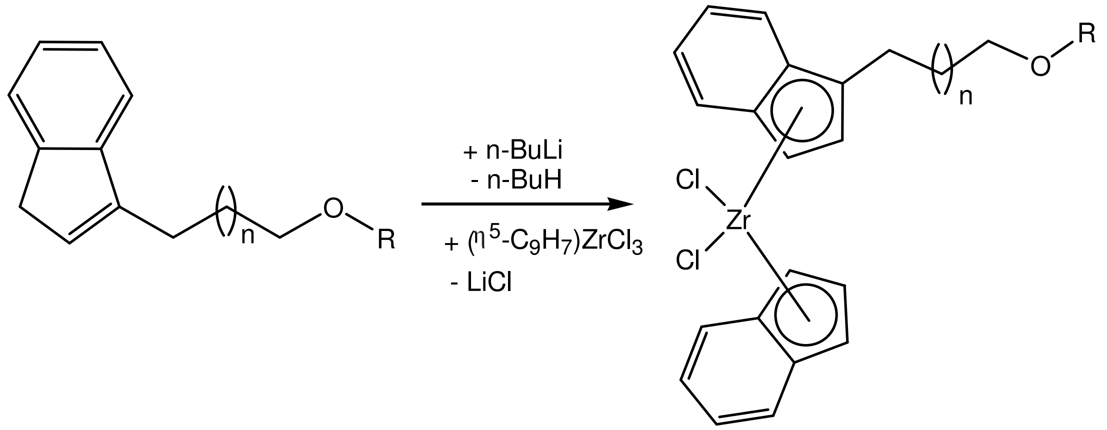

n = 1, 2, 3; R = substituted phenyl

The second part of this work deals with the synthesis of bis (indenyl) zirconium dichloride complexes bearing bulky 9-methyl fluorenyl substituents.

9-Methyl fluorenyl substituted indenyl compounds can be synthesized by the reaction of ω-bromo-1-indenylalkanes with the lithium salt of 9-methyl fluorene. The reaction of zirconium tetrachloride with the lithium salts of the substituted indenyl compounds afford the bis (indenyl) zirconium dichloride complexes in good yields.

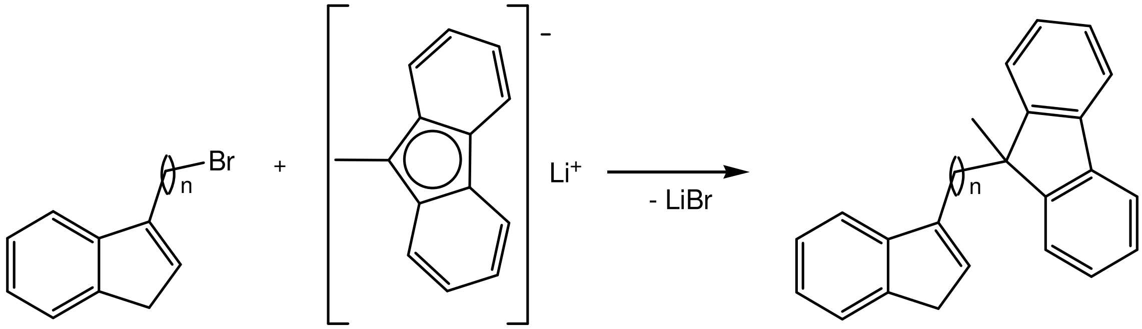

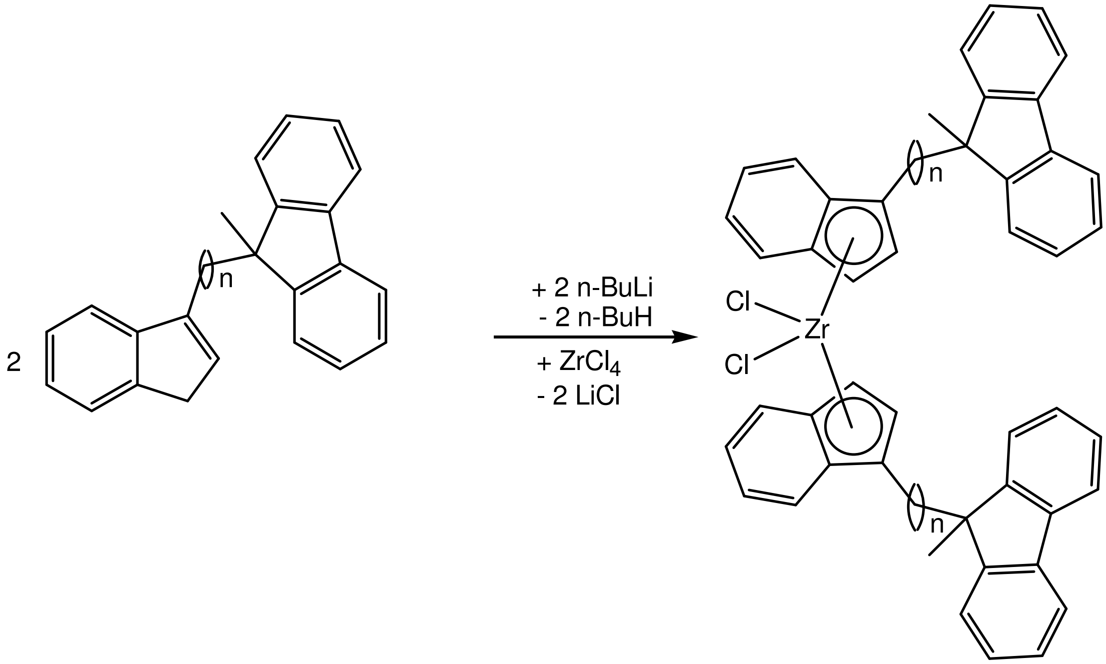

n = 2, 3, 4

Asymmetric chelating diamide complexes of titanium and zirconium were also synthesized and tested for ethylene polymerization as a part of the project.

Reaction of the desired aniline with an appropriate dibromoalkane compound affords the N-substituted bromoalkyl aniline derivative which can react with tertiary butyl amine to yield the desired asymmetric diamine compound.

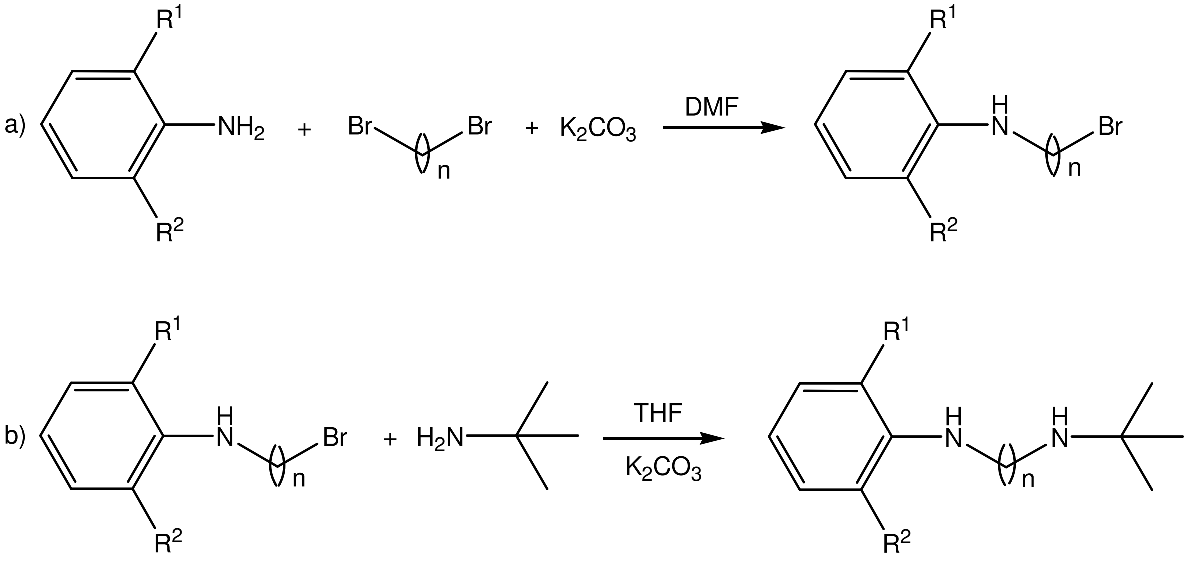

$R^1 = R^2 =$ alkyl; n = 2, 3

Deprotonation of the diamine compounds with n-butyllithium followed by the reaction with titanium tetrachloride or zirconium tetrachloride yields the desired chelating diamide complexes.

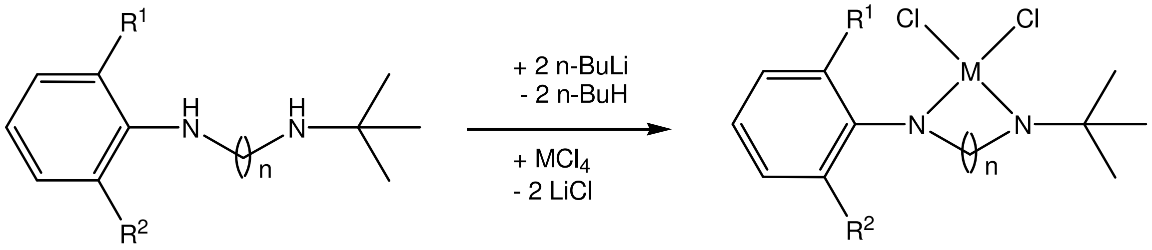

$R^1 = R^2 =$ alkyl; n = 2, 3; M = Ti, Zr

Titanium and zirconium complexes with a Schiff base derivative of 2-(2-aminophenyl)benzothiazole were also synthesized. The reaction of 2-(2-aminophenyl)benzothiazole with benzaldehyde yields its Schiff base derivative which can react with titanium tetrachloride or zirconium tetrachloride to afford the desired complexes.

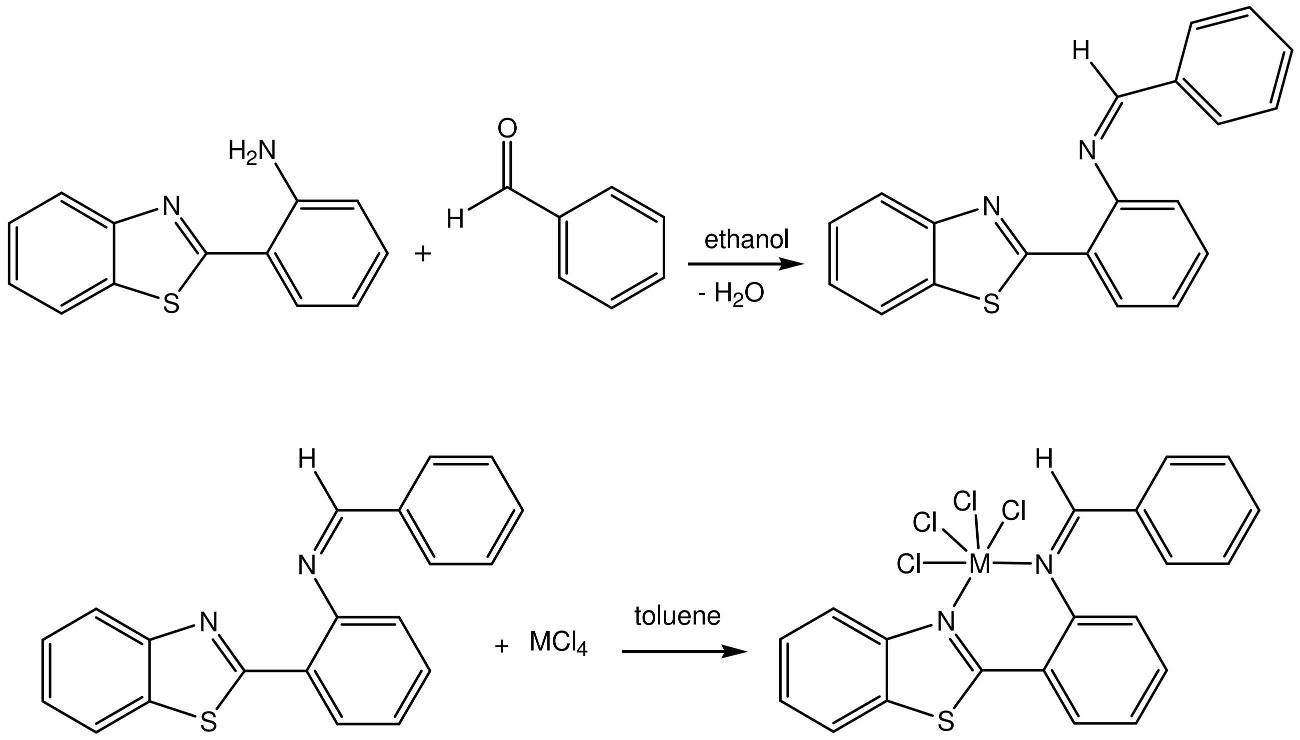

M = Ti, Zr

The above mentioned complexes were used for homogeneous ethylene polymerization after activation with MAO (M:Al = 1:2000).

The alkoxy substituted metallocene catalysts showed good to moderate activities which depend on the length of the bridging alkylidene chain between alkoxy group and indenyl ligand of the zirconocene dichloride complex as well as the steric bulk of the alkoxy substituent. The activity maximum (27467 kg PE/mol cat. h) was found for a chain length of four carbon atoms (catalyst **19**). Further increase or decrease in the chain length resulted in a decrease of activity. The decrease of steric bulk at the phenoxy group also resulted in a decrease of activity.

The 9-methyl fluorenyl substituted metallocene catalysts showed good activities towards ethylene polymerization. The catalyst **42** with butylidene bridge between 9-methyl fluorenyl group and indenyl ligand showed the maximum activity (15786 kg PE/mol cat. h).

The activated asymmetric chelating diamide complexes of titanium and zirconium (M:Al = 1:1000) showed low activities. The complex **48** bearing bulky isopropyl groups at the aniline moiety showed the highest activity (263 kg PE/mol cat. h). The activity decreased by decreasing the steric bulk at the aniline moiety.

Titanium and zirconium complexes of the Schiff base derivative of 2-(2-aminophenyl) benzothiazole also showed low activities (432 and 276 kg PE/mol cat. h) after activation with MAO (M:Al = 1:2000). A possible reason for the low activity could be the coordination of the sulphur atom to the active species.

The obtained polyethylenes were analyzed by differential scanning calorimetry (DSC) and viscometry analysis.

The symmetric alkoxy substituted metallocene catalysts produced polyethylenes of low melting points, melting enthalpies, crystallinities and viscosity average molecular weights (112.9 J/mol, 126 ˚C, 0.39 and 270000 g/mol (catalyst **23**)) than their asymmetric analogues (155.3 J/mol, 137.2 ˚C, 0.54 and 420000 g/mol (catalyst **33**)).

The polyethylenes produced by 9-methyl fluorenyl substituted metallocene catalysts are of medium melting points, melting enthalpies and crystallinities (142 J/mol, 129.3 ˚C and 0.49 (catalyst **42**)). The polyethylenes produced by the asymmetric chelating diamide catalysts have medium melting points but low melting enthalpies and crystallinities (137.8 J/mol, 116.5 ˚C and 0.44 (catalyst **52**)).

Zusammenfassung

Ziel dieser Arbeit war die Synthese und Charakterisierung neuer Gruppe IV Übergangsmetallkomplexe und die Untersuchung ihrer katalytischen Eigenschaften hinsichtlich der homogenen Polymerisation von Ethen. Dazu wurde eine Reihe verschiedener Ligandvorstufen und deren Metallkomplexe hergestellt und nach Aktivierung mit MAO für die Polymerisation von Ethen getestet.

Der erste Teil dieser Arbeit befasst sich mit der Synthese symmetrischer und asymmetrischer Metallocenkomplexe mit sterisch anspruchsvollen Alkoxy- substituierten Indenyl-Einheiten und die Untersuchung ihrer katalytischen Eigenschaften. Diese substituierten Indenyle können einfach durch die Umsetzung von ω-Brom-1-Indenalkanen in siedendem Phenol oder Naphthol mit Kaliumcarbonat und katalytischen Mengen 18-Krone-6 in Aceton hergestellt werden. Höhere Ausbeuten können durch die Umsetzung von ω-Brom-1-Phenoxyalkanen mit Indenyllithium erreicht werden.

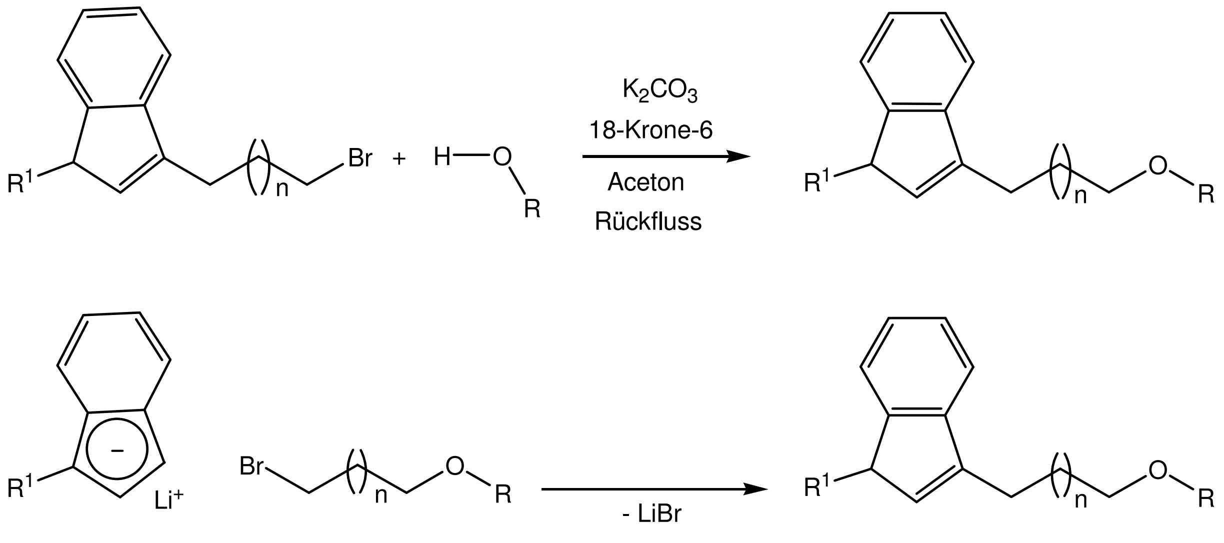

n = 1, 2, 3; R^1 = H, Me; R = substituiertes Phenyl

Die Darstellung der symmetrischen Koordinationsverbindungen erfolgte durch Deprotonierung der Indenylverbindungen mit n-BuLi und anschließender Umsetzung mit den entsprechenden Metalltetrachloriden.

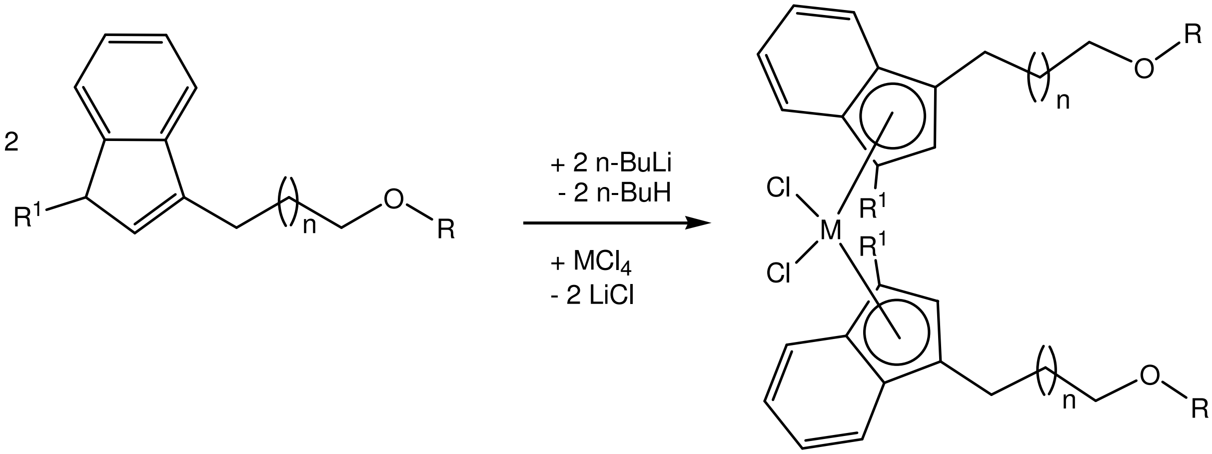

M = Zr, Hf; n = 1, 2, 3; R^1 = H, Me; R = substituiertes Phenyl

Die Darstellung der asymmetrischen Komplexe erfolgte nach Deprotonierung durch die Umsetzung mit Indenylzirkoniumtrichlorid.

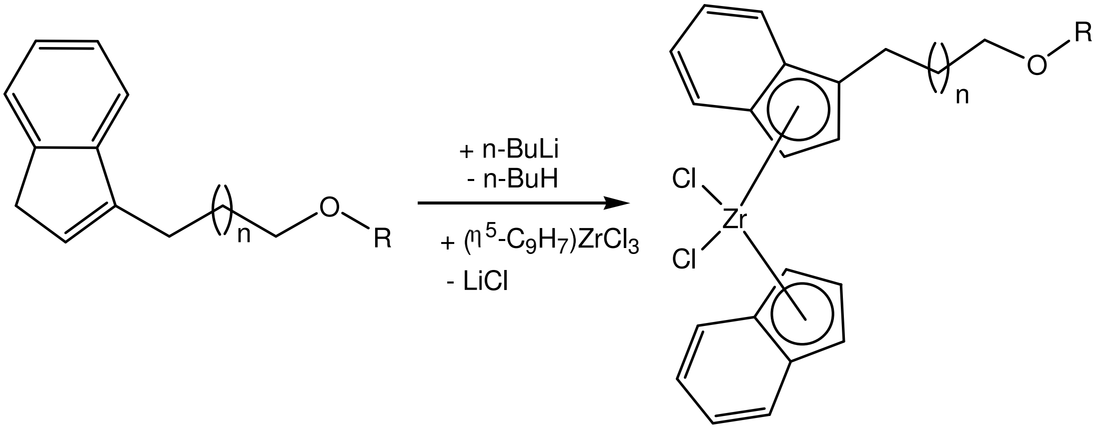

n = 1, 2, 3; R = substituiertes Phenyl

Der zweite Teil der Arbeit beschreibt die Synthese von Bis(indenyl)zirkoniumkomplexen mit sterisch anspruchsvollen 9-Methyl-fluorenyl Substituenten. Diese können durch die Reaktion von ω-Brom-1-Indenylalkanen und dem Lithiumsalz des 9-Methylfluorens erzeugt werden. Die Darstellung der Koordinationsverbindungen mit Zirkoniumtetrachlorid aus den entsprechenden Lithiumsalzen der substituierten Indenyle erfolgte in guten Ausbeuten.

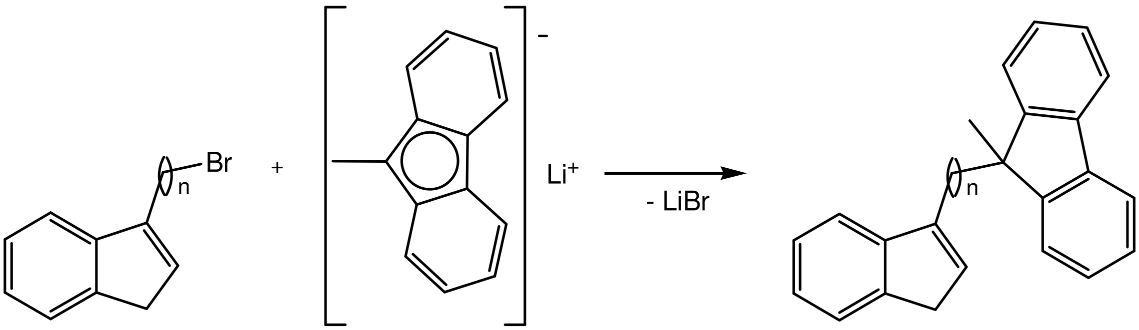

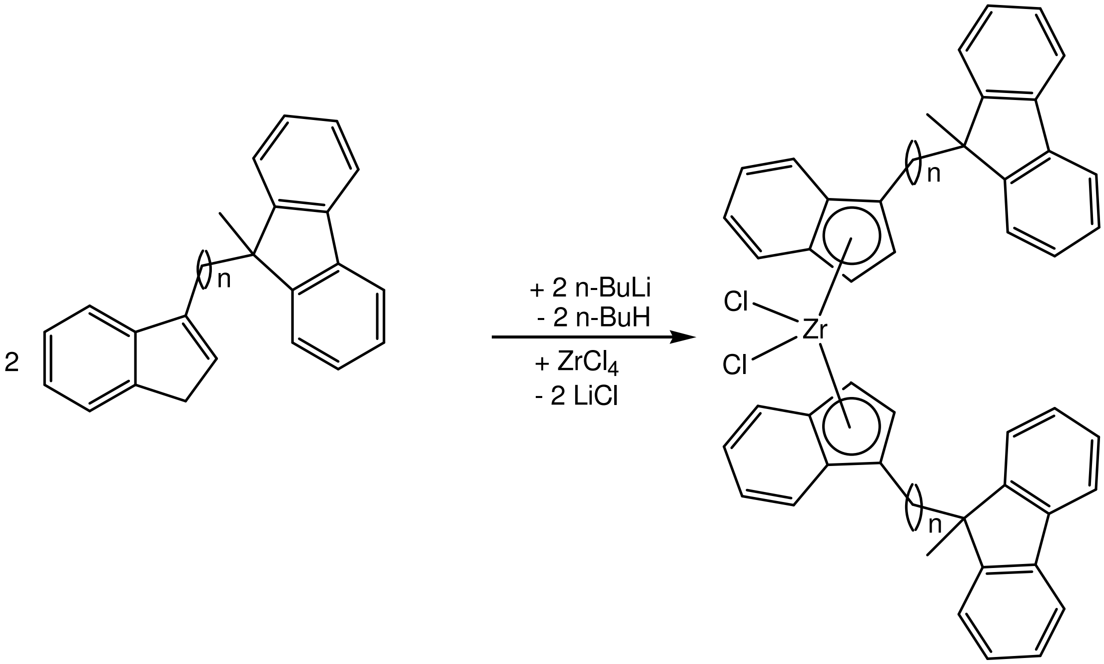

n = 2, 3, 4

In einem weiteren Kapitel wurden asymmetrische chelatisierende Diamid- verbindungen und deren Koordinationsverbindungen mit Titan und Zirkonium dargestellt und hinsichtlich der Polymerisation von Ethen untersucht. Die Reaktion eines Anilins mit dem entsprechenden Dibromalkan die N-substituierten Bromalkylaniline, welche mit t-Butyl-Amin zum gewünschten asymmetrischen Diamin umgesetzt werden können.

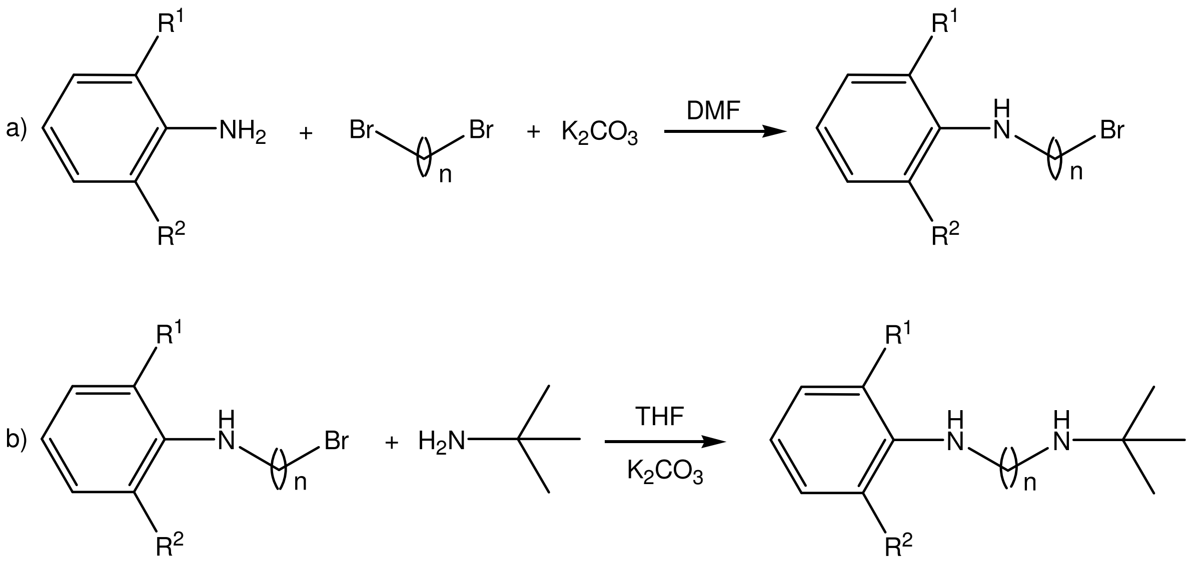

$R^1 = R^2 =$ Alkyl; n = 2, 3

Nach Deprotonierung mit n-BuLi und Reaktion mit Titan- bzw. Zirkoniumtetrachlorid wurden die Diamid-Chelatkomplexe erhalten.

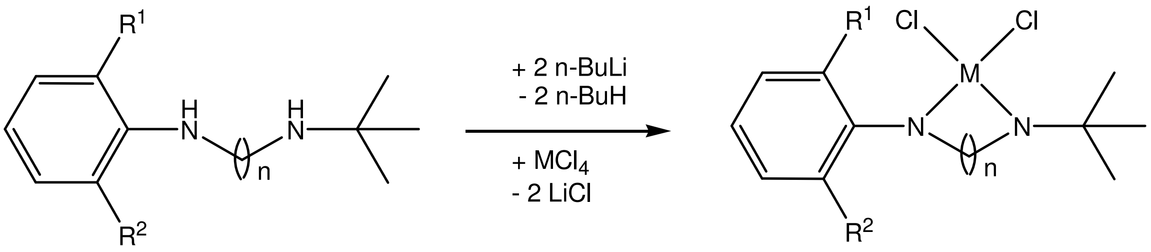

$R^1 = R^2 =$ Alkyl; n = 2, 3; M = Ti, Zr

Es wurden auch Titan- und Zirkoniumkomplexe mit einem 2-(2-Aminophenyl)benzthiazolderivat hergestellt. Die Schiff-Base Reaktion von 2-(2-Aminophenyl)benzthiazol mit Benzaldehyd ergab die gewünschte organische Verbindung, welche mit Titan- bzw. Zirkoniumtetrachlorid komplexiert wurde.

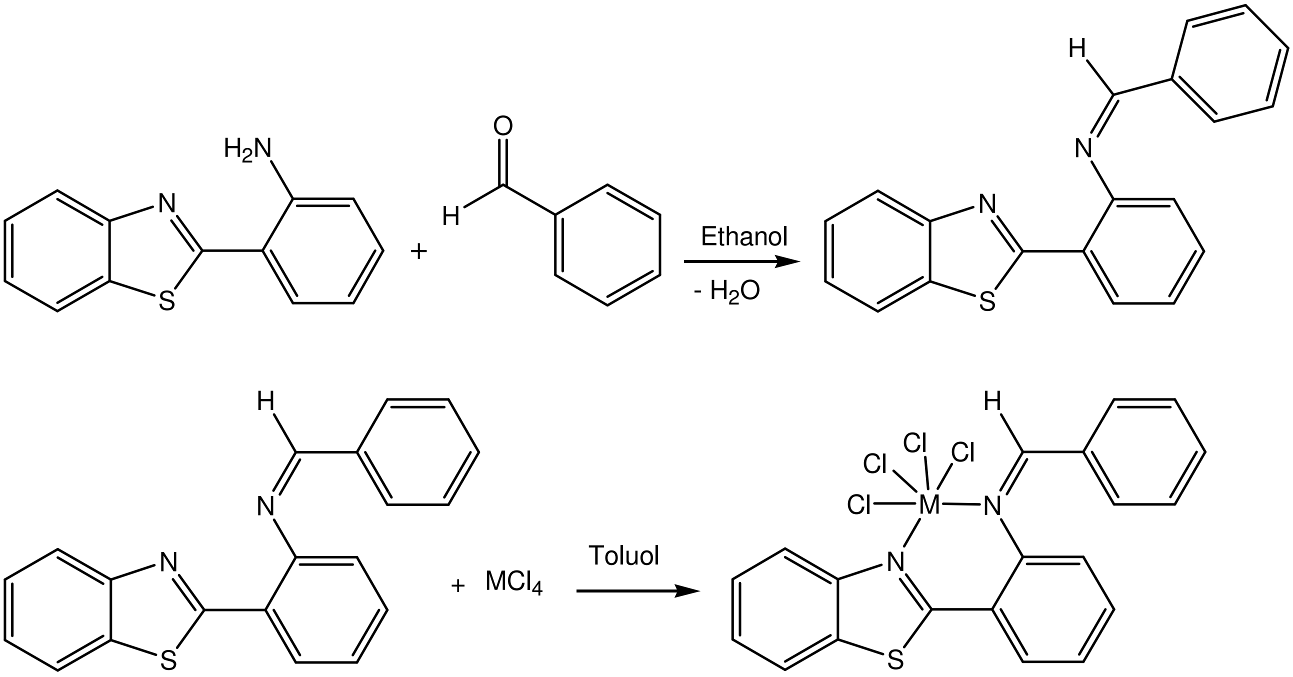

M = Ti, Zr

Die hier erwähnten Komplexe wurden mit MAO (M:Al = 1:2000) aktiviert und zur katalytischen Polymerisation von Ethen getestet.

Metallocenkomplexe mit Alkoxy Substituenten wiesen mittlere bis hohe Aktivitäten auf. Diese waren erheblich von der Länge der verbrückenden Alkylkette und dem sterischen Anspruch des Substituenten abhängig. Das Maximum der Aktivität lag bei einer Alkylkettenlänge von 4 Kohlenstoffen (27467 kg PE/mol cat. h (Komplex **19**)). Alle längeren oder kürzeren Ketten wiesen geringere Aktivitäten auf. Der sterische Anspruch der Substituenten verhielt sich indirekt proportional zu den gefundenen Aktivitäten.

Komplex **42** hatte mit 15786 kg PE/mol cat. h die höchste Aktivität dieser Substitutionsreihe.

Die asymmetrischen Amidkomplexe von Titan und Zirkonium (M:Al = 1:1000) zeigten geringere Aktivitäten. Komplex **48** mit Isopropylgruppen am Anilinfragment zeigte die höchste Aktivität dieser Reihe (263 kg PE/mol cat. h).

Die Titan- und Zirkoniumkomplexe mit dem Schiff-Base Derivat 2-(2-Aminophenyl)benzthiazol wiesen geringe Aktivitäten auf (432 und 276 kg PE/mol cat. h), vermutlich aufgrund der Koordination des Schwefels an der Metall.

Die erhaltenen Polyethylene wurden mittels DSC (differential scanning calorimetry) und Viskosimetrie analysiert.

Die Polymere der Metallocenkomplexe mit Alkoxysubstituenten hatten in der Regel niedrige Schmelzpunkte, Schmelzenthalpien, Kristallinitätsgrade und Molekulargewichte. Für die symmetrischen Komplexe ergaben sich 112.9 J/mol, 126 °C, 0.39 und 270000 g/mol (Komplex **23**), für die asymmetrischen Komplexe 155.3 J/mol, 137.2, 0.54 und 420000 g/mol (Komplex **33**) als gefundene Werte. Die 9-Methylfluorenyl substituierten Metallocenkomplexe erzeugten Polyethylene mit mittleren Schmelzpunkten, aber niedrigen Schmelzenthalpien und Kristallinitätsgraden (142 J/mol, 129.3 °C und 0.49 (Komplex **42**). Die asymmetrischen Diamidkomplexe erzeugten PE mit mittleren Schmelzpunkten aber niedrigen Enthalpien und Kristallinitätsgraden (137.8 J/mol, 116.5 °C und 0.44 (Komplex **52**).

References

[1] J. R. Severn, J. C. Chadwick, R. Duchateau, N. Friederichs, *Chem. Rev.* **2005**, *105*, 4073.

[2] Neufeldt, *Chronik der Chemie 1800-1980*, VCH, Weinheim, **1987**.

[3] R. B. Seymour, T. Cheng, *History of Polyolefins*, **1986**, Riedel Pub. Co., New York.

[4] J. P. Hogan, R. L. Banks, *Belg. Pat. 530617*, **1955**; *U. S. 2825721*, **1958**.

[5] K. Ziegler, H. Gellert, H. Kühlhorn, H. Martin, K. Meyer, K. Nagel, H. Sauer, K. Zosel, *Angew. Chem*. **1952**, *64*, 323.

[6] K. Ziegler, H. Kühlhorn, H. Breil, H. Martin, *Angew. Chem.* **1955**, *67*, 541.

[7] G. Natta, *Angew. Chem*. **1956**.

[8] K. Ziegler, *Angew. Chem*. **1964**, *76*, 545.

[9] G. Natta, *Angew. Chem*. **1964**, *76*, 553.

[10] D. S. Breslow, N. R. Newburg, *J. Am. Chem. Soc*. **1957**, *79*, 5072.

[11] G. Natta, P. Pino, G. Mazzanti, V. Giannini, *J. Am. Chem. Soc*. **1957**, *79*, 2975.

[12] H. Sinn, W. Kaminsky, H. J. Vollmer, *Angew. Chem*. **1980**, *92*, 396.

[13] H. Sinn, W. Kaminsky, *Adv. Organomet. Chem*. **1980**, *99*, 18.

[14] P. Cossee, *J. Catal.* **1964**, *3*, 80.

[15] E. J. Arlman, *J. Catal.* **1964**, *3*, 89.

[16] E. J. Arlman, P. Cossee, *J. Catal*. **1964**, *3*, 99.

[17] M. Peuckert, W. Keim, *Organometallics* **1983**, *2*, 594.

[18] W. Keim, A. Behr, B. Limbacker, C. Kruger, *Angew. Chem., Int. Ed. Engl*. **1983**, *22*, 503.

[19] W. Keim, A. Behr, G. Kraus, *J. Organomet. Chem.* **1983**, *251*, 377.

[20] M. Peuckert, W. Keim, *J. Mol. Catal.* **1984**, *22*, 289.

[21] W. Keim, R. P. J. Schulz, *Mol. Catal.* **1994**, *92*, 21.

[22] M. Brookhart, L. K. Johnson, C. M. Kilian, S. Mecking, D. J. Temple, *Polym. Prepr. (*Am. Chem. Soc., Div. Polym. Chem.), **1996**, *37*, 254.

[23] L. K. Johnson, C. M. Kilian, M. Brookhart, *J. Am. Chem. Soc.* **1995**, *117*, 6414.

[24] L. K. Johnson, S. Mecking, M. Brookhart, *J. Am. Chem. Soc.* **1996**, *118*, 267.

[25] D. J. Scollard, D. H. McConville, N. C. Payne, J. J. Vittal, *Macromolecules* **1996**, *29*, 5241.

[26] D. J. Scollard, D. H. McConville, *J. Am. Chem. Soc.* **1996**, *118*, 10008.

[27] B. L. Small, M. Brookhart, *J. Am. Chem. Soc.* **1998**, *120*, 7143.

[28] B. L. Small, M. Brookhart, A. M. A. Bennett, *J. Am. Chem. Soc.* **1998**, *120*, 4049.

[29] G. J. P. Britovsek, V. C. Gibson, B. S. Kimberley, P. J. Maddox, S. J. McTavish, G. A. Solan, A. J. P. White, D. J. Williams, *Chem. Commun*. **1998**, 849.

[30] G. J. P. Britovsek, V. C. Gibson, B. S. Kimberley, P. J. Maddox, S. J. McTavish, G. A. Solan, A. J. P. White, D. J. Williams, *J. Am. Chem. Soc.* **1999**, *121*, 8728.

[31] Y. Chen, R. Chen, C. Qian, X. Dong, J. Sun, *Organometallics* **2003**, *22*, 4312.

[32] K. P. Tellmann, V. C. Gibson, A. J. P. White, D. J. Williams, *Organometallics* **2005**, *24*, 280.

[33] C. Bianchini, G. Giambastiani, I. Guerrero Rios, A. Meli, E. Passaglia, T. Gragnoli, *Organometallics* **2004**, *23*, 6087.

[34] A. S. Abu-Surrah, K. Lappalainen, U. Piironen, P. Lehmus, T. Repo, M. Leskelä, *J. Organomet. Chem.* **2002**, *648*, 55.

[35] N. V. Semikolenova, V. A. Zakharov, E. P. Talsi, D. E. Babushkin, A. P. Sobolev, L. G. Echevskaya, M.M. Khysniyarov, *J. Mol. Catal. A* **2002**, *182–183*, 283.

[36] G. J. P. Britovsek, V. C. Gibson, O. D. Hoarau, S. K. Spitzmesser, A. J. P. White, D. J. Williams, *Inorg. Chem*. **2003**, *42*, 3454.

[37] G. B. Galland, R. Quijada, R. Rojas, G. Bazan, Z. J. A. Komon, *Macromolecules* **2002**, *35*, 339.

[38] R. Quijada, R. Rojas, G. Bazan, Z. J. A. Komon, R. S. Mauler, G. B. Galland, *Macromolecules* **2001**, *34*, 2411.

[39] T. Fujita, Y. Tohi, M. Mitani, S. Matsui, J. Saito, M. Nitabaru, K. Sugi, H. Makio, T. Tsutsui (Mitsui Chemicals, Inc.), *EP 0874005*, **1998**.

[40] S. Matsui, M. Mitani, J. Saito, Y. Tohi, H. Makio, H. Tanaka, T. Fujita, *chem. Lett.* **1999**, 1065.

[41] S. Matsui, M. Mitani, J. Saito, Y. Tohi, H. Makio, N. Matsukawa, Y. Takagi, K. Tsuru, M. Nitabaru, T. Nakano, H. Tanaka, N. Kashiwa, T. Fujita, *J. Am. Chem. Soc*. **2001**, *123*, 6847.

[42] S. Matsui, T. Fujita, *Catalysis Today*, **2001**, *66*, 63.

[43] H. Makio, N. Kashiwa, T. Fujita, *Adv. Synth. Catal*. **2002**, *344*, 477.

[44] N. Matsukawa, S. Matsui, M. Mitani, J. Saito, K. Tsuru, N. Kashiwa, T. Fujita, *J. Mol. Catal. A: Chem.* **2001**, *169*, 99.

[45] S. Ishii, J. Saito, M. Mitani, J. Mohri, N. Matsukawa, Y. Tohi, S. Matsui, N. Kashiwa, T. Fujita, *J. Mol. Catal. A: Chem.* **2002**, *179*, 11.

[46] Ishii, R. Furuyama, N. Matsukawa, J. Saito, M. Mitani, H. Tanaka, T. Fujita, *Macromol. Rapid Commun.* **2003**, *24*, 452.

[47] H.W. Gschwend, H.R. Rodriguez, *Org. React.* **1979**, *26*, 1.

[48] H. Sinn, W. Kaminsky, *Adv. Organomet. Chem.* **1980**, *18*, 99.

[49] K. P. Stahl, G. Boche, W. Massa, *J. Organomet. Chem.* **1984**, *277*, 113.

[50] J. Amarasekera, T. B. Rauchfuss, *Inorg. Chem.* **1989**, *28*, 3875.

[51] N. Piccolrovazzi, P. Pino, G. Consiglio, A. Sironi, M. Moret, *Organometallics* **1990**, *9*, 3098.

[52] R. F. Jordan, *Adv. Organomet. Chem.* **1991**, *32*, 325.

[53] P. Burger, J. Diebold, S. Gutmann, H.-U. Hund, H.-H. Brintzinger, *Organometallics* **1992**, *11*, 1319.

[54] T.J. Marks, *Acc. Chem. Res.* **1992**, *25,* 57.

[55] M. Aulbach, F. Küber, *Chem. Unser. Z.* **1994**, *28*, 197.

[56] C. Qian, D. Zhu, *J. Chem. Soc. Dalton Trans.* **1994**, 1599.

[57] H.-H. Brintzinger, D. Fischer, R. Mülhaupt, B. Rieger, R. M. Waymouth, *Angew. Chem.* **1995**, *107*, 1255.

[58] H. G. Alt, A. Köppel, *Chem. Rev.* **2000**, *100*, 1205.

[59] H. G. Alt, E. H. Licht, A. I. Licht, K. J. Schneider, *Coord. Chem. Rev.* **2006**, *250*, 2.

[60] H. Plenio, D. Burth, *J. Organomet. Chem.* **1996**, *519*, 269.

[61] E. Barsties, S. Schaible, M.-H. Prosenc, U. Rief, W. Röll, O. Weyand, B. Dorer, H.-H. Brintzinger, *J. Organomet. Chem.* **1996**, *520*, 63.

[62] H. J. G. Luttikhedde, R. P. Leino, C.-E. Wilén, J. H. Näsman, M. J. Ahlgrén, T. A. Pakkanen, *Organometallics* **1996**, *15*, 3092.

[63] P, Jutzi, T. Redeker, B. Neumann, H.-G. StammLer, *Organometallics* **1996**, *15*, 4153.

[64] J. A. Ewen, R. L. Jones, M. J. Elder, A. L. Rheingold, L. M. Liable-Sands, *J. Am. Chem. Soc.* **1998**, *120*, 10786.

[65] C. A. G. Carter, R. McDonald, J. M. Stryker, *Organometallics* **1999**, *18*, 820.

[66] P. Witte, T. K. Lal, R. M. Waymouth, *Organometallics* **1999**, *18,* 4147.

[67] S. Knüppel, J.-L. Fauré, G. Erker, G. Kehr, M. Nissinen, R. Fröhlich, *Organometallics* **2000**, *19*, 1262.

[68] T. Dreier, G. Erker, R. Fröhlich, B. Wibbeling, *Organometallics* **2000**, *19*, 4095.

[69] T. Dreier, G. Unger, G. Erker, B. Wibbeling, R. Fröhlich, *J. Organomet. Chem.* **2001**, *622*, 143.

[70] C. Alonso-Moreno, A. Antiñolo, F. Carrillo-Hermosilla, P. Carrión, I. López-Solera, A. Otero, S. Prashar, J. Sancho, *Eur. J. Inorg. Chem.* **2005**, 2924.

[71] F. Lin, J. Sun, X. Li, W. K. Lang, H. F. Li, H. Schumann, *Eur. Polym. J.* **2007**, *43*, 1436.

[72] X. Xiao, J. Sun, X. Lia, H. F. Li, Y. Wang, *J. Mol. Cat. A: Chem*. **2007**, *267*, 86.

[73] X, Xiao, B. Zhu, X. Zhao, Y. Wang, J. Sun, *Inorg. Chim. Acta* **2007**. *360,* 2432.

[74] Y. Nie, J. Sun, J. Cheng, H. Ren, H. Schumann, *J. Appl. Polym. Sci.* **2008**, *108*, 3702.

[75] G. Erker, B. Temme, *J. Am. Chem. Soc.* **1992**, *11*, 44004.

[76] G. Erker, M. Aulbach, M. Knickmeier, D. Winbermühle, C. Krüger, S. Werner, *J. Am. Chem. Soc.* **1993**, *115*, 4590.

[77] G. W. Coates, R. M. Waymouth, *Science* **1995**, *267*, 217.

[78] E. Hauptman, R. M. Waymouth, *J. Am. Chem. Soc.* **1995**, *117*, 11586.

[79] R. Kravchenko, A. Masood, R. M. Waymouth, *Organometallics* **1997**, *16*, 3635.

[80] J. L. M. Petoff, M. D. Bruce, R.M. Waymouth, A. Masood, T. K. Lal, R. W. Quan, S. J. Behrend, *Organometallics* **1997**, *16*, 5909.

[81] M. D. Bruce, G. W. Coates, E. Hauptman, R. M. Waymouth, J. W. Ziller, *J. Am. Chem. Soc.* **1997**, *119*, 11174.

[82] M. D. Bruce, R. M. Waymouth, *Macromolecules* **1998**, *31*, 2707.

[83] Y. Hu, M. T. Krejchi, C. D. Shah, C. L. Myers, R. M. Waymouth, *Macromolecules* **1998**, *31*, 6908.

[84] J. L. M. Petoff, T. Agoston, T. K. Lal, R. M. Waymouth, *J. Am. Chem. Soc.* **1998**, *120*, 11316.

[85] S. Lin, E. Hauptman, T. K. Lal, R. M. Waymouth, R. W. Quan, A. B. Ernst, *J. Mol. Catal.* **1998**, *136*, 23.

[86] Y. Hu, E. D. Carlson, G. G. Fuller, R. M. Waymouth, *Macromolecules* **1999**, *32*, 3334.

[87] C. D. Tagge, R. L. Kravchenko, T. K. Lal, R. M. Waymouth, *Organometallics* **1999**, *18*, 380.

[88] R. Schmidt, H. G. Alt, *J. Organomet. Chem.* **2001**, *621*, 304.

[89] R. Schmidt, M. Deppner, H. G. Alt, *J. Mol. Catal.* **2001**, *172*, 43.

[90] R. Kravchenko, R. M. Waymouth, *Macromolecules* **1998**, *31*, 1.

[91] N. E. Grimmer, N. J. Coville, C. B. de Koning, *J. Organomet. Chem.* **2002**, *642*, 195.

[92] W. A. Herrmann, M. Denk, R. W. Albach, J. Behm, E. Herdtweck, *Chem. Ber.* **1991**, *124*, 683.

[93] H. C. S. Clark, F. G. N. Cloke, P. B. Hitchcock, J. B. Love, A. P. Wainwright, *J. Organomet. Chem*. **1995**, *501*, 333.

[94] J. D. Scollard, D. H. McConville, J. J. Vittal, *Organometallics* **1995**, *14*, 5478.

[95] S. Tinkler, R. J. Deeth, D. J. Duncalf, A. McCamLey, *J. Chem. Soc., Chem. Commun.* **1996**, 2623.

[96] K. Aoyagi, P. K. Gantzel, K. Kalai, T. D. Tilley, *Organometallics* **1996**, *15*, 923.

[97] T. H. Warren, R. R. Schrock, W. M. Davis, *Organometallics* **1996**, *15*, 562.

[98] A. D. Horton, J. de With, A. J. van der Linden, H. van de Weg, *Organometallics* **1996**, *15*, 2672.

[99] F. G. N. Cloke, T. J. Geldbach, P. B. Hitchcock, J. B. Love, *J. Organomet. Chem.* **1996**, *506*, 343.

[100] J. D. Scollard, D. H. McConville, J. J. Vittal, *Organometallics* **1997**, *16*, 4415.

[101] J. D. Scollard, D. H. McConville, J. J. Vittal, N. C. Payne, *J. Mol. Catal.* **1998**, *128*, 201.

[102] C. H. Ahn, M. Tahara, T. Uozumi, J. Jin, S. Tsubaki, T. Sano, K. Soga, *Macromol. Rapid Commun.* **2000**, *21*, 385.

[103] T. Uozumi, S. Tsubaki, J. Z. Jin, T. Sano, K. Soga, *Macromol. Chem. Phys*. **2001**, *202*, 3279.

[104] S. Tsubaki, J. Jin, C. H. Ahn, T. Sano, T. Uozumi, K. Soga, *Macromol. Chem. Phys.* **2001**, *202*, 482.

[105] P. Souza, J. A. Garcia-Vazquez, J. R. Masaguer, *Synth. React. Inorg. Met. Org. Chem.* **1985**, *15*, 247.

[106] C. Molleda, J. A. Garcia-Vazquez, J. R. Masaguer, *Transition Met. Chem.* **1987**, *12*, 249.

[107] C. Molleda, J. R. Masaguer, J. A. Garcia-Vazquez, *Synth. React. Inorg. Met. Org. Chem.* **1989**, *19*, 181.

[108] P. Souza, J. A. Garcia-Vazquez, J. R. Masaguer, *Transition Met. Chem.* **1984**, *9*, 318.

[109] G. Seth, M. K. Samota, J. Kaur, *Indian J. Chem.* **2006**, *3*, 25.

[110] G. S. Reddy, K. K. Reddy, *Current Sci.*, **1976**, *45*, 535.

[111] D. Hawkins, J. M. Lindley,; I. M. McRobbie, O. Meth-Cohn, *J. Chem. Soc. Perkin Trans. 1*, **1980**, 2387.

[112] A. S. Kiselyov, M. Hojjat, K. Van Aken, L. Strekowski, *Heterocycles* **1994**, *37*, 775.

[113] S. Billeau, F. Chatel, M. Robin, R. Faure, J.-P. Galy, *Magn. Reson. Chem.* **2006**, *44*, 102.

[114] R. K. J. Bott, D. L. Hughes, M. Schormann, M. Bochmann, S. J. Lancaster, *J. Organomet. Chem.* **2003**, *665*, 135.

[115] Q. Chen, J. Huang *Appl. Organomet. Chem.* **2006**, *20*, 758.

[116] H. Zhang, S. Katao, K. Nomura, J. Huang, *Organometallics* **2007**, *26*, 5967.

[117] G. Alesso, M. Sanz, M. E. G. Mosquera, T. Cuenca, *Eur. J. Inorg. Chem*. **2008**, 4638.

[118] R. Vollmerhaus, M. Rahim, R. Tomaszewski, S. Xin, N. J. Taylor, S. Collins, *Organometallics* **2000**, *19,* 2161.

[119] R. Gómez, R. Duchateau, A. N. Chernega, J. H. Teuben, F. T. Edelmann, M. L. H. Green, *J. Organomet. Chem*. **1995**, *491*, 153.

[120] L. F. Groux, F. Bélanger-Gariépy, D. Zargarian, R. Vollmerhaus, *Organometallics* **2000**, *19*, 1507.

[121] J. R. Ascenso, A. R. Dias, J. A. Fernandes, A. M. Martins, S. S. Rodrigues, *Inorg. Chim. Acta* **2003**, *356*, 279.

Erklärung

Hiermit erkläre ich, dass ich die Arbeit selbständig verfassst und keine anderen als die angegebenen Quellen und Hilfsmittel benutzt habe.

Ferner erkläre ich, dass ich nicht andersweitig mit oder ohne Erfolg versucht habe, eine Dissertation zu diesem oder gleichartigem Thema einzureichen oder mich der Doktorprüfung zu unterziehen.

Bayreuth, den 10. Februar 2010

Khalil Ahmad